Numerical **Weather Prediction**

Forecasting Research
Technical Report No. 259

Report on pre-operational trials of the new microphysics scheme in the mesoscale model

by

J. Radcliffe, B. Chalcraft, C. Wilson, B. Macpherson, D. Wilson and P. Clark

December 1998

The Met.Office

Excelling *in weather services*

Forecasting Research
Technical Report No. 259

Report on pre-operational trials of the new microphysics scheme in the mesoscale model

by

J. Radcliffe, B. Chalcraft, C. Wilson, B. Macpherson,
D. Wilson and P. Clark

December 1998

Meteorological Office
NWP Division
Room 344
London Road
Bracknell
Berkshire
RG12 2SZ
United Kingdom

Tel: 44 (0)1344 856245 Fax: 44 (0)1344 854026 e-mail: jsarmstrong@meto.gov.uk

Report on pre-operational trials of the new microphysics scheme in the mesoscale model

Jonathan Radcliffe, Byron Chalcraft, Clive Wilson, Bruce Macpherson,
Damian Wilson and Pete Clark

December 1998

Abstract

Pre-operational trials of a new cloud microphysics scheme, and new visibility diagnostic, have been shown to have a strong beneficial effect on mesoscale model forecasts. The new microphysics scheme uses more physical arguments in its treatment of water types, with ice becoming a prognostic variable. The new visibility diagnostic is now based on the assumption of a distribution of relative humidity within the grid-box. After a series of case studies and a parallel trial, biggest forecast improvements have been seen in fog probabilities, visibility and screen temperature.

1. Introduction

A new cloud/precipitation microphysics scheme has been developed at the Met Office (Wilson and Ballard, 1998) for use in the unified model. Currently it is used in the climate and operational mesoscale forecast models. Preliminary tests showed it to have potential to improve markedly mesoscale forecasts, especially forecasts of low cloud. This report gives details of the pre-operational trials leading up to its acceptance and operational implementation on 4th August 1998.

The trials consisted of two stages: studies of the performance of the new scheme on selected forecasts from the previous 18 months; and with the new scheme running in parallel with the current operational model over approximately four weeks, mostly during July 1998. The forecasts of surface fields, precipitation and cloud cover from the new scheme and that of the operational model were assessed and compared, objectively and subjectively.

2. Description of the new scheme

A full description of the new scheme is given in Wilson and Ballard (1998).

2.1 Shortcomings in the old scheme

The most important distinction of the new scheme is how the amounts of liquid water/ice are calculated. Previously, the condensate was partitioned as a function of temperature only, above 0 °C it was all liquid, below -9 °C all was ice, with the diagnosed ice allowed to fall, but not the liquid water.

A serious consequence of this was the incorrect prediction, by the model, of fog from ice fallout, commonly seen by forecasters. With temperatures below freezing in the boundary layer and stratocumulus cloud, the precipitation scheme would fall ice out of the cloud top, resulting in a downward moisture flux and fog. In reality, with temperatures just below 0 C, there will be very few ice nuclei present to fall to lower levels.

Another problem is found when the cloud base is near to or above 0 C. Ice falling from above melts and causes a build up of moisture just above the melting layer. Only crude parametrizations of autoconversion and accretion, not based on physical processes and very tunable, allow precipitation to form as a balance.

2.2 The new precipitation/cloud scheme

In the new scheme, ice becomes a prognostic variable, and the large scale precipitation scheme uses physical processes and values to separate water between vapour, liquid droplets, raindrops and frozen water (ice), Figure 2.1. Ice is advected around the model domain by tracer advection. It is based on the work of Rutledge and Hobbs (1983) and was used in the UKMO's old non-hydrostatic model, described by Golding (1992).

Starting from the top layer, the precipitation scheme works sequentially through a set of eleven transfer terms for the water content. Ice and rain may fall to the next level (rain is diagnostic and falls out in one timestep) where they are used in those transfer equations. The cloud scheme now only predicts liquid water, at all temperatures.

2.3 Changes to the assimilation of cloud data

The mesoscale data assimilation scheme (Macpherson et al. 1996) makes use of 'MOPS' cloud and precipitation data prepared by the Nimrod nowcasting system, where MOPS is the Moisture Observation Pre–processing System. The cloud assimilation for the old microphysics is based on that scheme's unique relationship between grid–box mean RH and cloud fraction. In the new microphysics, with prognostic ice content, this relationship no longer holds where ice is present. A new version of the cloud assimilation therefore had to be developed, and this is described in detail in the Appendix. The version which emerged from this development was tested on 5 cases studies prior to embarking on more extensive pre–operational trials.

Each case was run with assimilation from T–12 and forecast to T+18, using the same boundary file for the whole run, taken from a LAM run with DT of T–12. The cases chosen were DT's 12z 05/12/97, 06z 08/1/97, 12z 01/12/97, 12z 16/12/97 and 00z 31/08/97. Summary forecast verification scores are presented in Figure 2.3.1. As well as giving an encouraging preliminary view of the impact of the new microphysics itself, these cases showed how the impact of assimilating cloud data varies from the old to the new microphysics. The new assimilation appeared to be working quite satisfactorily.

From Figure 2.3.1(a), the improvement in cloud cover is greatest at the very start of the forecast, when the benefit of assimilation is larger with the new scheme. The overall benefit of cloud data assimilation on total cloud cover is marginal from T+6, though in individual cases (not shown), it is longer lasting. From Figure 2.3.1(b), there is a suggestion that the benefit of cloud data for temperature forecasts is larger with the new scheme than the old one. It may be that even if we are not getting better total cover beyond T+6 from the cloud data, they may be improving the 3–d cloud structure and hence the radiation balance. One must be careful, however, not to place too much weight on results from only 5 cases. Improved fog probability is a feature of the new scheme (Figure 2.3.1(c)). In the old scheme, cloud data can make the errors worse, probably through providing extra forcing of the ice fallout problem. In the new scheme, the impact of cloud data on errors in fog is closer to neutral.

3. Case studies

The case studies were rerun at version 4.4 of the UM, using the pre-June 1998 mesoscale domain and resolution (0.15 °, 17 km, and 31 levels). In each case, two configurations were run: the control (using the operational setup) and test (with the new microphysics - 3A LS precipitation scheme, 2A cloud scheme). Both test and control reruns consisted of a first, spin-up, assimilation cycle from T-9 to T-3, followed by an assimilation and forecast cycle T-3 to T+24. Boundary conditions were taken from the LAM at T-6 and T+0, and observations files including MOPS every three hours from T-9 to T+0.

The results of the reruns were judged both objectively and subjectively against observations. For the objective verification data from up to 289 stations were retrieved from the SDB, to calculate biases and r.m.s. errors for fields. These included relative humidity, winds, pmsl, screen temperature, visibility, fog probability and cloud cover. Each case was studied separately, looking at the improvement (or otherwise) of the test physics over the control, then a set of means of biases and errors over all cases was calculated for the separate fields. Finally, a mean of the r.m.s. errors over all fields was worked out.

Precipitation forecasts were verified against the set of 42 stations used to assess the operational mesoscale precipitation forecasts. Equitable threat, Hanssen & Kuipers and

frequency bias scores were calculated. The subjective verification compared the available model output fields against station observations, radar rainfall and satellite imagery.

3.1 Description of the cases

Fourteen cases were rerun, covering a variety of synoptic and mesoscale conditions. The new scheme was tested under the weather types described by WGOS (working Group on the Operational System) in the Mesoscale Model Change Procedure (the cases which were chosen solely for this reason are indicated by an asterisk in the list below). Other tests were done for conditions for which improved model guidance was expected. The dates and times are listed below, together with a short phrase describing the weather type or the operational model shortcomings.

1	October 13th 1996, 0z	amounts of ST underdone, especially at 0900, in a cyclonic southerly
2	December 4th 1996, 6z	excessive CU/SC in an unstable west to northwesterly
3	December 22nd 1996, 6z	excessive precipitation in anticyclone over northern England
4	January 5th 1997, 0z	excessive fog forecast due to ice fallout in very cold northeasterly type
5	January 9th 1997, 6z	as 5th
6	January 15th 1997, 0z	freezing fog incorrectly cleared by model in slack southerly in a ridge
7	May 12th 1997, 6z	showers & thunderstorms under-forecast in an unstable, cyclonic southwesterly
8	May 29th 1997, 0z*	clear summer day in anticyclone
9	August 5th 1997, 6z*	model incorrectly lost area of stratus over NE England in the evening
10	August 28th 1997, 6z	false impression of drier slots in unstable, cyclonic & brisk southwesterly
11	September 27th 1997, 6z	incorrectly cleared stratocumulus in anticyclone
12	December 1st 1997, 0z*	mixed snow and rain in cold northerly to the rear of a slow-moving low
13	December 10th 1997, 0z*	land gales in association with a deep low centre crossing S Scotland
14	February 2nd 1998, 0z*	clear winter night in a developing ridge

These dates come from a list maintained by Byron Chalcraft. Half each are from 0z and 6z runs, and half come from winter months DJF, the remainder spread May through to October.

Forecasts were made up to T+24, with model output every 3 hours.

3.2 Objective assessment

The results from the objective verification were very encouraging, showing improvements in r.m.s. errors where expected, and no serious detrimental effects on scores, in either the required cases or those specifically chosen for this trial, in any forecast fields. At a glance, Fig 3.2.1 gives the per cent change in r.m.s.e. averaged over all, and key, fields case by case as a time series. Some of the main features of the objective assessment from each case are given below. These are followed by summary statistics which give means of biases and r.m.s. errors over the cases.

October 13th 1996

Total cloud amounts show an improvement in r.m.s. errors at T+3, from reducing the positive bias, although studying just the low cloud amount reveals that the new microphysics has not increased the stratus which was lacking from the control. The stratus probability r.m.s.e. from the verification is not improved over the control, which ranges from 0.2 to 0.5. There is a slight detriment to the visibility r.m.s. error from the new microphysics up to T+9, but otherwise the errors are similar to that of the control.

December 4th 1996

The new scheme loses a lot of the low cloud put in by the control around the east Midlands and East Anglia, agreeing more closely with the satellite image. The 1.5m RH value is improved over the control during the day, as is the fog probability score, but these both worsen after T+15. Forecast visibility bias is increased by the new microphysics, improving r.m.s.e. at all times.

December 22nd 1996

Fog, mist and stratus probabilities are decreased by the test scheme, although the effect on r.m.s.e. is less consistent. Visibility r.m.s.e. is improved by over 10% in the second half of the forecast through decreasing the negative bias.

January 5th 1997

The total cloud bias (Fig. 3.2.2(c)) in the control shows a strong negative bias - cloud having descended excessively to form fog which was not observed (Fig. 3.2.2(a)). The test forecast keeps more cloud, and reduced the fog probability bias to practically zero, with a greatly reduced r.m.s. error (Fig 3.2.2(b)). Similar behaviour is seen in mist and stratus probabilities. A knock-on effect is to increase the screen temperatures and visibility, both of which are underforecast by the control (Figs 3.2.2(d), 3.2.2(e)), there is little change to the temperature r.m.s. errors, although the visibility error is more than halved at many forecast times (Fig 3.2.2(f)).

January 9th 1997

The positive 1.5 m RH bias is well reduced by the new microphysics, and improves the r.m.s.e. by over 10% throughout the forecast. Most of the fog is cleared by the new scheme, and doesn't develop the following night when the control forecast covers mainland UK with fog. There are subsequent improvements in verification scores, although the total cloud cover errors are worse than the control after T+6 with too little being forecast. However, the stratus probability bias and r.m.s.e. are much reduced Little impact is seen on the forecast temperatures.

January 15th 1997

This case showed how the new scheme could also beneficially keep fog, when the control dispersed it (Fig. 3.2.3(a)). The effect on other forecast fields is particularly noticeable after T+12 (midday local time). In this case the control has too high screen temperatures, which the test forecast goes some way to correcting (Fig. 3.2.3(b)), reducing the r.m.s. error at T+15 by over 15%.

May 12th 1997

The 1.5 m RH bias has been reduced by the new scheme in the verification, but with little effect on the r.m.s. error. Also the negative visibility bias has been reduced. Total cloud amounts are not changed, but the total cloud max/rand (which is the field included as a key field) bias is lowered, and the r.m.s.e. increased. There is little change in other fields.

May 29th 1997

Very little change in most verification r.m.s. error fields, except visibility which shows an improvement of about 10% after 9 hours due to the new microphysics. The cloud amounts have been increased by the new microphysics, reducing the slight negative bias, but not changing the r.m.s. error substantially.

August 5th 1997

Fog and visibility r.m.s. errors improved, the new microphysics introduces a more positive cloud bias giving decreased r.m.s. errors in both cloud fields to 12 hours, but no improvement thereafter. Little change in other fields.

August 28th 1997

The new scheme has reduced cloud r.m.s. errors (Fig. 3.2.4(a)), and daytime screen temperature r.m.s. errors are generally improved by about 0.1 K of 1.5 - 2 K (Fig. 3.2.4(b)).

September 27th 1997

Verification scores show that the negative bias in the total cloud amount has been substantially reduced and decreased the r.m.s. errors. The new scheme also outperforms the control forecast in 1.5 m RH, 10 m winds, screen temperature and dewpoint.

December 1st 1997

Although the positive cloud bias is consistently reduced from about 0.5 to half that by the effect of the new microphysics, the r.m.s.e. remains at about 2.4 oktas until T+18 and beyond when it increased above that of the control forecast (Fig. 3.2.5). However after the same time, the fog probability r.m.s.e. of the test is seen to improve substantially over the control (its bias was consistently lower and closer to zero), and visibility is consistently better forecast in the test version.

After T+18 the vector wind r.m.s.e. and positive bias are lowered by over 0.1 m/s, and the pmsl has its negative bias and r.m.s.e. reduced by over 0.1 hPa.

December 10th 1997

This case shows the test scheme to be significantly lowering the screen temperature and pmsl rmses at T+12, 15 and 18 as two fronts cross the UK (Fig. 3.2.6(a) and (b)). Before and after this event, fog probability scores are improved.

February 2nd 1998

There are improvements by the new microphysics scheme early in the forecast to screen temperature, and later to RH and stratus probability. Visibility r.m.s. errors are improved throughout.

Meaned statistics

Errors and biases have been meaned according to forecast time over all the cases. Also, for individual fields the percentage change due to the test scheme relative to the control, at each forecast time and averaged over all times, has been calculated (Fig. 3.7). Finally, the average percentage change in r.m.s.e. over all fields was found.

The largest effects are seen, as we would expect, in fog probability (Figs 3.2.8) and visibility (Figs 3.2.9) which give time averaged improvements of 19% and 14% respectively. Other significant improvements are seen in RH, which has about a 4% reduction in its r.m.s. errors after T+6. Screen temperature is systematically increased by up to 0.1 K in the test, with a reduction of 1.7% in r.m.s.e..

Cloud amounts have their r.m.s.e. improved by 2.4% when averaged over all the forecast times, but this hides some systematic detrimental behaviour when at T+9 and T+12 the r.m.s.e. is degraded. Studying 0z and 6z run times separately we see that the detriments generally come during the day, and the improvements at night.

The r.m.s. errors in wind fields are affected only slightly, but in the right direction, generally showing a reduction in r.m.s. errors of between 0 and 1%. The pmsl similarly sees a 1% reduction in time-averaged r.m.s.e..

When the r.m.s. errors are averaged over all fields we see a consistent improvement of between 2 and 5%, averaging out at 3.7% over all times. If we just take the key fields (screen temperature, visibility, 10 m vector wind and cloud cover) and average, this gives practically the same improvement of 3.8% (Fig 3.2.10). Again, there is some evidence of a diurnal cycle in both of these compilations, with greatest improvements seen at night.

3.3 Precipitation and visibility scores

Contingency tables of forecast precipitation and visibility were constructed, for each forecast period, comparing against observations at the 42 stations which are used routinely to measure the performance of the operational mesoscale. Each table was constructed for all the cases considered together to improve the sample size. Mean results for the first 24 hours will be presented here.

The 6h forecast accumulations of precipitation show equal or better equitable threat (ETS) scores for low to moderate thresholds (0.1–2.4 mm/6h), Fig 3.3.1(a). The improved low threshold score reflects the removal of light rain and drizzle from erroneous fall–out of ice. The frequency of erroneous prediction has also been reduced (Fig3.3.2(a)). The higher accumulations have mostly worse ETS compared to the control, but the observed frequency over this sample of cases is extremely small (Fig 3.3.2(b)) and so is not reliable. The 95% confidence intervals are indicated by the vertical bars in Fig3.3.1, which show that none of the

changes in ETS can be regarded as statistically significant from this sample of cases studies. The Hanssen and Kuipers score (Fig.3.3.1(b)) which is more sensitive to missed events also shows the test new microphysics version to have improved for low to moderate thresholds.

For visibility both the ETS and Hanssen and Kuipers score are clearly improved at the thick fog, fog and mist thresholds (<200m, <1km, <5km), Figs 3.3.3(a), 3.3.3(b). The frequency bias for prediction of fog and mist is also appreciably improved (Fig.3.3.4(a)), although it should be noted that nearly 85% of the observations have visibilities greater than 5km (Fig.3.3.4(b)) so these results are for a relatively small sample, especially at the lowest threshold of 200m. However the ETS improvements are mostly significant at the 95% level as shown by the separation between the confidence error bars.

3.4 Subjective Assessment

October 13th 1996

For both rainfall and surface temperature there were no significant differences between the runs. The trial cloud forecast was slightly preferred, for having less high cloud over southeast England at T+3, otherwise no significant differences in cloud or in fog and stratus probabilities, so no improvement on the operational run's lack of widespread Stratus at 0900.

December 4th 1996

The trial run was slightly preferred for precipitation distribution in the first half of the forecast. The trial cloud output was preferred for having less low cloud from T+0 to T+15 over parts of E Midlands and E Anglia. Temperatures were a little better on the trial early in the forecast, and a little worse on later frames - hence no preference.

December 22nd 1996

The trial run was preferred overall for having less spurious ("spotty high syndrome") light precipitation over N England and Scotland. This is shown in fig. 3.4.1. The precipitation rate is too light for a radar frame to be a fair verification but surface observations support the reduction over land. On just one forecast frame (T+6) from this run there was actually a little *more* spurious precipitation on the trial run in the south of England. There was no preference in both cloud and temperature outputs. But the reduction of fog probabilities in the trial run over the Scottish Highlands was also preferred.

January 5th 1997

From T+9 to T+24 the trial run had less very light precipitation than the operational run over both land and sea, especially at T+21 and T+24. This was preferred, since by T+9 there was little if any precipitation being observed. There was no preference for temperatures. For cloud the trial was slightly preferred for having a little more low cloud over Eire in early frames and for having low cloud extending further southeast into the Continent on later frames. Stratus probabilities were much reduced in the trial run and this was also preferred as most parts had Stratocumulus reported at around 2000 feet. Fog probabilities were also much reduced in the trial run from T+3 onwards and this was very much better than the operational run. Fig. 3.4.2 shows this marked reduction in fog probability, at T+24, and fig.3.4.3 the reduction in largely spurious light precipitation.

January 9th 1997

The trial run was again preferred overall for precipitation in having less light precipitation than the operational over many inland parts from T+12 to T+18, and more generally from T+21 to T+24. There was no preference regarding temperatures and cloud. However, from T+0 to T+9 the operational run was preferred because the trial run reduced the fog probabilities too much, such that there was less indication of hill fog in an actual area of fog and low cloud over northern France. Then from T+12 to T+24 the trial was the better in having a much reduced fog probability over a large part of England, Scotland and the Continent and since this covered a larger area for longer the trial run's fog probabilities were preferred overall.

January 15th 1997

There were no significant differences for precipitation. Fog probabilities were correctly higher on the trial run from T+9 to T+24, with the greatest improvement on the T+12 and T+15 frames. Fig.3.4.4 shows this better fog retention, with supporting 'visible' satellite image (surface observations confirmed fog). The trial run was also better for having higher Stratus probabilities from T+12 to T+24 over parts of England. Also, the trial T+12, 15 & 18 frames also had more low cloud in the fog area. The effects on surface temperatures was also beneficial in the fog area, with values correctly 2 to 4 degrees lower over the East Midlands and East Anglia from T+12 to T+18, as shown in Figs.3.4.5a and 3.4.5b. Overall, the trial run was much preferred.

May 12th 1997

For rainfall the operational run was marginally preferred for having a slightly better shower distribution over S England at (only) T+6, as shown in Fig.3.4.6. The trial run cloud frames at T+18 & 21 had much less high cloud over France than the operational run (but this could not be verified since no satellite imagery was available, and there are very few observations of cloud over France at night). By T+24 there were no significant differences in the cloud fields once again. The operational run was also slightly preferred for temperature, especially at T+9 & 12, when the trial run was incorrectly a little cooler over some inland areas.

May 29th 1997

There was a little more very light precipitation on early frames of the trial run, but neither run was preferred, and there were no significant differences in the other fields.

August 5th 1997

There were only small differences in all fields, with no overall preferences, including low cloud over northeast England in later frames, i.e. no improvement in the operational run's loss of the low cloud cover there. The trial run did increase the amount of *high* cloud in this area, though.

August 28th 1997

For rainfall the trial run is slightly preferred over the operational for having a marginally better shower distribution at T+0 and T+3 and again at T+15 and T+24. No significant differences were seen in the cloud or temperature fields.

September 27th 1997

There was no preference for rainfall since there was very little difference between the runs, just a few more patches of very light precipitation throughout on the trial run, mainly over the sea, and not properly verifiable. There were no significant differences in the cloud, temperature or fog and stratus probabilities.

December 1st 1997

The operational run's precipitation distribution was slightly preferred on a couple of frames. No significant differences were seen in surface temperatures, and there were only small differences in the cloud fields. For Stratus probabilities however there were some differences of note, mainly reductions over northeast Scotland and southwest England on early frames and a reduction in the size of high Stratus probability in the main rain area over S England on a couple of later frames but there was no overall preference. Fog probabilities were again preferred on the trial run, though. This was due to a correct reduction in fog probability over northern Scotland from T+9 to T+24, and from T+18 to T+24 over central southern England.

December 10th 1997

There were only small, insignificant differences in fields generally, therefore there was not a preferred run.

February 2nd 1998

Some small differences in shower distribution over sea and western coastal areas were seen but overall there was not a preference for precipitation fields. There were no significant differences with regards temperature or cloud. But small areas of reduced Stratus probability in the trial over the N Sea, especially on later frames, and also over northeast Scotland and northern France at T+24 was preferred. Lower fog probabilities in the trial from T+12 onwards over northern Scotland, part of the North Sea and Continent, especially at T+24, was also slightly preferred.

Summary of Subjective Assessment

Out of the 14 runs examined the trial output was preferred overall in 5, no preference for either run in 8 and the operational run was preferred, and only slightly, in just one case, the 12th of May. The greatest benefit from the new microphysics was seen in 1) a large reduction of the spurious high fog probabilities associated with ice fallout in cold easterly types and 2) an improvement in the maintenance of freezing radiation fog. No serious detrimental impact was seen in other synoptic types. There also appears to be benefit from some reduction of spurious light precipitation in anticyclones, known as the "spotty high" syndrome.

4. Parallel trials

From late June through July, the mesoscale model with the new microphysics scheme in place was run in parallel with the operational model (this phase of the trials was administered by Adam Maycock). Thus the test scheme would run with the same assimilation cycle as the control, picking up its own formed analyses, four times a day to T+36 (although the operational model in fact only ran to a maximum of T+30). The resolution of the operational model was increased to 0.11 °, 12 km, and 38 levels, on June 10th 1998, and it was at this

resolution (and over the extended domain) that all the parallel trials were run. MOPS files were provided for the new configuration.

These trials were run with a new visibility diagnostic, written by Pete Clark, also incorporated (as presented to WGOS at June 15th, 1998 meeting, Appendix B). From the objective verification of several case studies, a significant improvement in r.m.s. errors in log(visibility) had been seen.

4.1 Objective verification

From 22nd June to 30th July, sixty-nine forecasts were assessed using the mesoscale verification package, as used for the case studies. Again, the results were positive, with the new scheme producing better forecasts, verified against observations, than the operational in all but thirteen instances (Fig. 4.1.1).

As with the case studies, greatest improvements were seen in the fields of fog probability and visibility (Figs 4.1.2 and 4.1.3). The negative bias in log (visibility) was slightly overcompensated, especially at longer forecast times, but gave a systematic improvement in r.m.s.e. of just over 15%. Although fog was not common during the trial, the positive bias was still evident in the control forecasts, and largely cancelled out by the new scheme, giving a strong improvement in r.m.s.e..

A weakness found from the parallel trials, which was not seen in the case studies, was the under-forecast by the new scheme of total cloud amount (as measured by the max/random overlap) (Fig. 4.1.4) and stratus. Although both test and the operational models started with a negative cloud bias of - 0.7 oktas, after six hours the control has spun up to close to zero, whereas the test scheme reaches only - 0.4 oktas. This detriment shows through in the r.m.s.e., worsened by about 7%. However, this seems to have the knock-on effect of increasing screen temperatures, from a negative bias and so reducing the r.m.s.e. in this field (Fig. 4.1.5).

All other fields showed small reductions in r.m.s.e. on average (Fig. 4.1.6). The average change in r.m.s.e. across all fields and cases was a 2% improvement. More importantly, over the key fields of screen temperature, visibility, vector wind and total cloud amount, the change was a 2.8% improvement. It should also be noted that the scheme is expected to have the most benefit during the winter and so to see such a positive impact in the summer months is very encouraging.

4.2 Precipitation scores

There is quite a small difference between the control and test equitable threat scores for the precipitation rates averaged over the first 24 hours (Figure 4.2.1(a)). The new scheme scores slightly better at most thresholds, but error bars on the differences make them statistically not significant. Breaking the ETS down to six-hourly intervals does show some more significant pattern however. In the first six hours, the new microphysics scores better than the operational model at higher thresholds (> 2.4 mm/6hr), and at longer forecast times, T > 12, it fares better at lower thresholds (< 0.5 mm/6hr).

The Hanssen and Kuipers score, which is sensitive to missed events, rather than false alarms, is consistently better at all thresholds with the new microphysics scheme (Figure 4.2.1(b)). The bias (number forecast divided by number observed, at each threshold) (Figure 4.2.2(a)) is also higher in the new scheme than in the control. Both these measures tell us that the new scheme is forecasting more precipitation than the operational model, and imply that the false alarm rate is also somewhat higher, although fewer events are missed. Again, as with the case studies (section 3.3), the observed frequency (Figure 4.2.2(b)) at the highest thresholds (> 6.4

and 10.4 mm/6hr) are very small and so the improvements indicated for these may be less reliable.

4.3 Subjective assessment

A total of 73 runs were assessed during the period from 18th June to 20th July, inclusive. The fields compared were: precipitation rates, cloud cover, pmsl, surface temperature, and stratus and fog probabilities.

Precipitation

Differences in output were for the most part quite small and for the majority of runs there was not a preference. Quite a number of runs had no significant differences on any frames and a large number of others had slight improvements at some time frames, offset by small detriments at others. Of the 73 runs examined there was no overall preference in the output in 59, a slight preference for the current operational output in 6 and a slight preference for the new microphysics runs in 8. An example of an improvement is shown in Fig. 4.3.1.

Cloud

Differences were small and there was generally not a preference for either run, but it was found that for high cloud in particular the new microphysics output often had somewhat less cover near the boundary.

PMSL

No significant differences for nearly all runs but there were two cases in which the operational run produced spurious, temporary PMSL dipoles at short range, almost certainly a result of the latent heat nudging scheme. In the new microphysics runs this effect was virtually absent. This is shown in figure 4.3.2. The corresponding precipitation analysis frame from the new microphysics run was also slightly better, see figure 4.3.3.

Temperatures

For most runs there were no significant differences but where differences were seen these were mostly during daytime with the new microphysics run having (correctly) slightly higher temperatures (1–2 degrees C.) over some inland areas.

Fog probability

Fog was rare during the period. Even sea fog was less prevalent than normal due to the preponderance of polar maritime air in the trial period. The majority of runs therefore showed no significant differences but there was quite a large number where the new microphysics run showed a small reduction of fog probability, e.g. reduced the probability over small areas, from say 30% to 20%, usually in association with precipitation. This is difficult to verify but on the whole appears to be beneficial.

Stratus probability

Similar to that seen for fog, with the majority of runs showing no significant differences, but with a 10–20% reduction in probability over small areas on some new microphysics runs in precipitation areas. This is rated as being neutral as it appeared correct for some runs and not for others.

4.4 Model stability

During the parallel trials there were 3 interruptions to the continuous assimilation cycle. The first 2 were not due to the use of the new microphysics and it is highly unlikely that the third was either.

The first problem at the end of June was traced to a bug in the assimilation of screen temperatures over high orography, which also caused the operational mesoscale model to fail. This has been corrected.

The 2nd interruption over the 1st week-end of July was due to T3E problems.

The last failure was during the 18Z run on 20 July, when exceptionally high surface temperatures and convectively unstable air over Holland and Germany resulted in numerical instability. The operational model only just managed to survive this without failure. Reruns with the new microphysics and operational versions have shown the failure may be avoided by omitting MOPS cloud observations and latent heat nudging. The cloud observations themselves are not thought to be the cause of the problem but rather their interactions with the rest of the model, especially the convection scheme. This appears to be not effective enough at the higher horizontal resolution to prevent the dynamical adjustment from becoming numerically unstable. In these extreme cases, the convection scheme should be more frequently invoked to avoid failure. The half-timestep operational version will be available in the event of a recurrence of the extreme conditions.

The new microphysics version of the model is therefore concluded not to be any more prone to numerical instability than the current operational model, for which measures to reduce the likelihood of failure are actively being tested.

5. Timings

With the new scheme showing large improvements in the verification of forecasts, the only drawback to be considered is that of extra computing cost. Additional costs come from having ice as a prognostic variable and using tracer advection to move it around, and the additional complexity of the transfer equations. During the course of the case studies, the timings of several operational and test forecasts were compared. On average, user CPU time increased by 17%.

6. Conclusions

The new cloud/precipitation microphysics scheme uses more physical arguments in its treatment of water types, and rids the model of fairly arbitrary tuning parameters. As such, it significantly improves the overall forecast accuracy of the mesoscale model.

Case studies have shown it to have had a large positive impact on one of the model's primary weaknesses, that of predicting wintertime fog, and to have decreased the r.m.s.e. of all other fields, giving an average decrease over key fields of 3.5%. Even during the parallel trials in the summer, when less effect is expected, objective verification has again seen an improvement of almost 3% when the key fields are considered, in combination with the new visibility diagnostic.

Acknowledgements

We wish to thank Adam Maycock for running and monitoring the parallel trial.

References

Golding, B W, 1992: An efficient non-hydrostatic forecast model. *Meteorol. Atmos. Phys.*, **50**, 89-103

Macpherson B, Wright B J, Hand W H, and Maycock A J, 1996: The impact of MOPS Moisture data in the U.K. Meteorological Office Mesoscale Data Assimilation Scheme. *Mon. Weath. Rev.* **124**, 1746–1766

Rutledge, S A and Hobbs P V, 1983: The mesoscale and microscale structure and organization of clouds and precipitation in midlatitude cyclones. VIII: A model for the "seeder-feeder" process in warm-frontal rainbands. *J. Atmos. Sci.*, **40**, 1185-1206

Smith R N B, Gregory D, and Wilson C A, 1992: Calculation of saturated specific humidity and large–scale cloud. Unified Model Documentation Paper No 29.

Wilson, D R and Ballard S P, 1998: A microphysical based precipitation scheme for the UK Meteorological Office Unified Model. submitted to *Quart. Journal R. Met. Soc.*

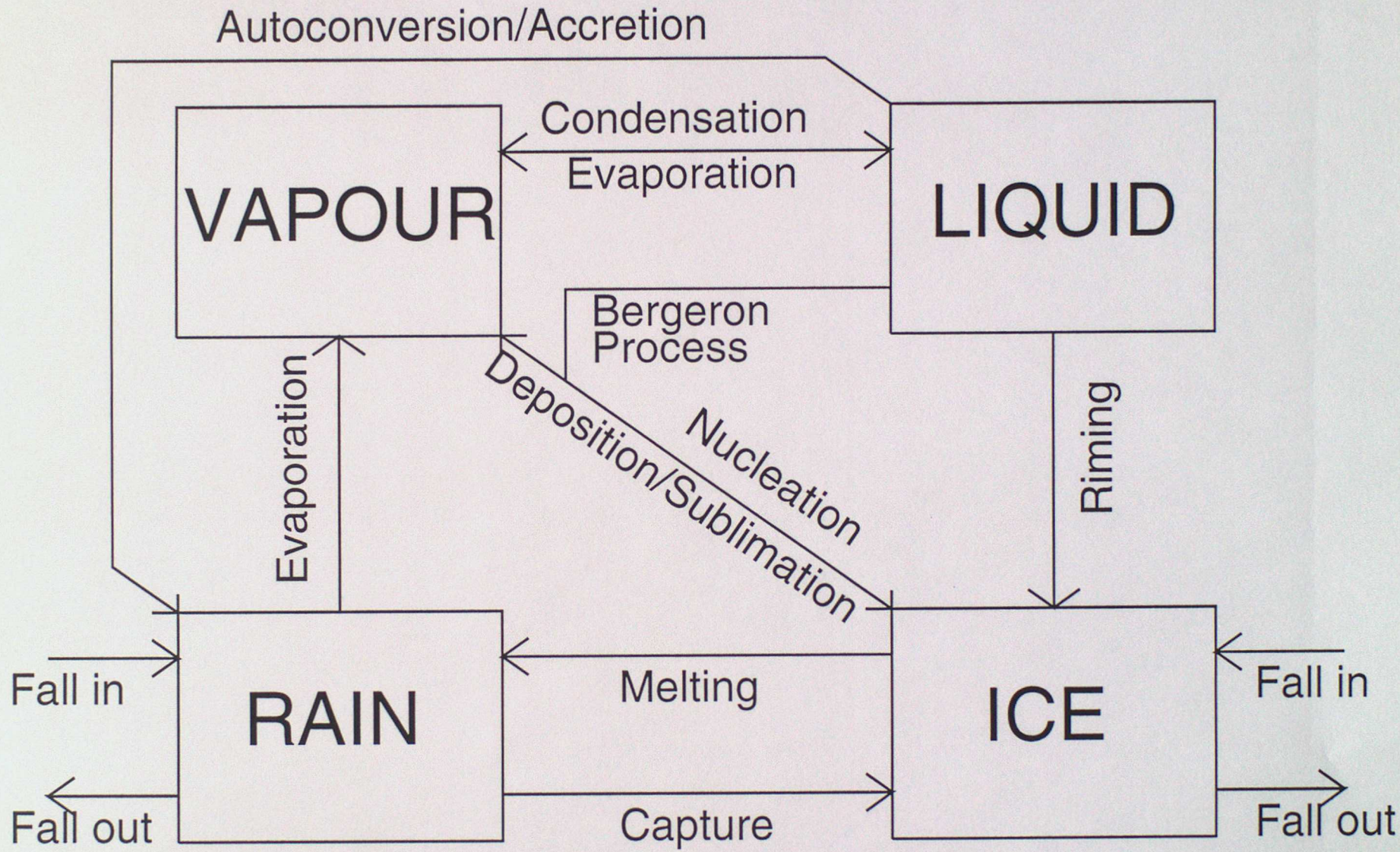

Figure 2.1 Transfer diagram

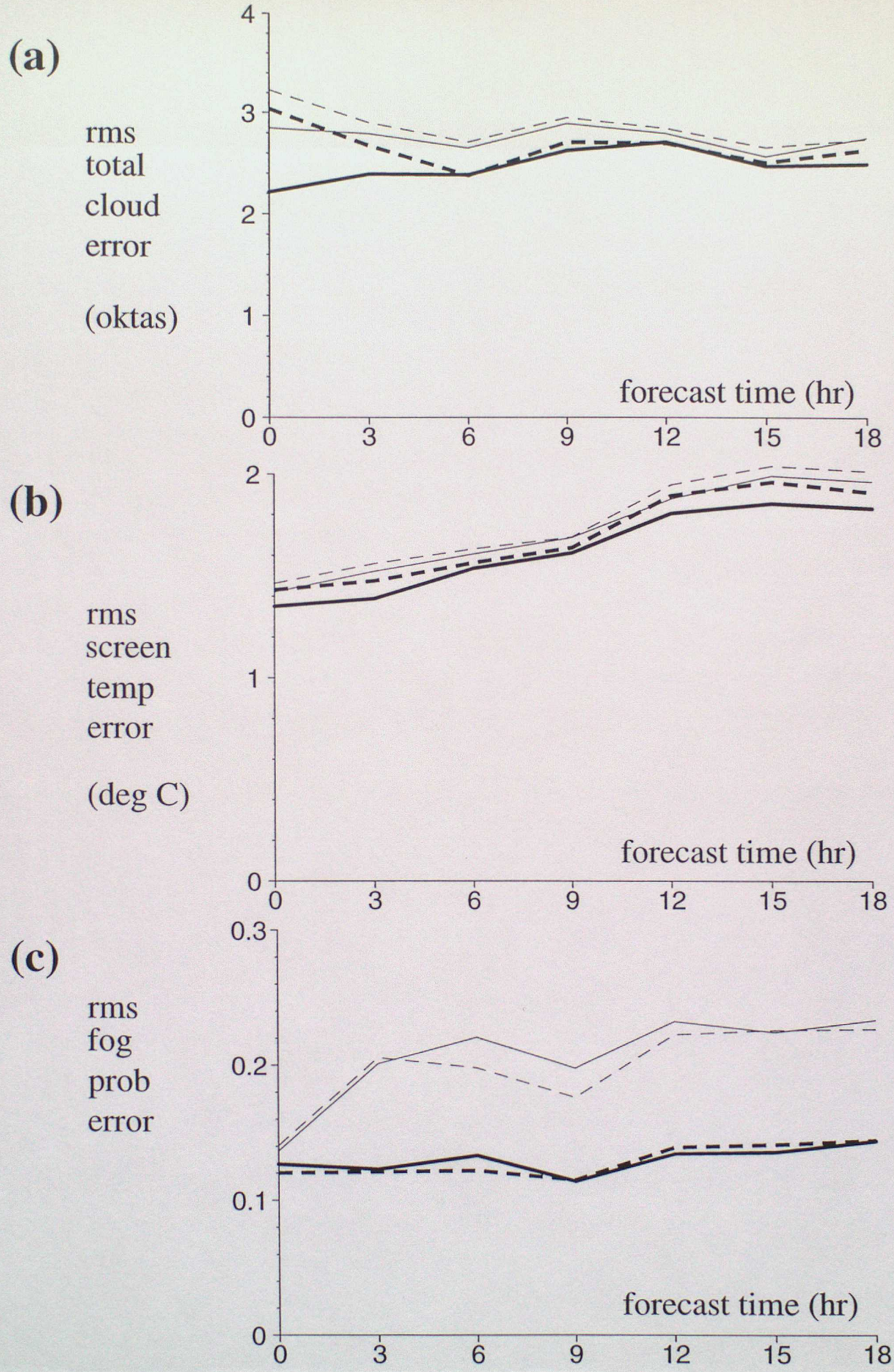

Figure 2.3.1: Verification results for assimilation tests with new microphysics (bold lines) and old microphysics (normal lines). Full lines are for runs assimilating cloud data. Dashed lines are for runs with NO cloud data assimilated.. Rms errors are averaged over 5 cases and a UK station list for (a) total cloud cover (b) screen temperature (c) fog probability

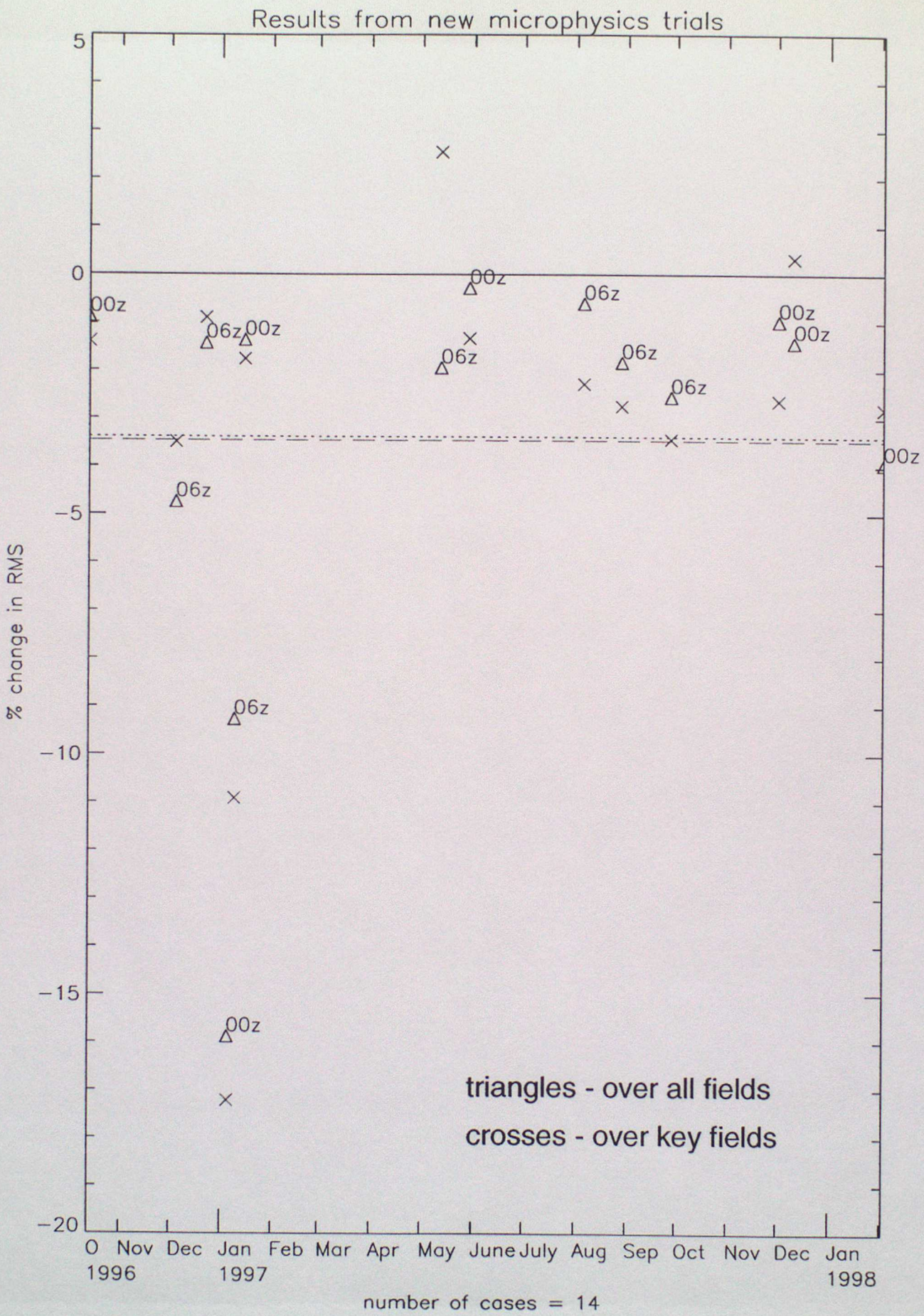

Fig. 3.2.1 % change in average rmse for each case

Fig. 3.2.2(a)

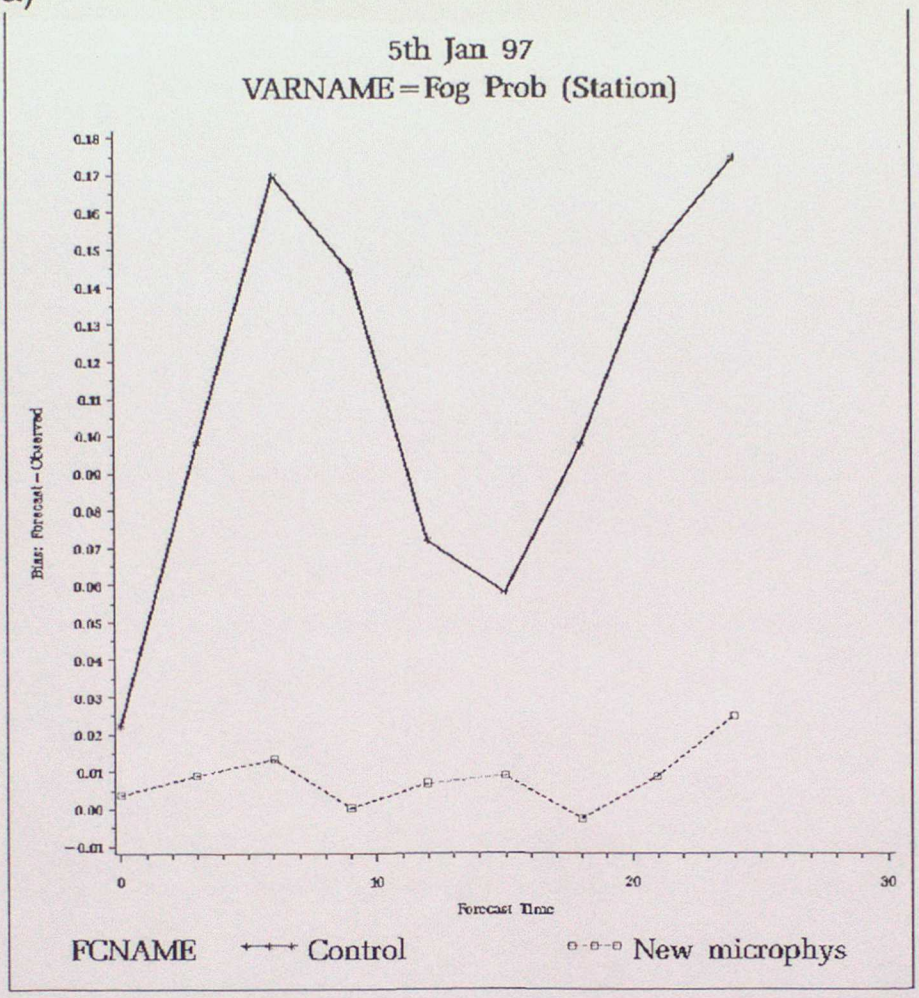

Fig. 3.2.2(b)

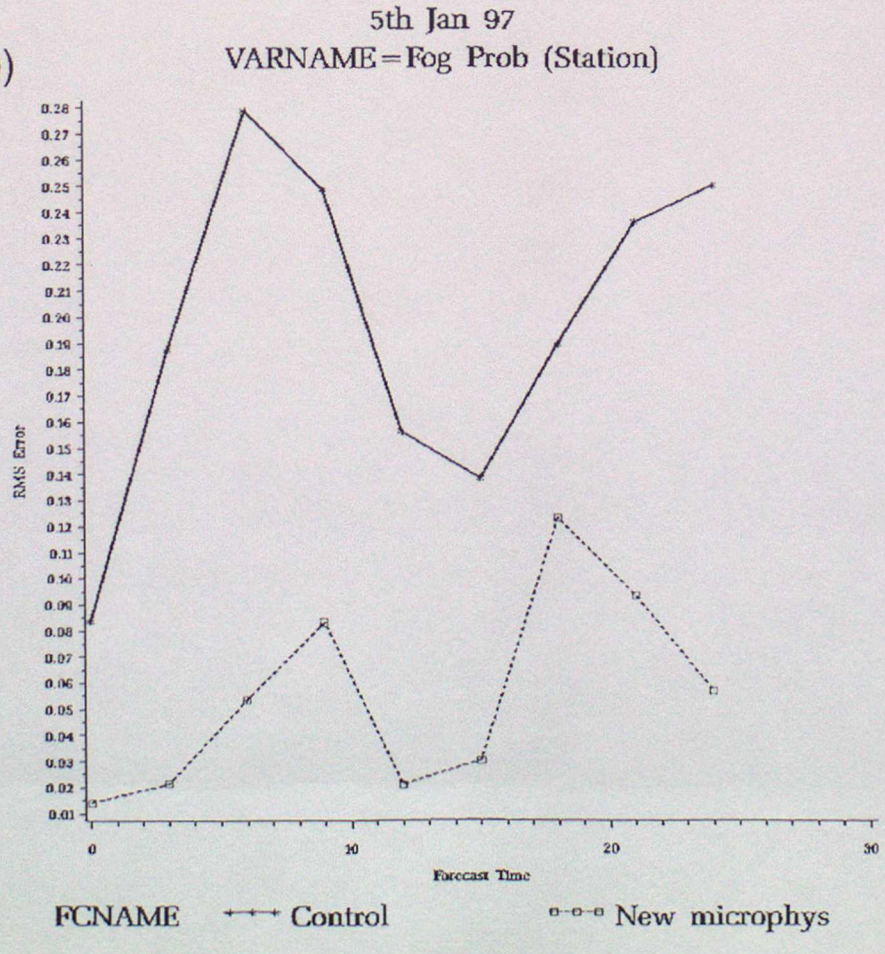

Fig. 3.2.2(c)

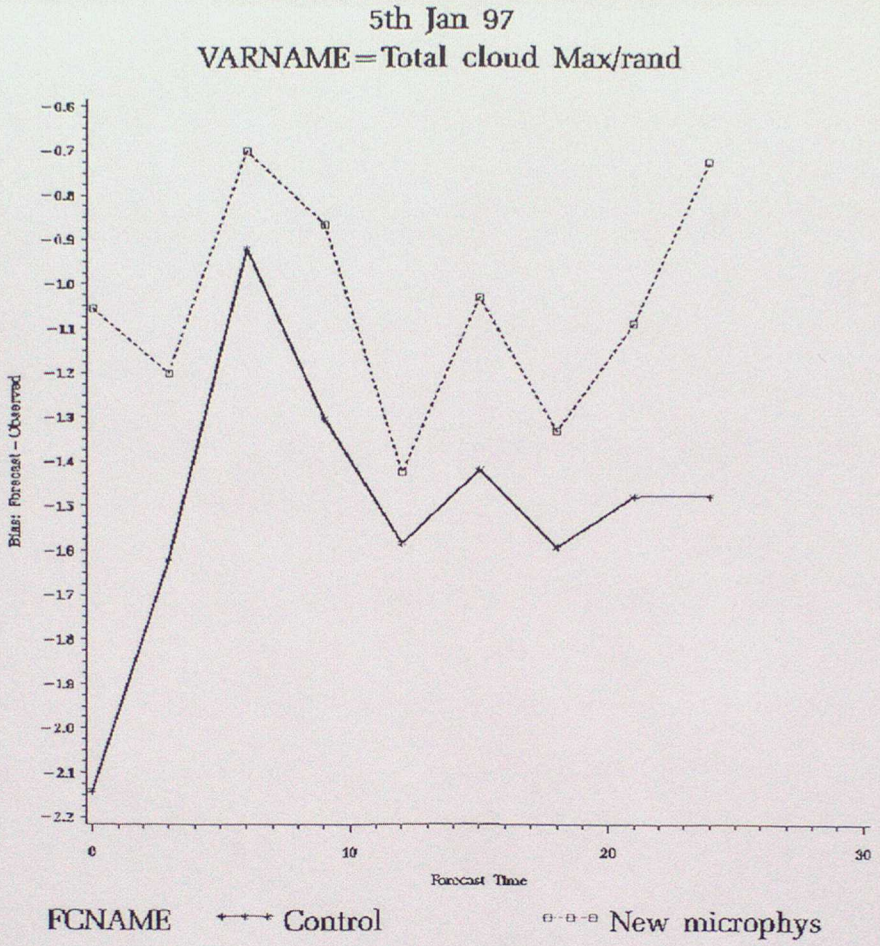

Fig. 3.2.2(d)

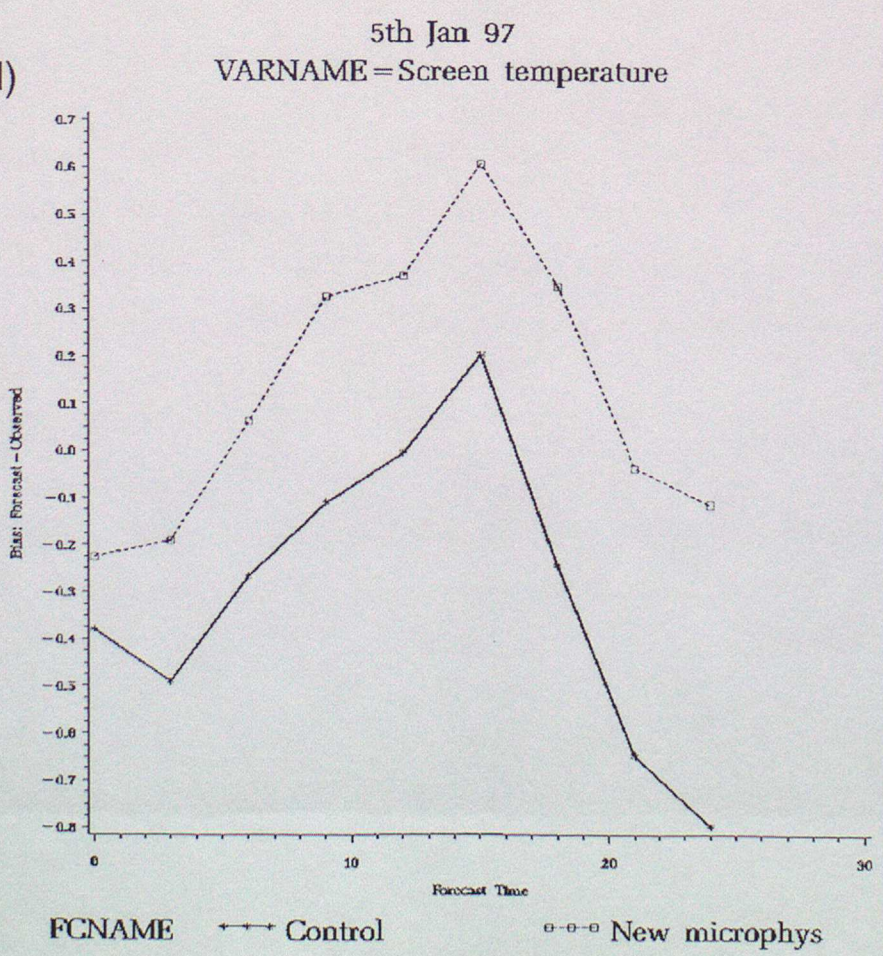

Fig. 3.2.2(e)

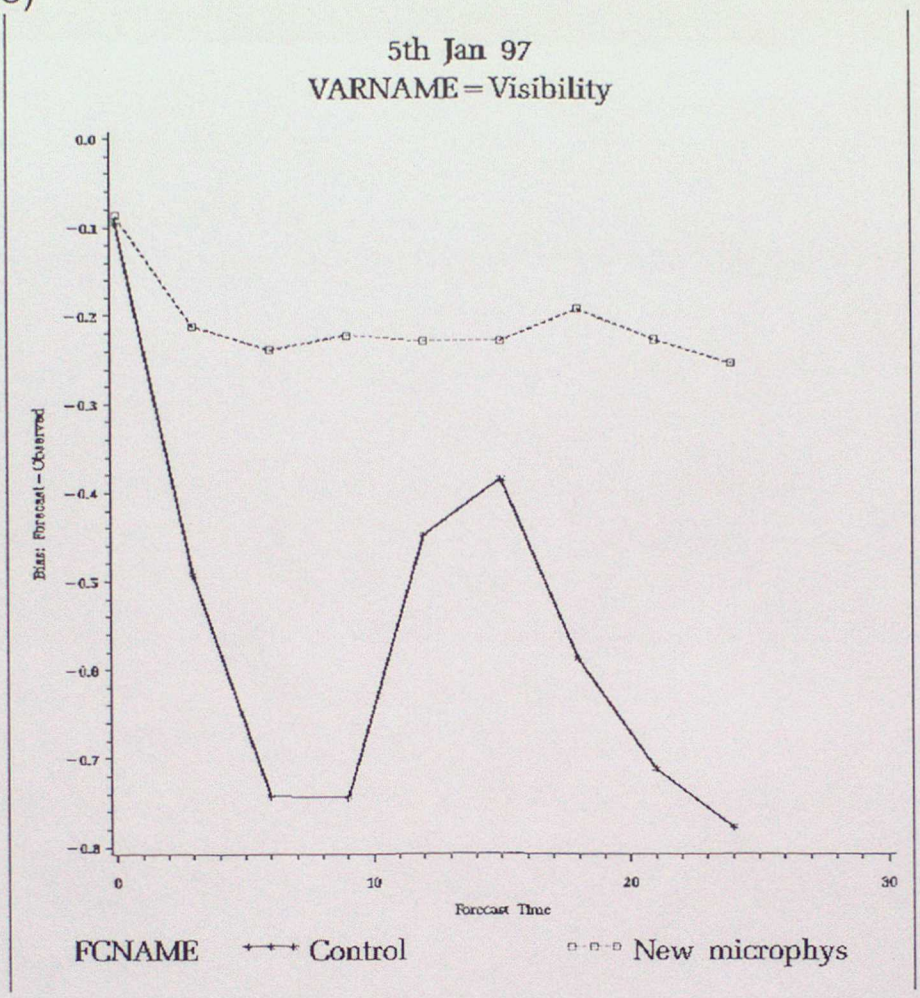

Fig. 3.2.2(f)

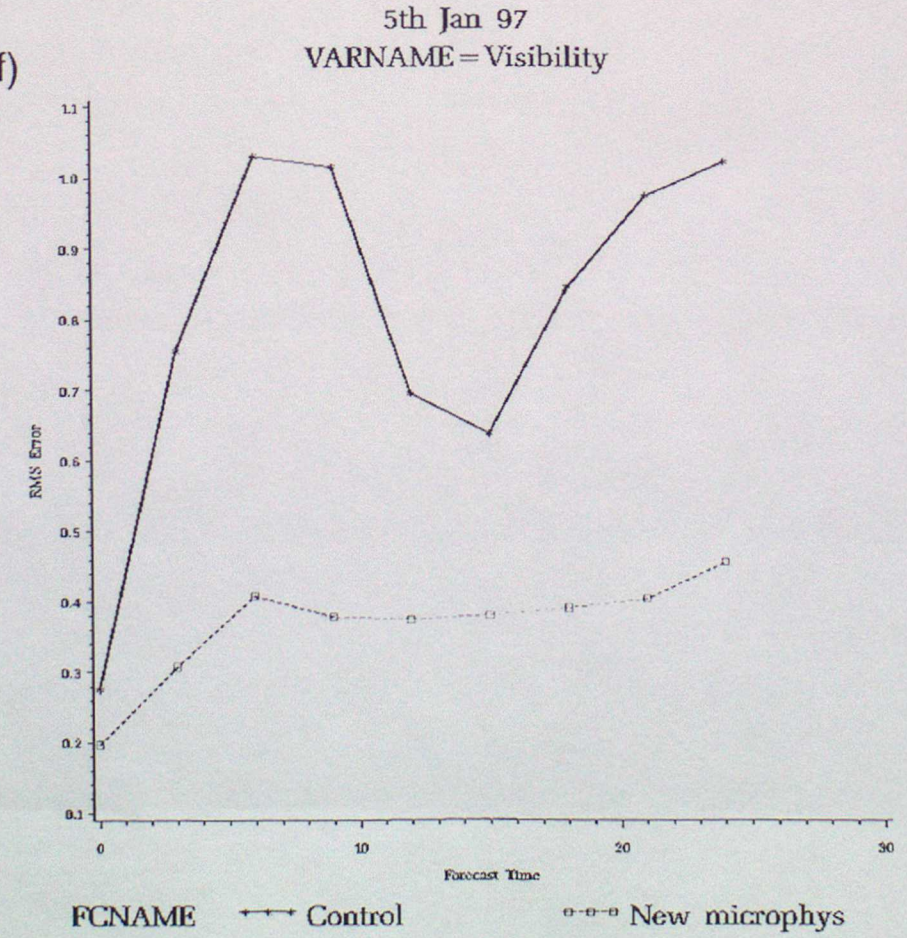

Fig. 3.2.3(a)

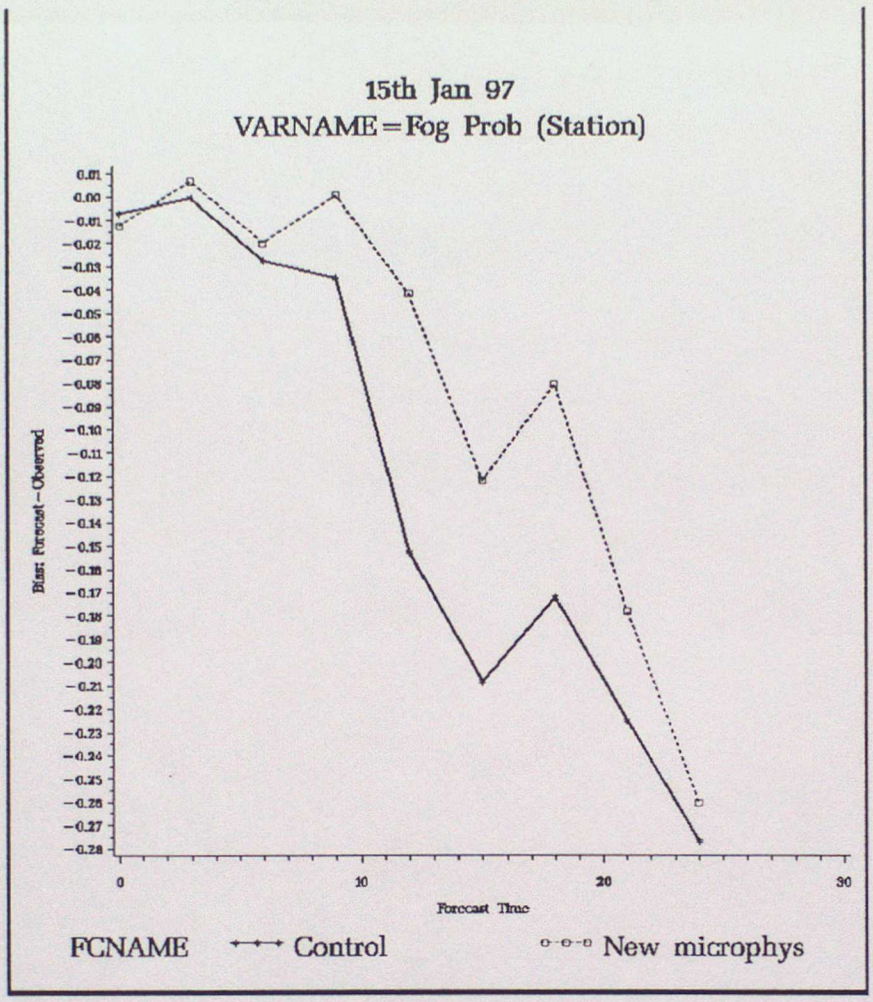

Fig. 3.2.3(b)

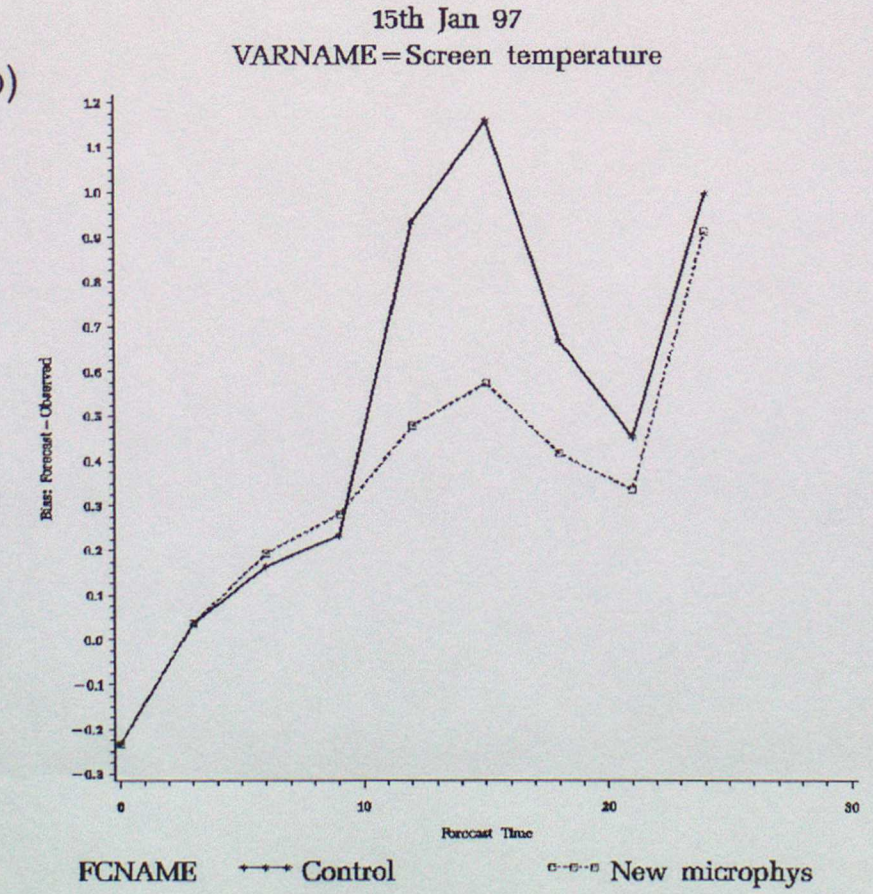

Fig. 3.2.4(a)

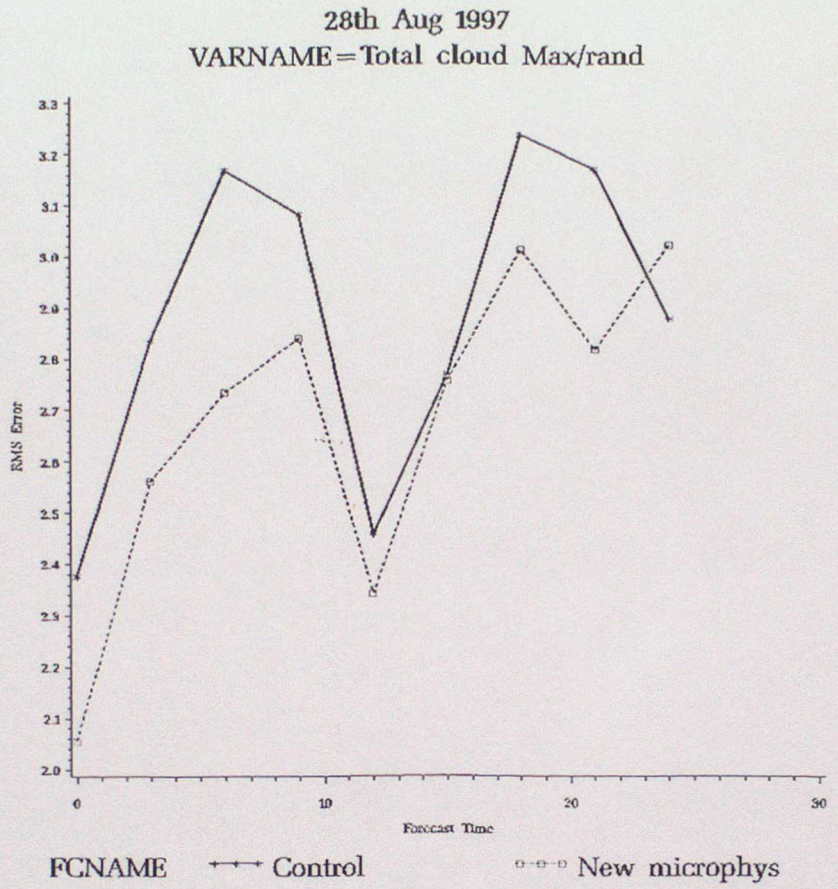

Fig. 3.2.4(b)

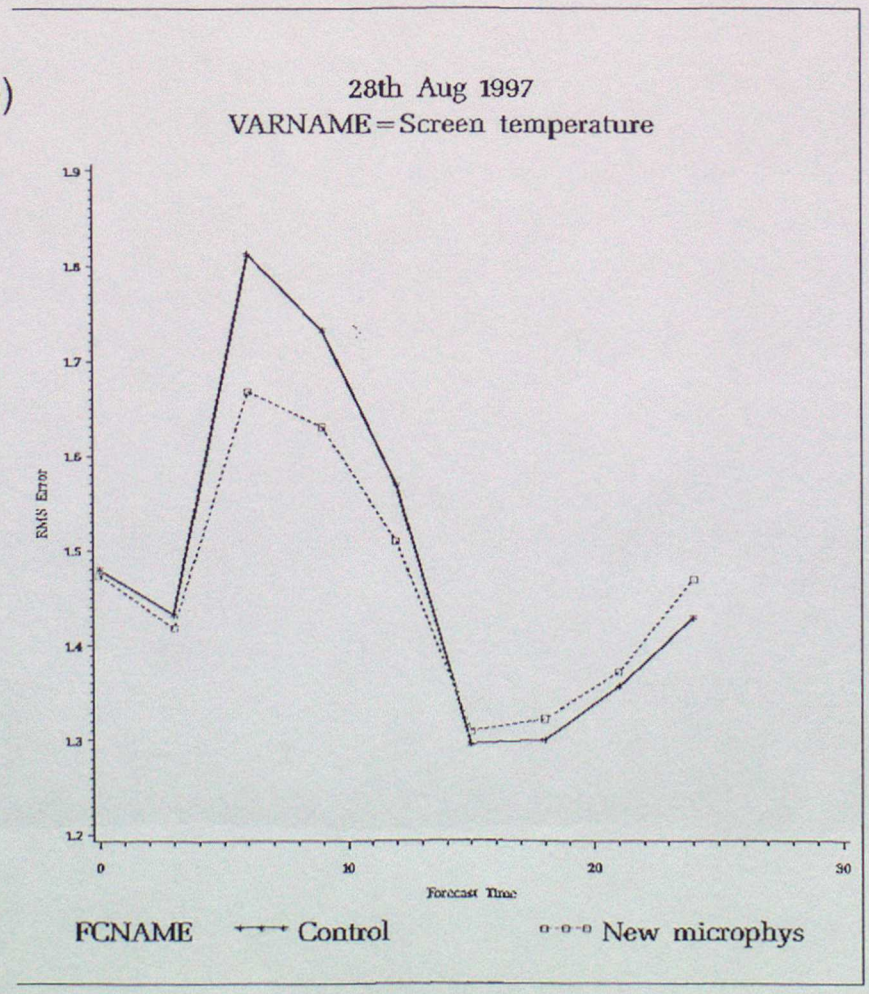

Fig. 3.2.5(a)

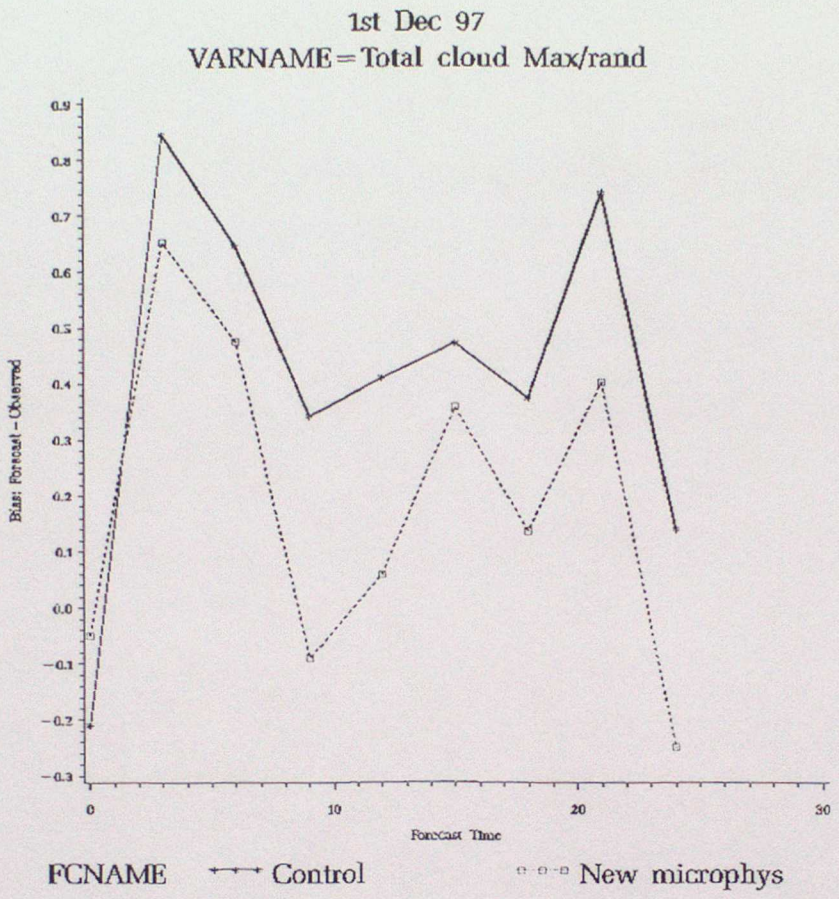

Fig. 3.2.5(b)

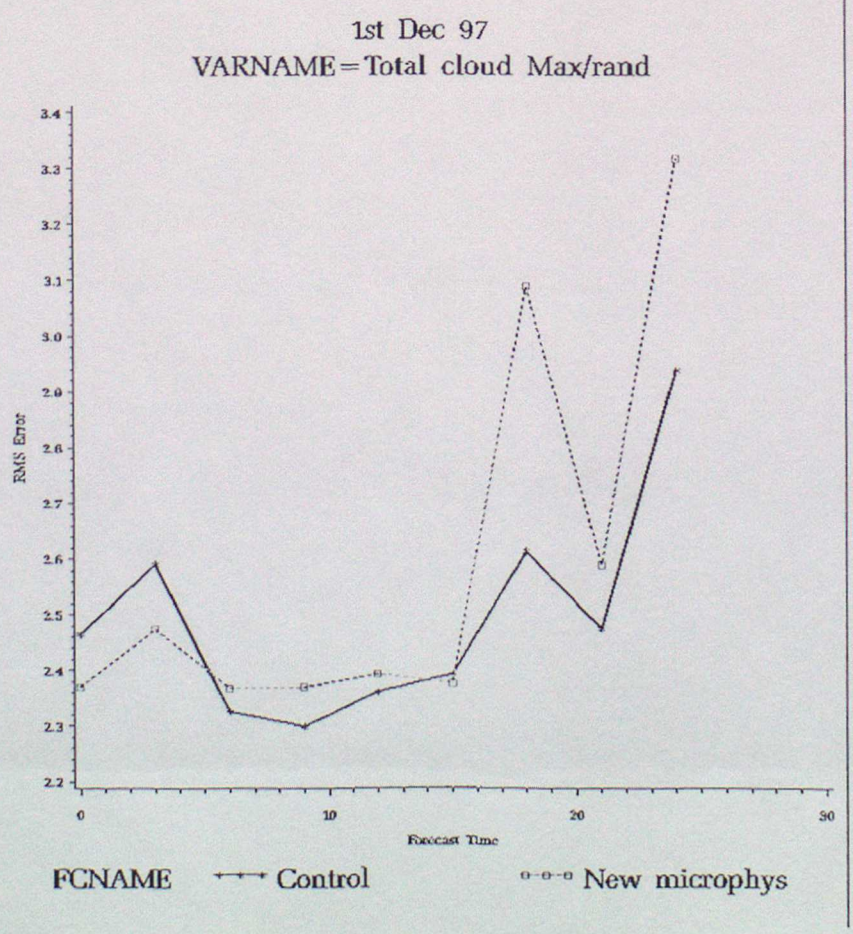

Fig. 3.2.6(a)

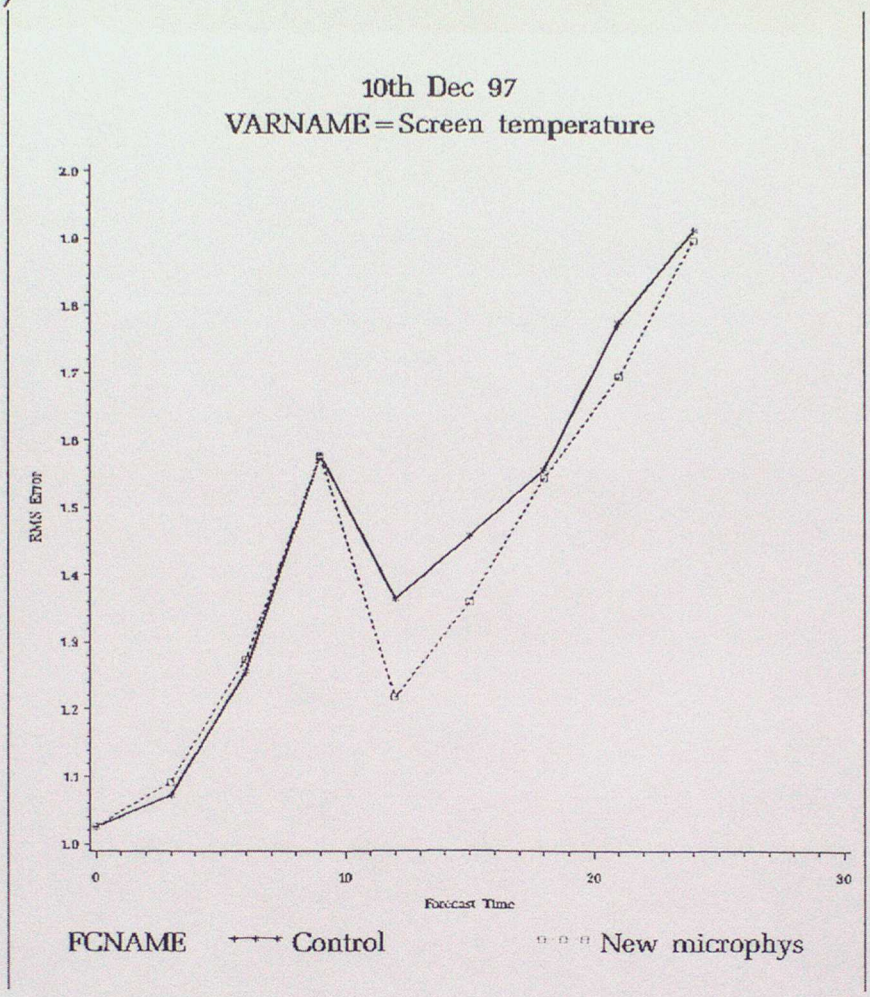

Fig. 3.2.6(b)

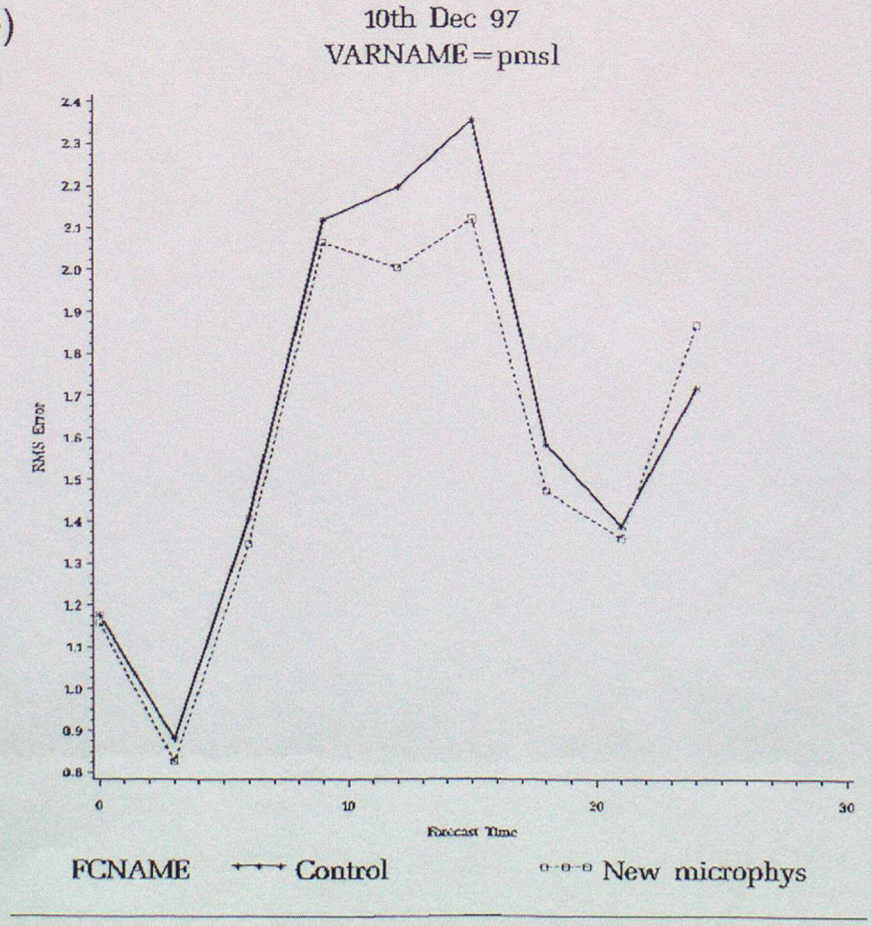

Results from new microphysics trials
% change in RMS
0
−5
−10
−15
−20
−25
Screen temperature
Visibility
1.5m RH
10m u−wind
10m v−wind
Fog Prob (Station)
Stratus Prob (Station)
Mist Prob (Station)
10 m wind speed
10 m wind direction
10 m Vector wind
PMSL
TD
Total cloud
Total cloud Max/rand
number of cases = 14

Fig. 3.2.7

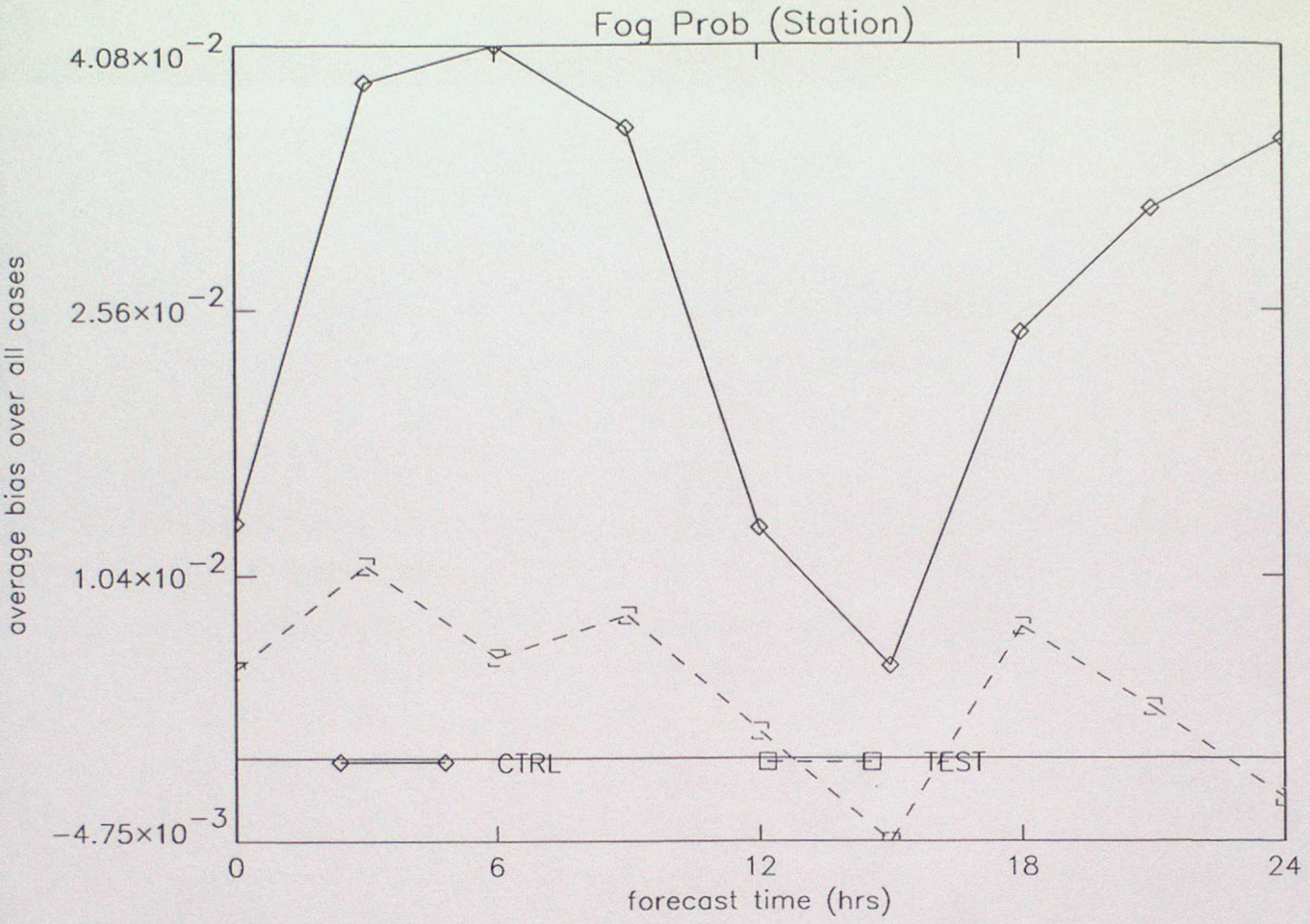
Fog Prob (Station)
4.08×10^-2
2.56×10^-2
1.04×10^-2
-4.75×10^-3
average bias over all cases
CTRL
TEST
0
6
12
18
24
forecast time (hrs)

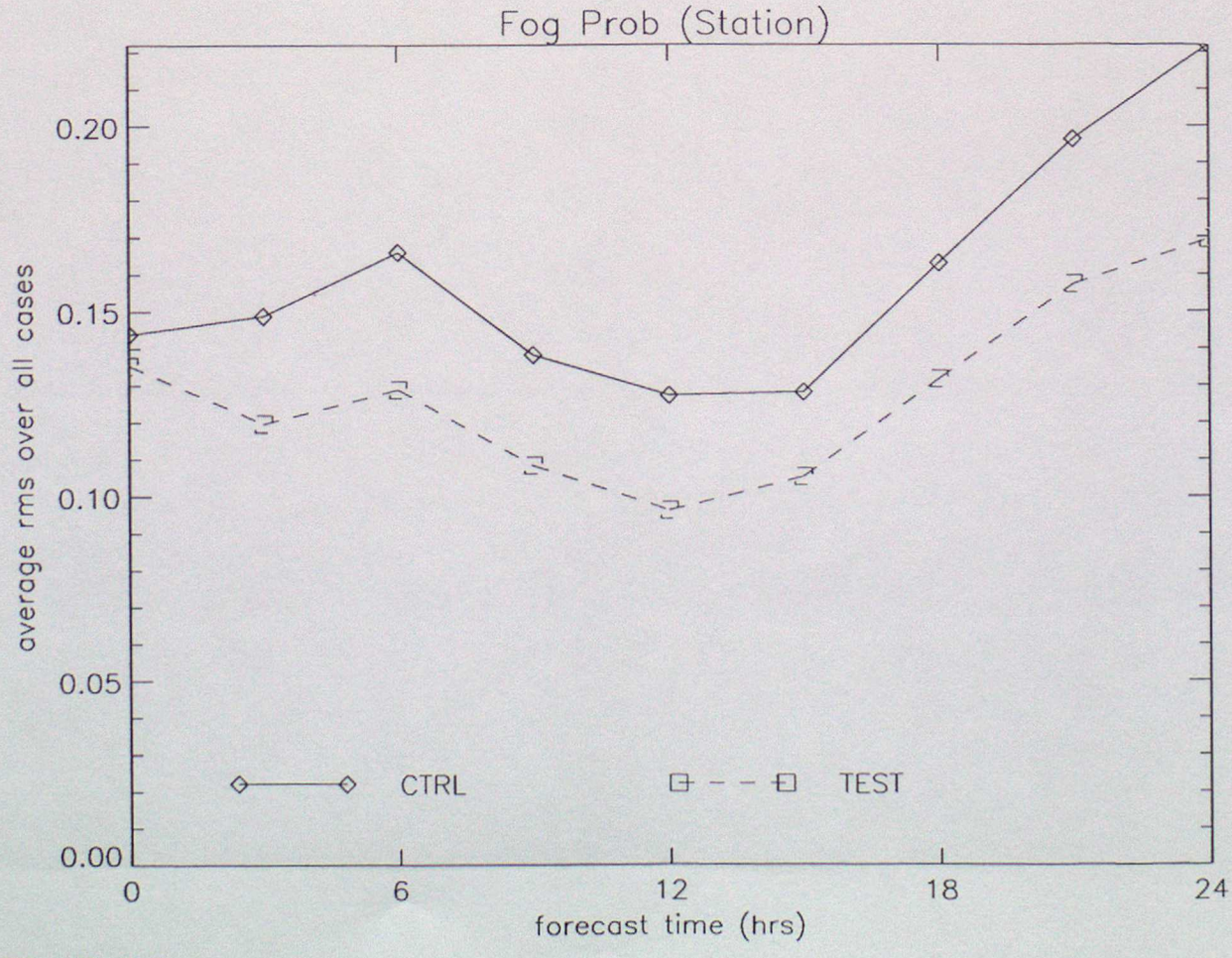
Fog Prob (Station)
0.20
0.15
0.10
0.05
0.00
average rms over all cases
CTRL
TEST
0
6
12
18
24
forecast time (hrs)

Fig. 3.2.8

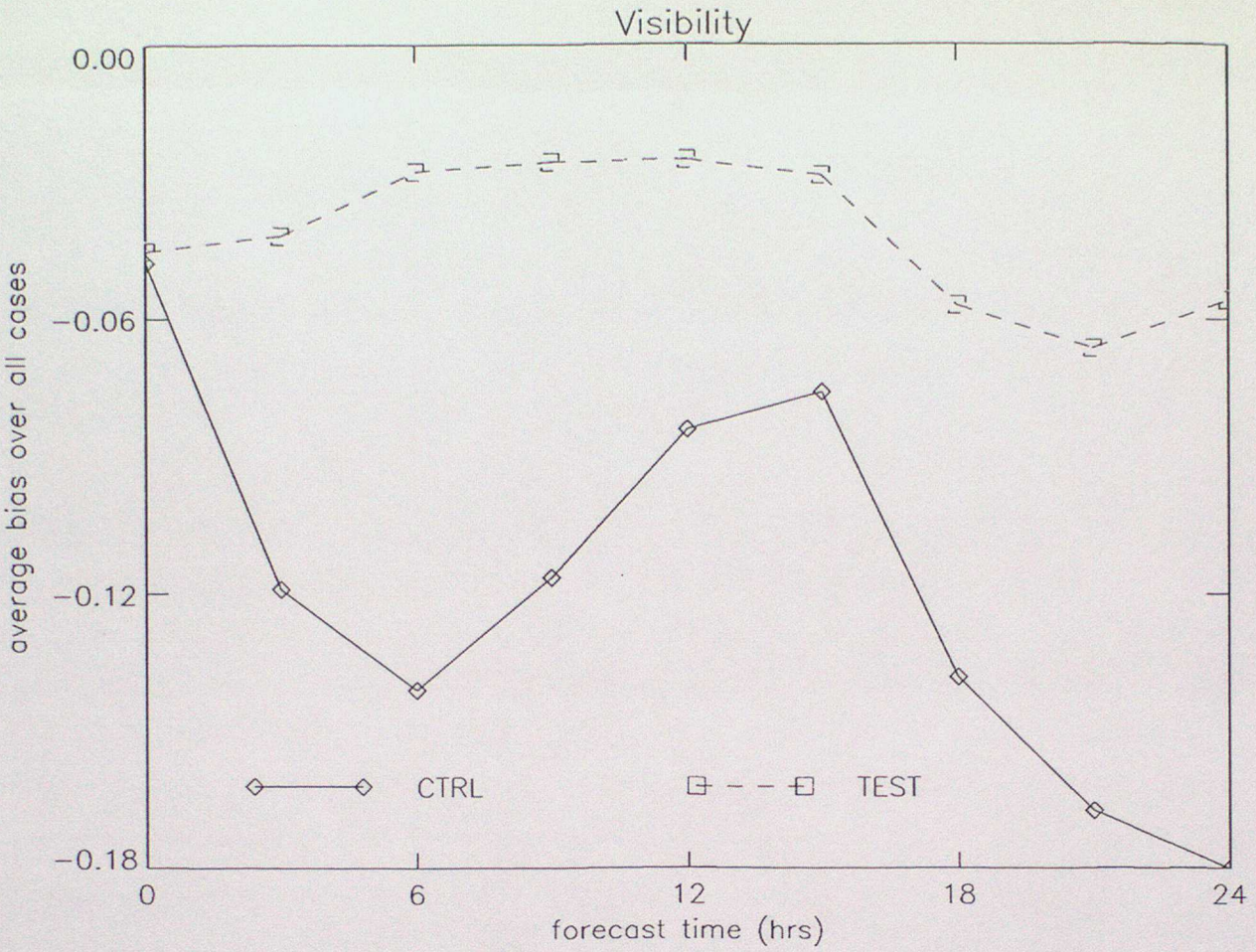
Visibility
0.00
−0.06
−0.12
−0.18
average bias over all cases
CTRL
TEST
0
6
12
18
24
forecast time (hrs)

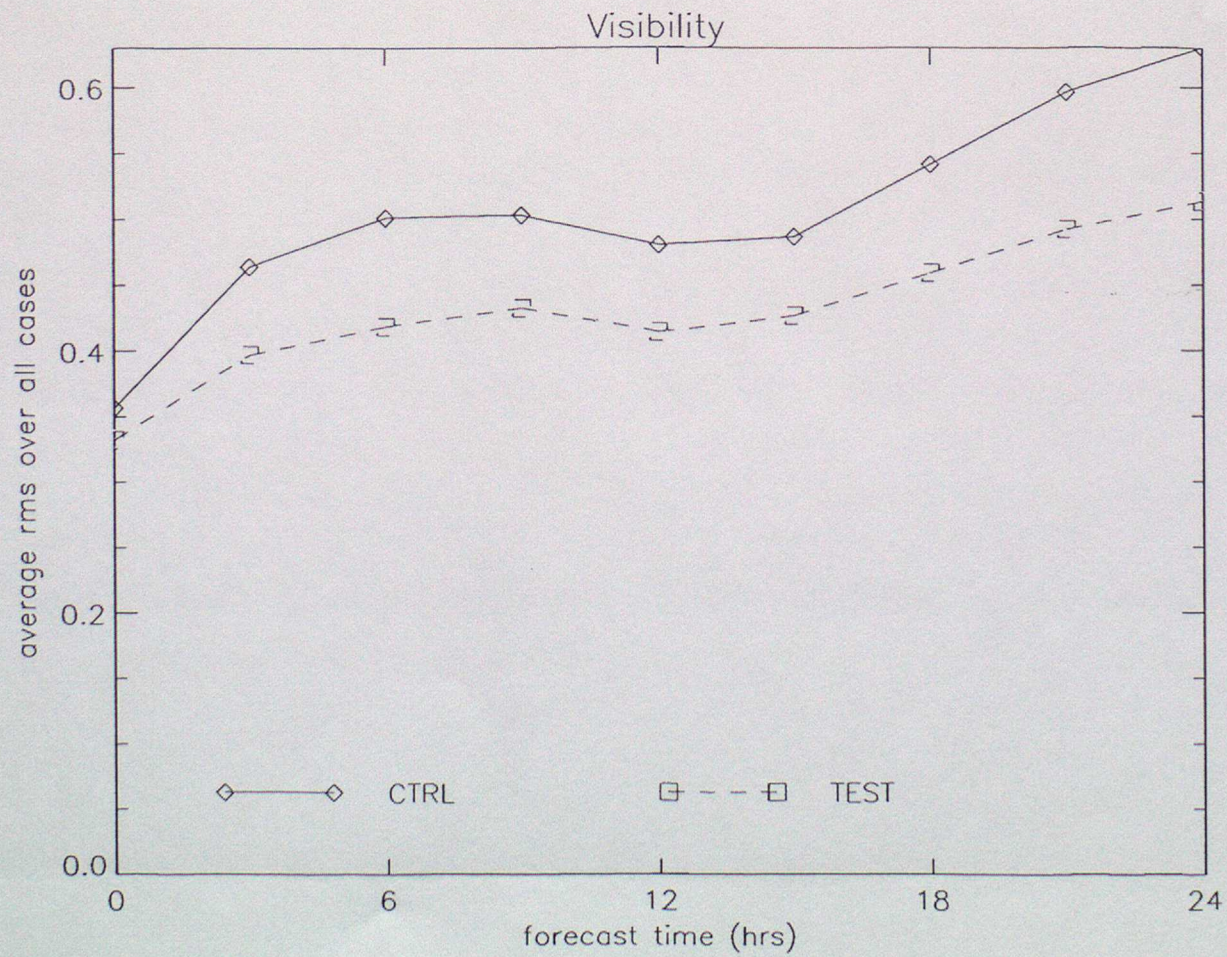
Visibility
0.6
0.4
0.2
0.0
average rms over all cases
CTRL
TEST
0
6
12
18
24
forecast time (hrs)

Fig. 3.2.9

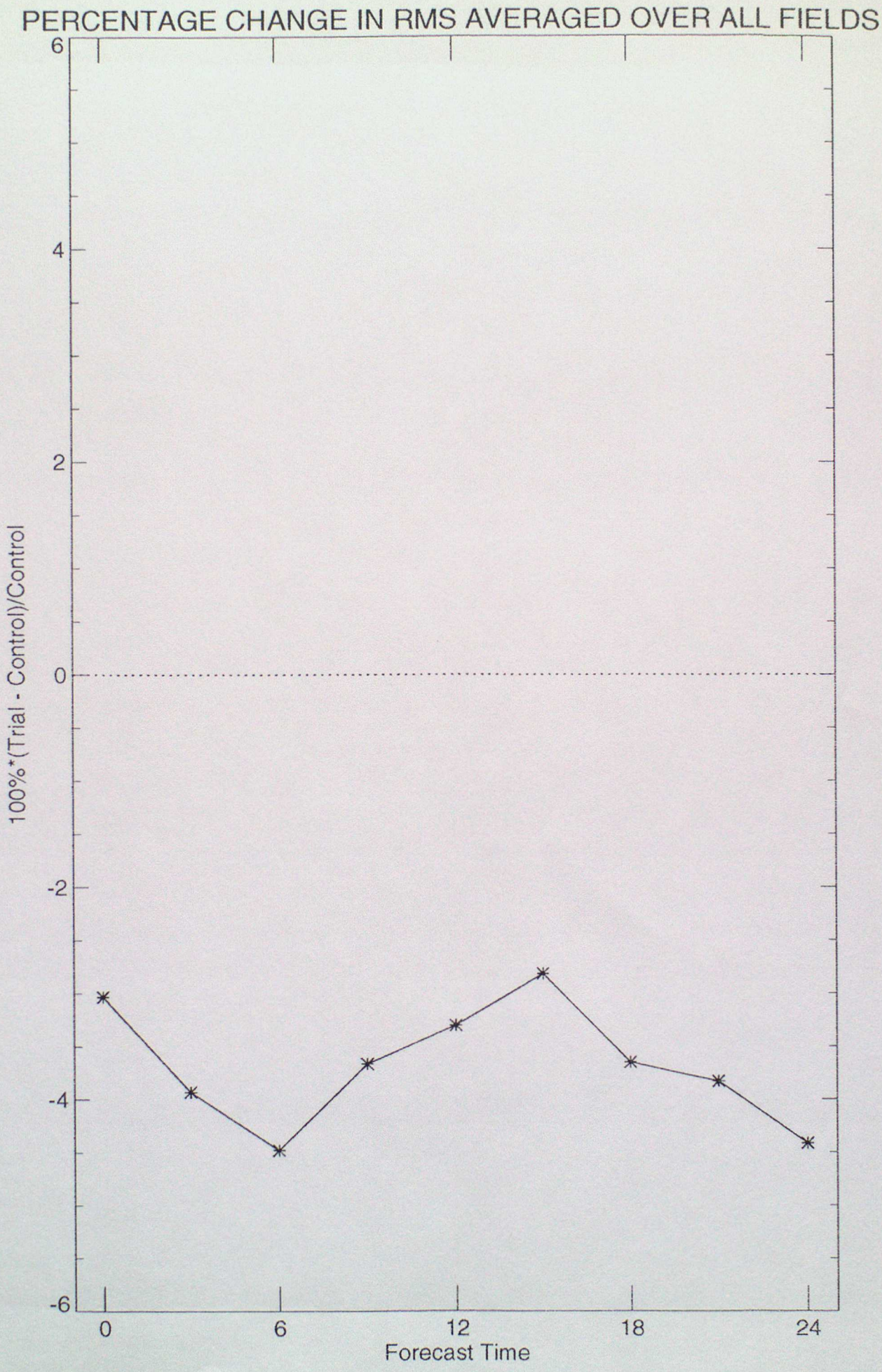
PERCENTAGE CHANGE IN RMS AVERAGED OVER ALL FIELDS
100%*(Trial - Control)/Control
6
4
2
0
-2
-4
-6
0
6
12
18
24
Forecast Time

Fig. 3.2.10

Fig 3.3.1(a)

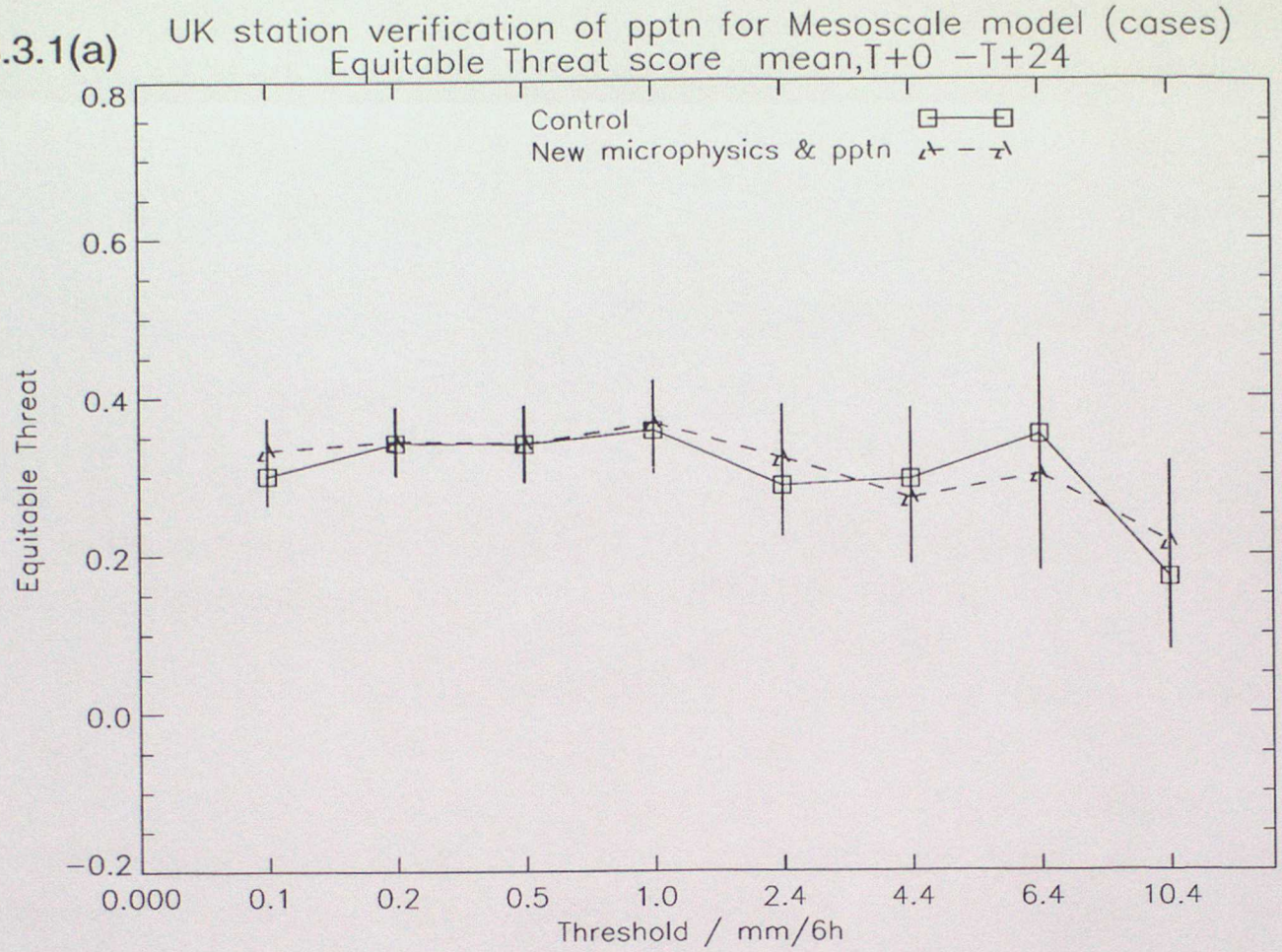

Fig 3.3.1(b)

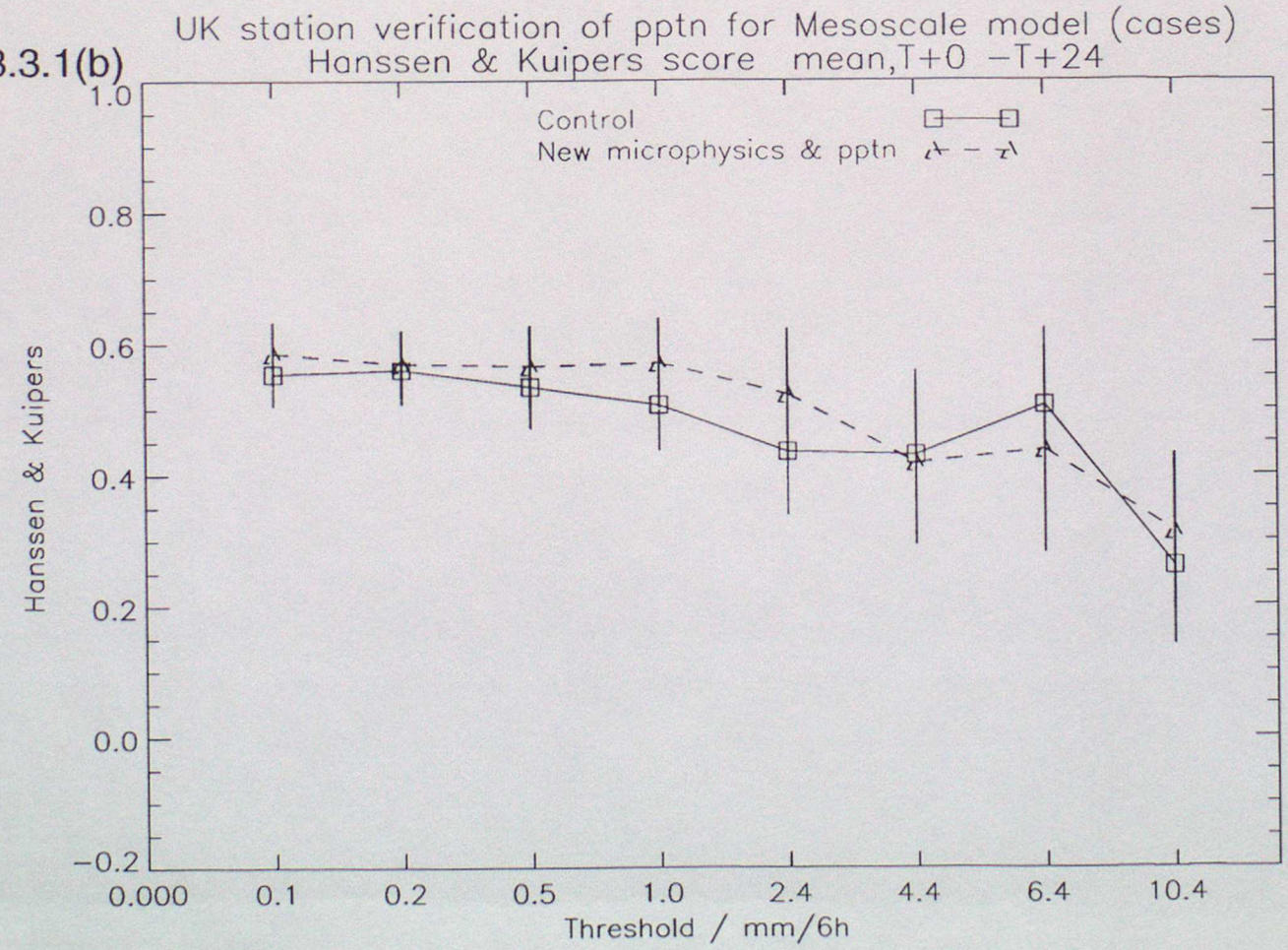

Fig 3.3.2(a)

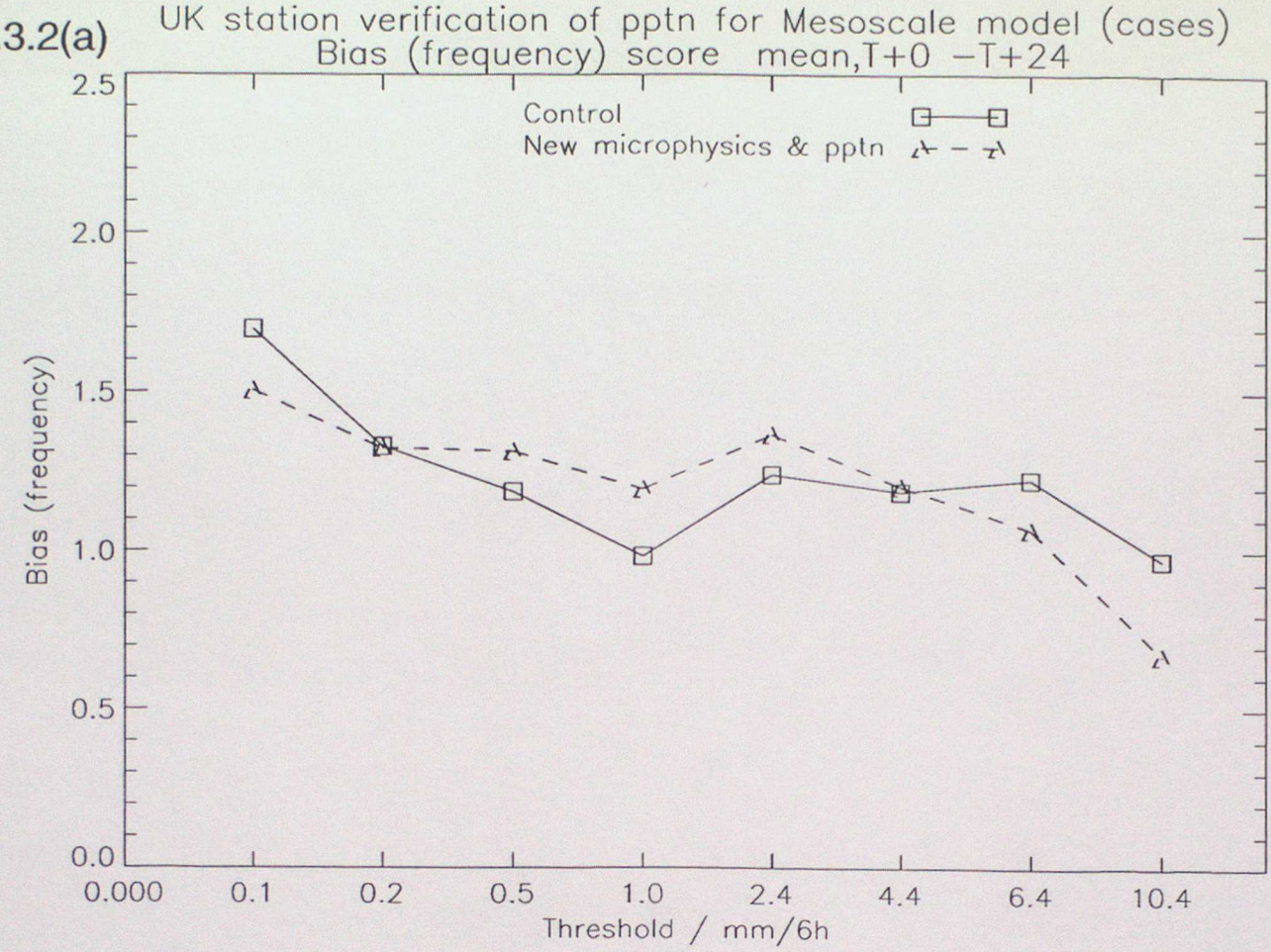

Fig 3.3.2(b)

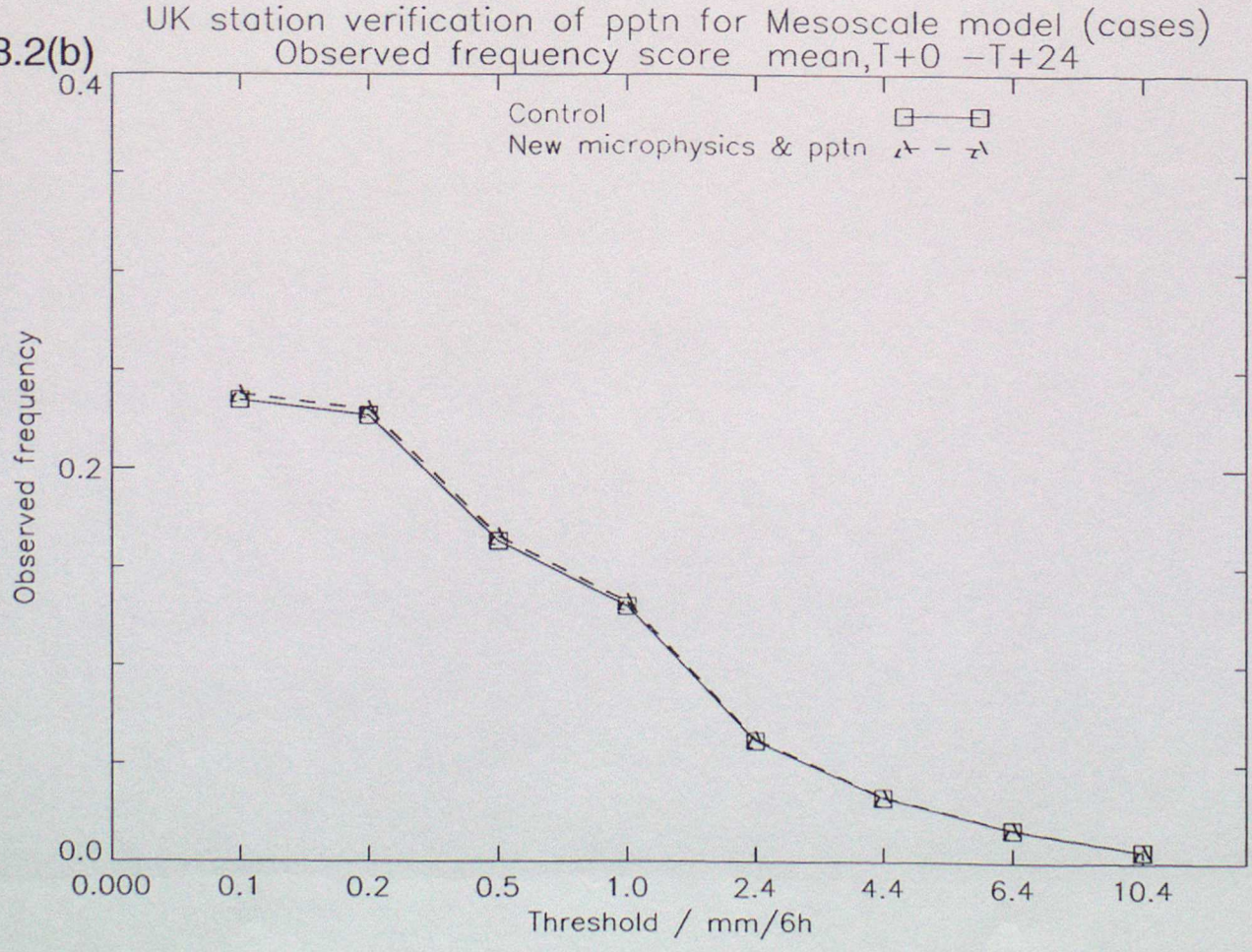

Fig 3.3.3(a)

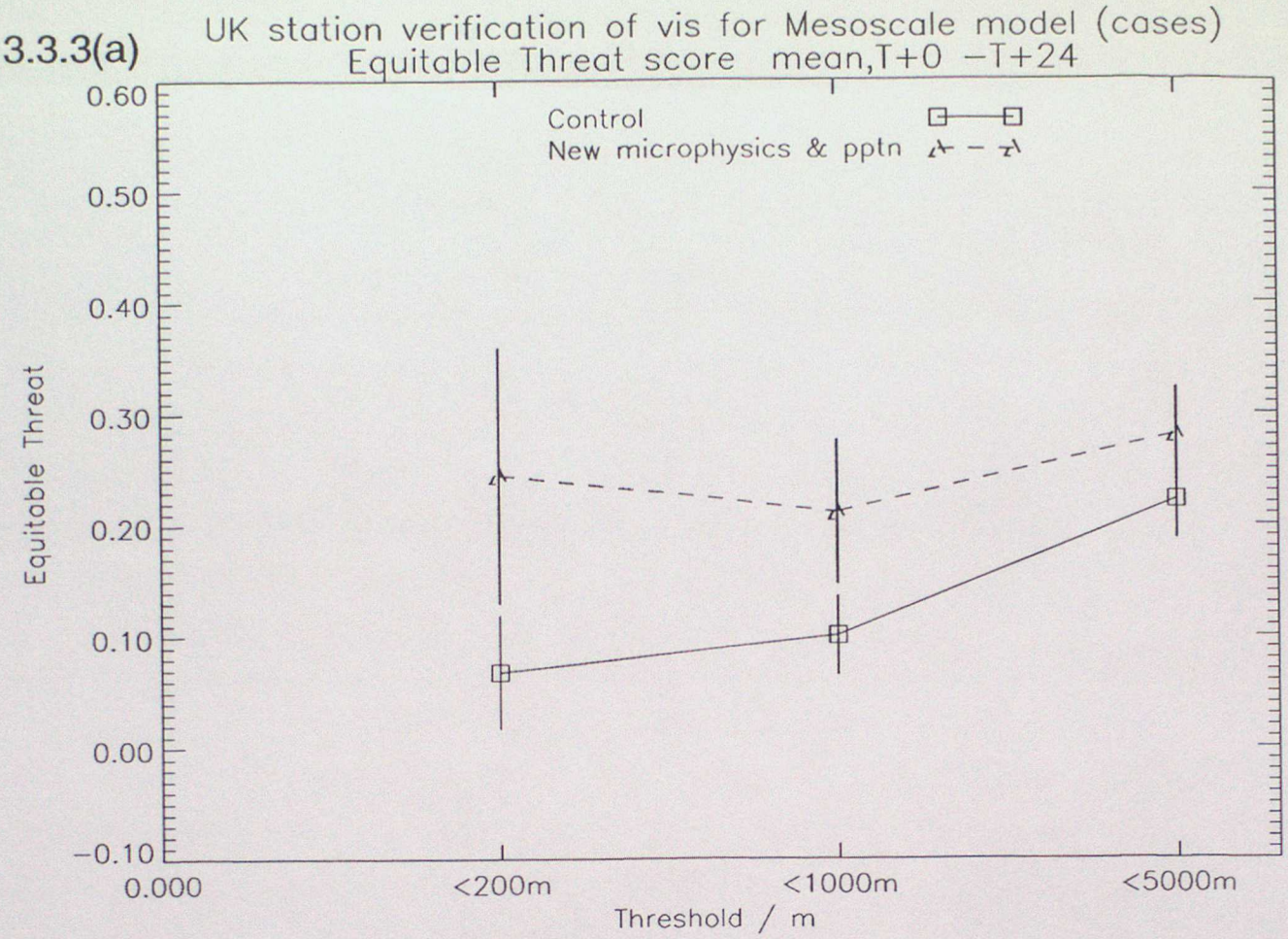

Fig 3.3.3(b)

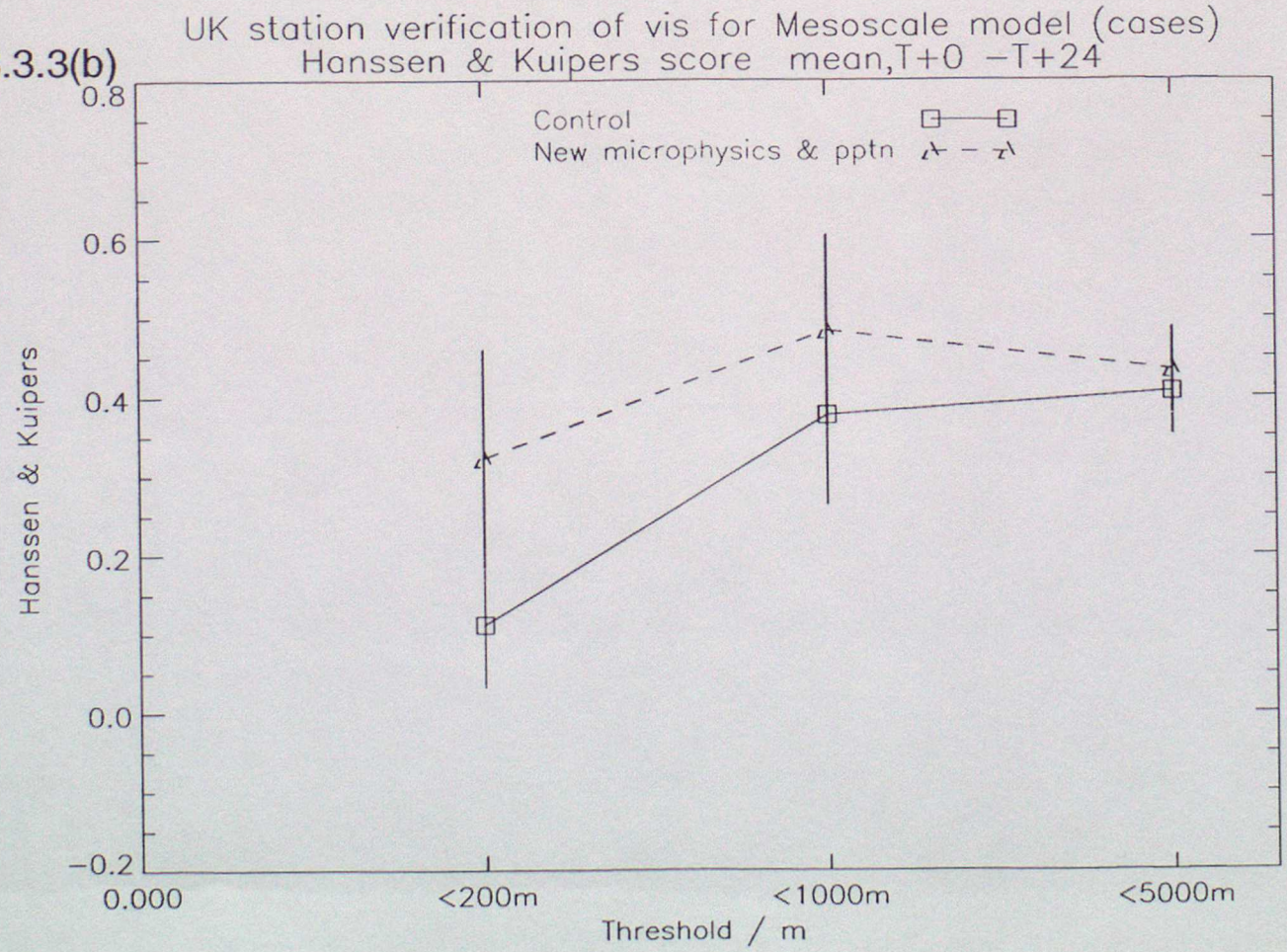

Fig 3.3.4(a)

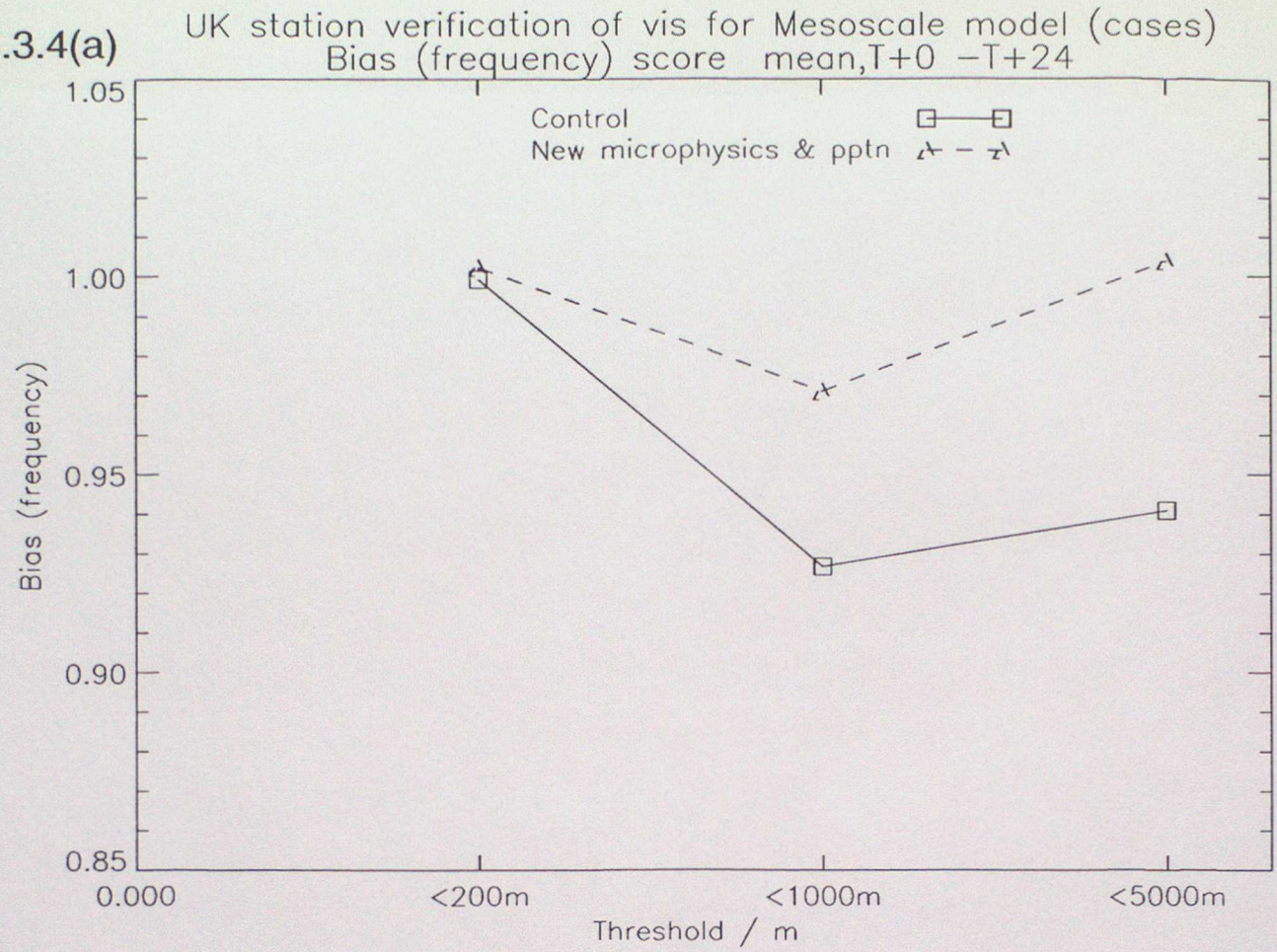

Fig 3.3.4(b)

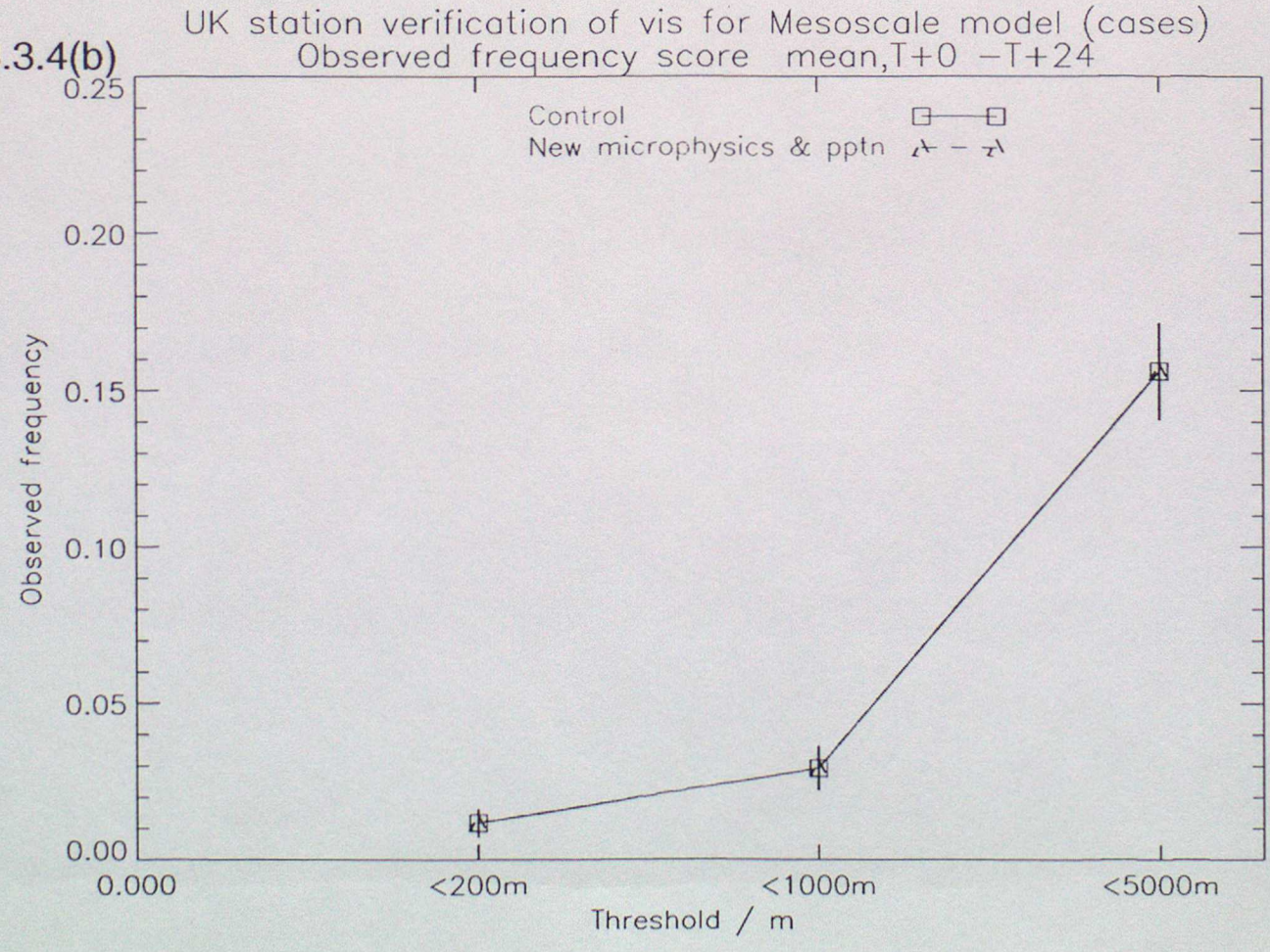

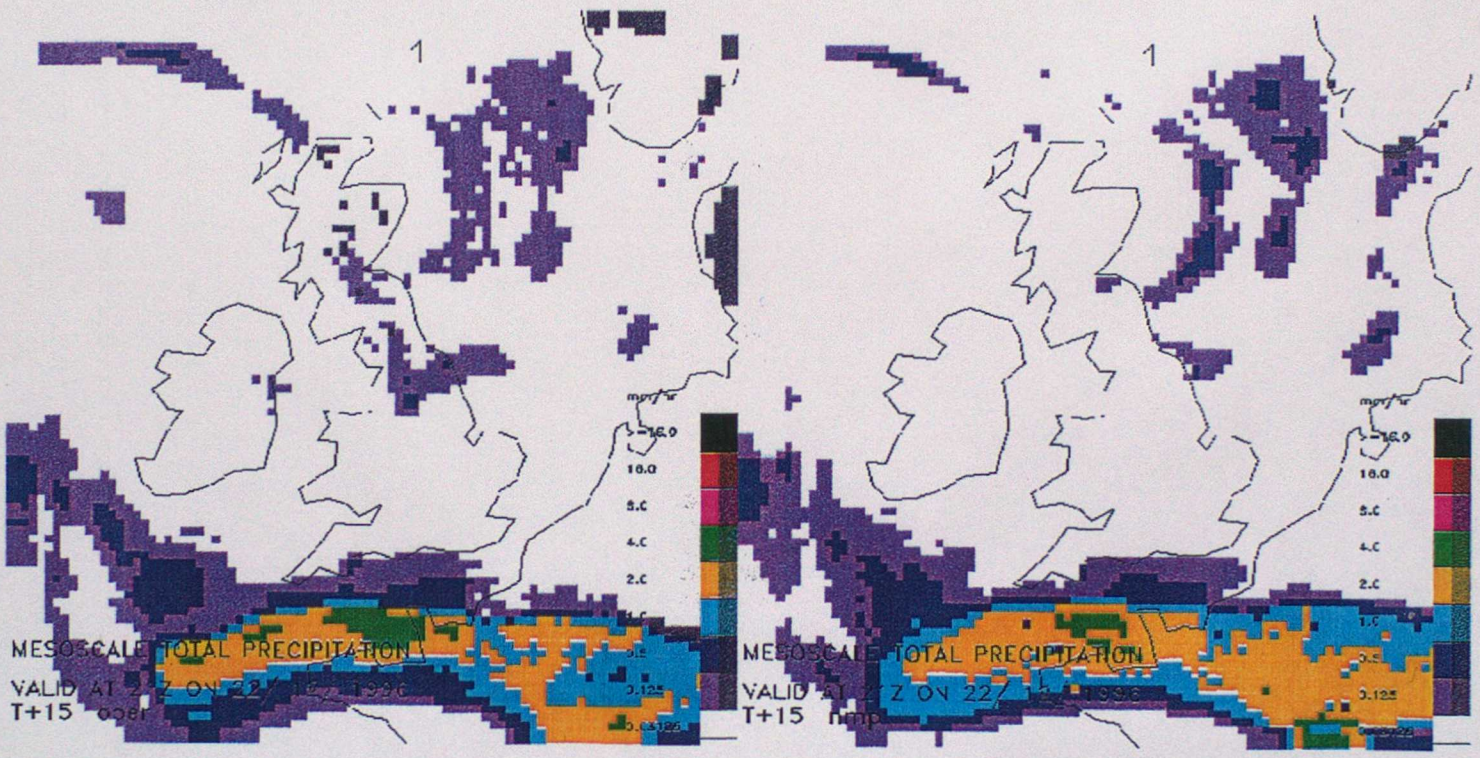

control test

Fig. 3.4.1 December 22nd 1996, 21z, T+6

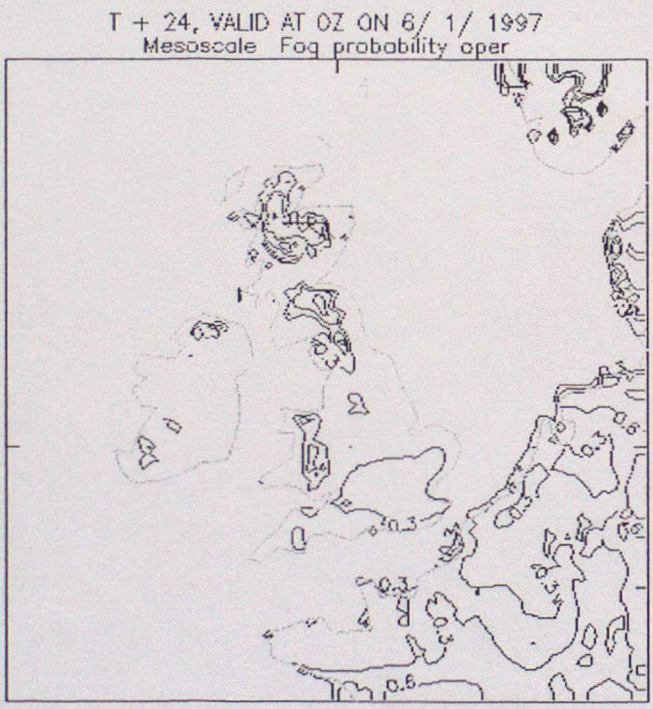

control

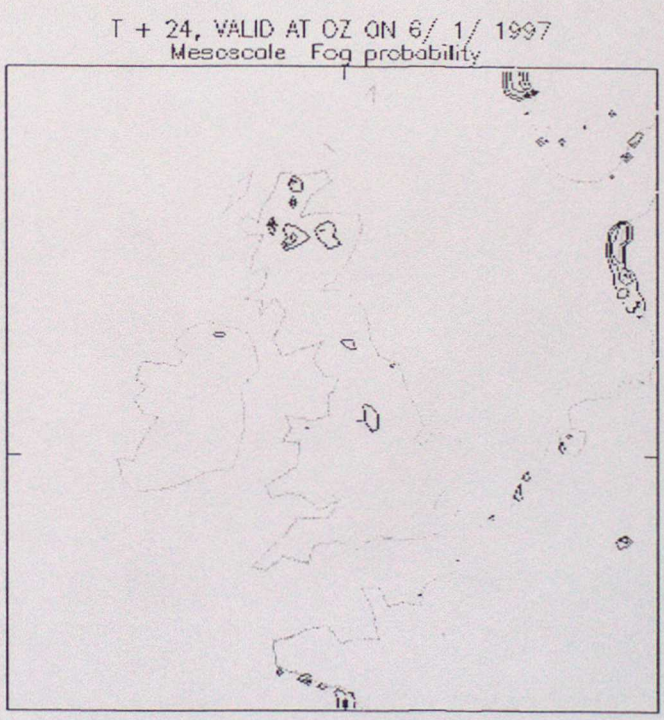

test

Fig. 3.4.2

Fig. 3.4.3 January 6th 1997, 0z, T+24

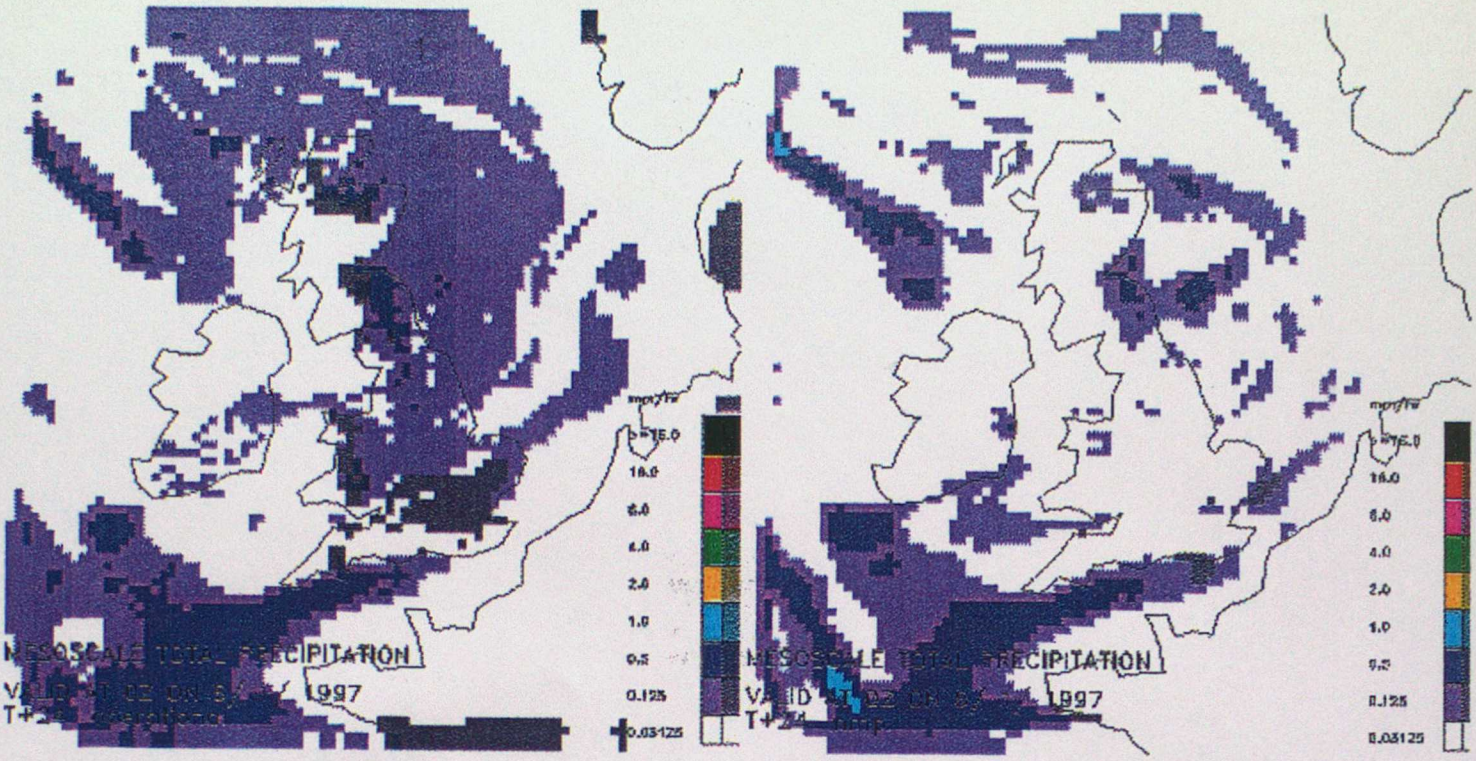

control test

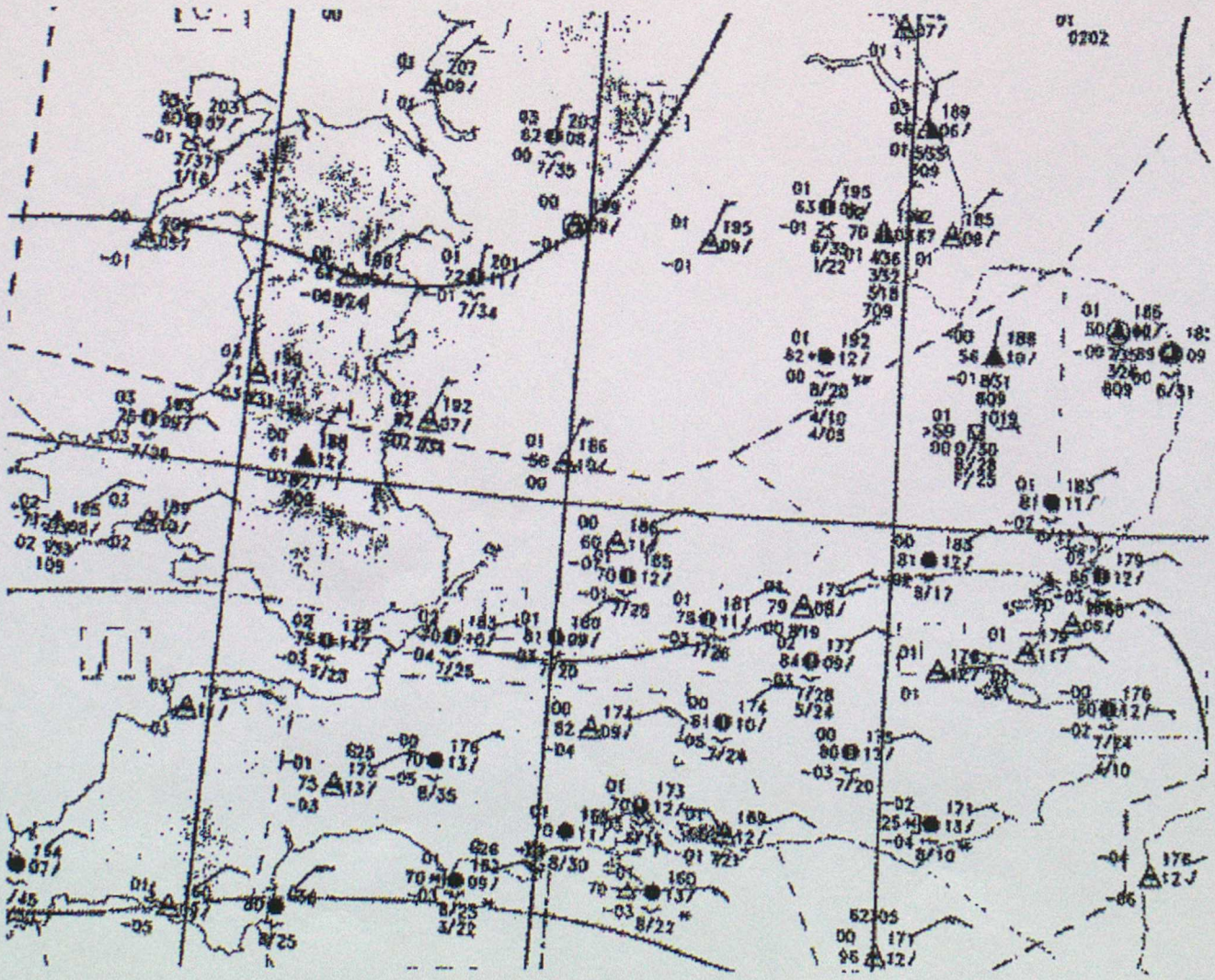

control

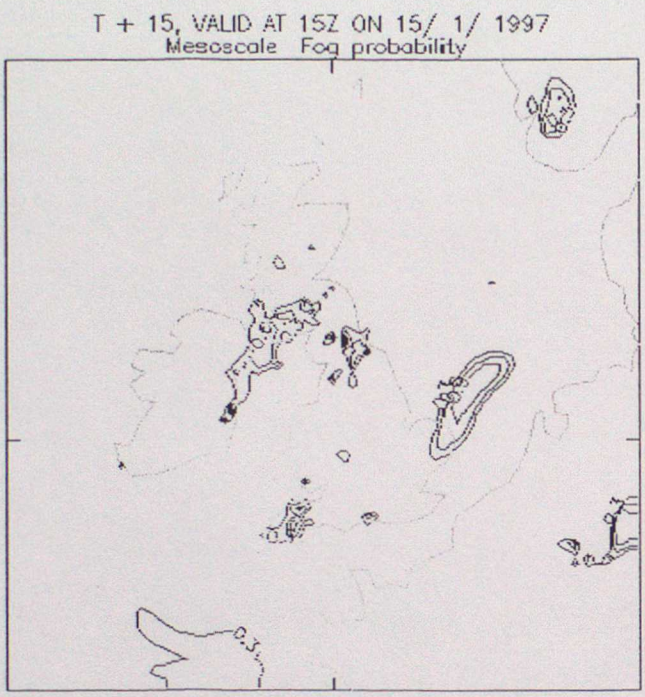

test

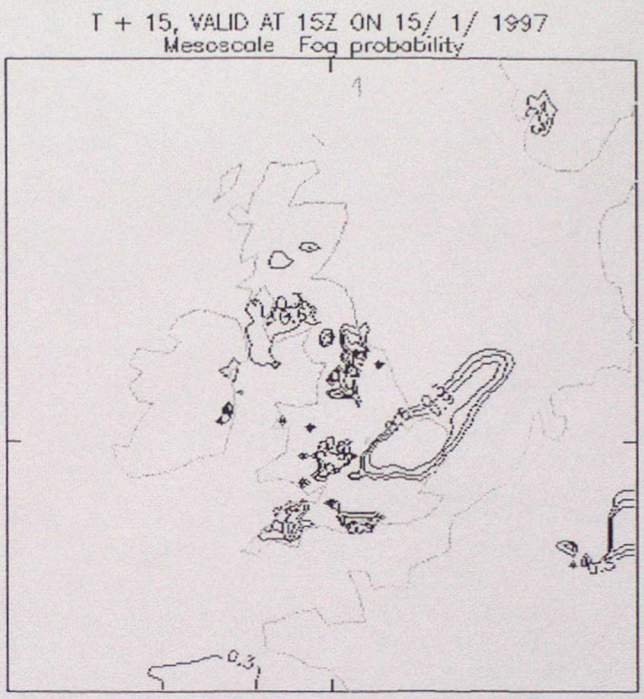

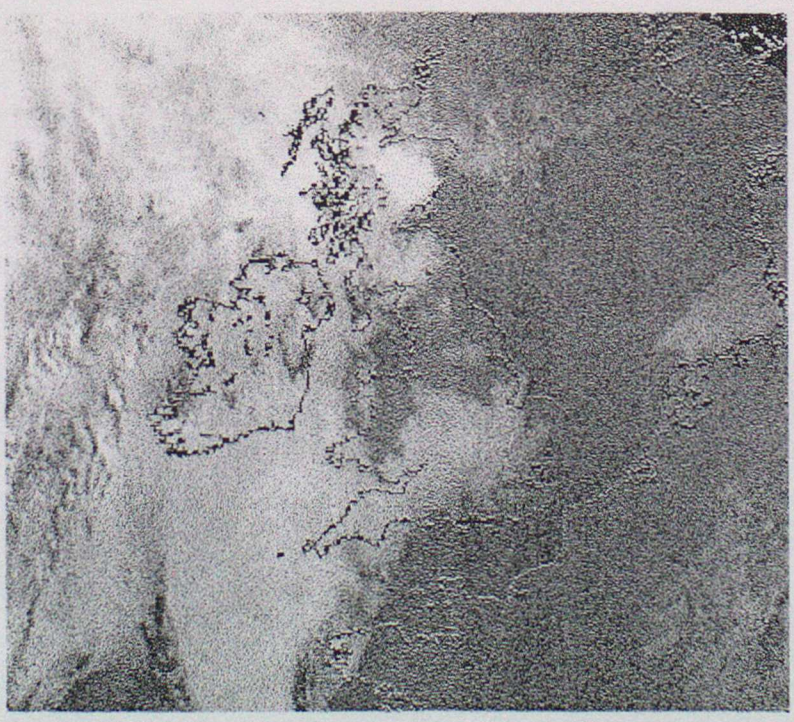

verifying visible satellite image

Fig. 3.4.4

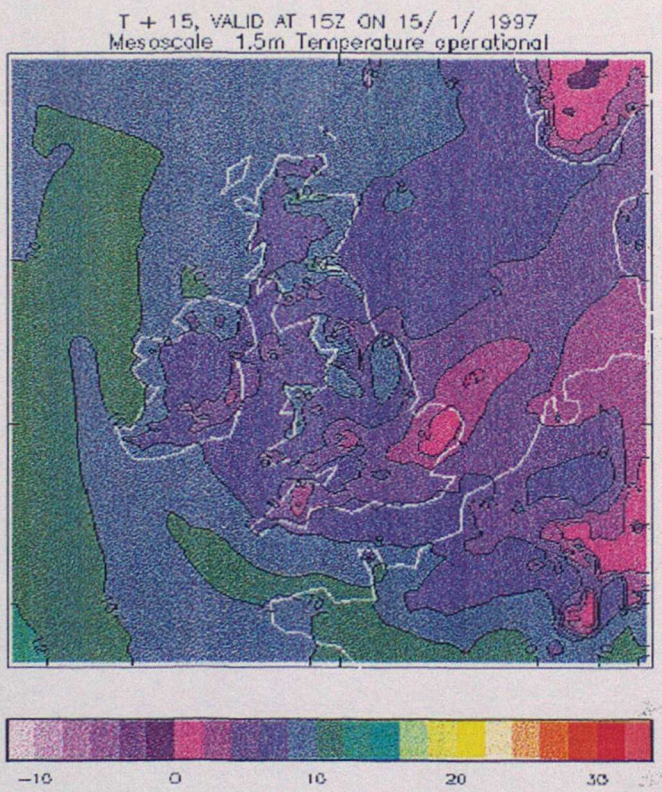

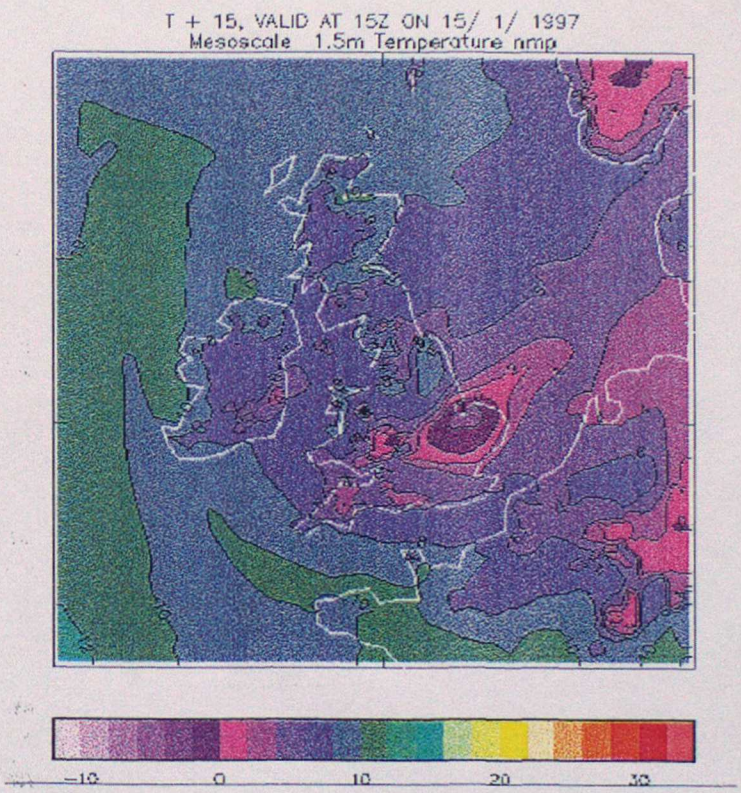

control

test

Fig. 3.4.5a

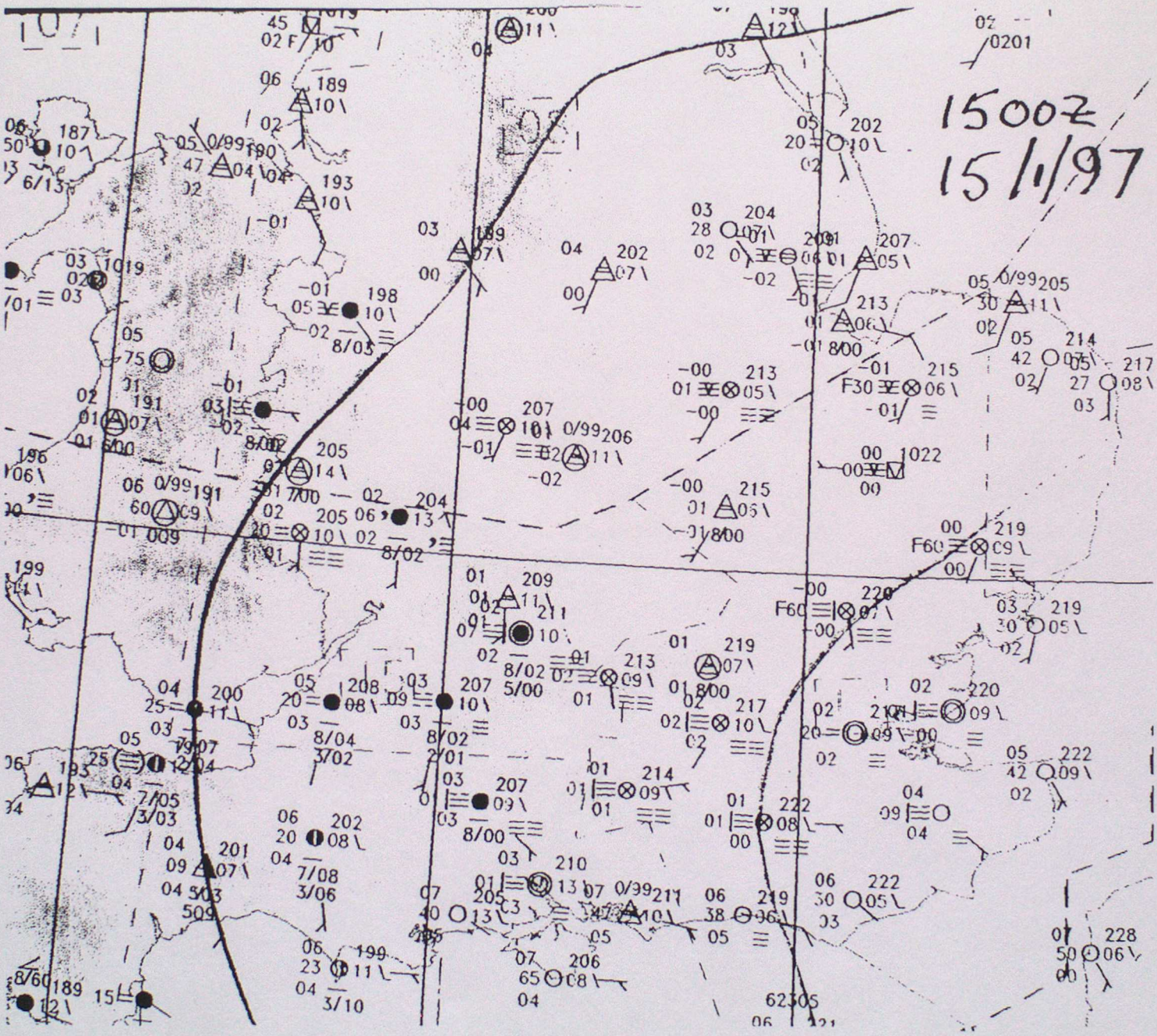

Fig. 3.4.5b Verifying chart for Fig. 3.4.5a

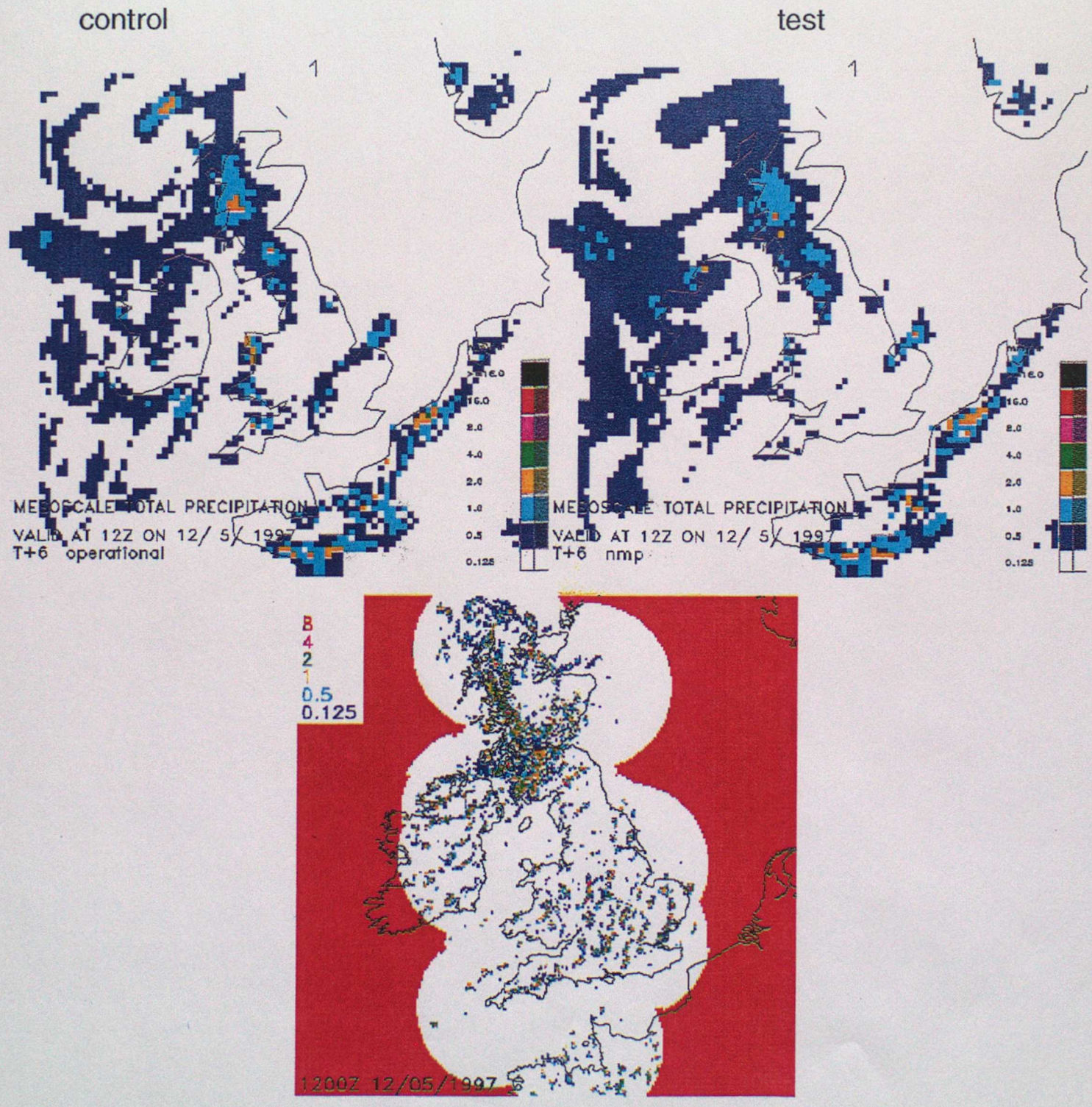

Fig 3.4.6 May 12th 1997, 12z, T+6

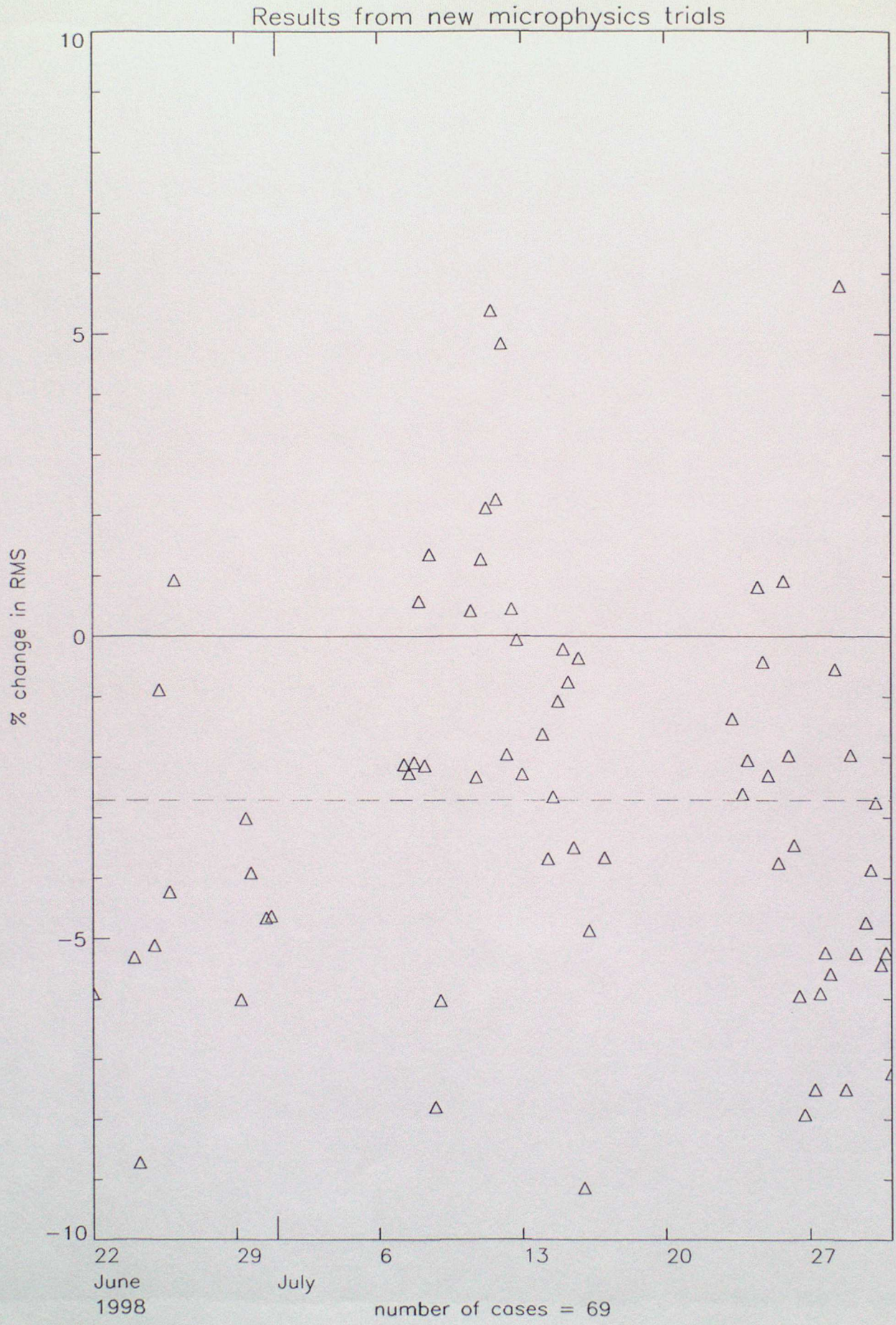
Results from new microphysics trials
10
5
0
−5
−10
% change in RMS
22
June
1998
29
July
6
13
20
27
number of cases = 69

Fig. 4.1.1

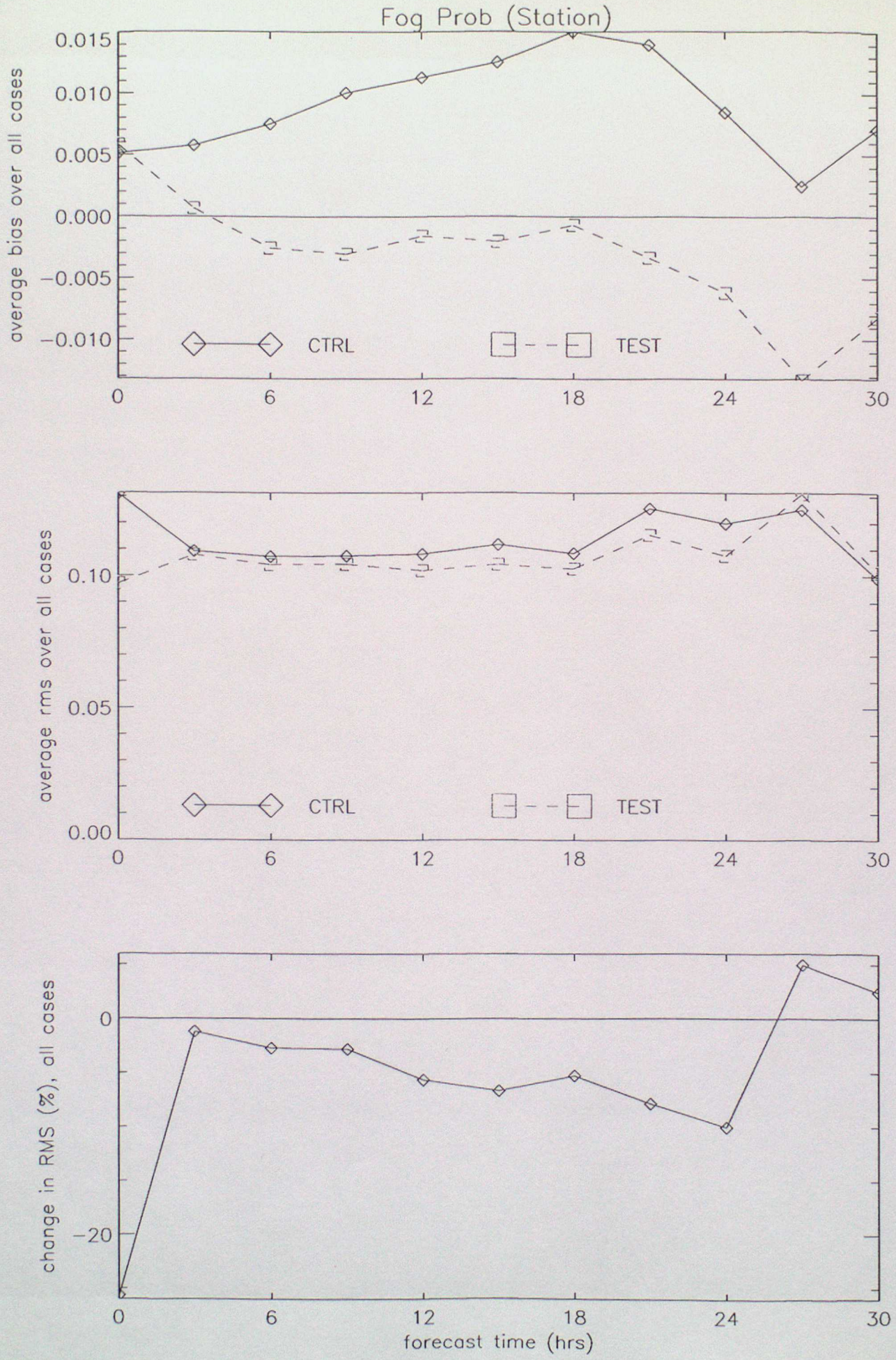
Fog Prob (Station)
average bias over all cases
0.015
0.010
0.005
0.000
−0.005
−0.010
CTRL
TEST
0
6
12
18
24
30
average rms over all cases
0.10
0.05
0.00
CTRL
TEST
0
6
12
18
24
30
change in RMS (%), all cases
0
−20
0
6
12
18
24
30
forecast time (hrs)

Fig. 4.1.2

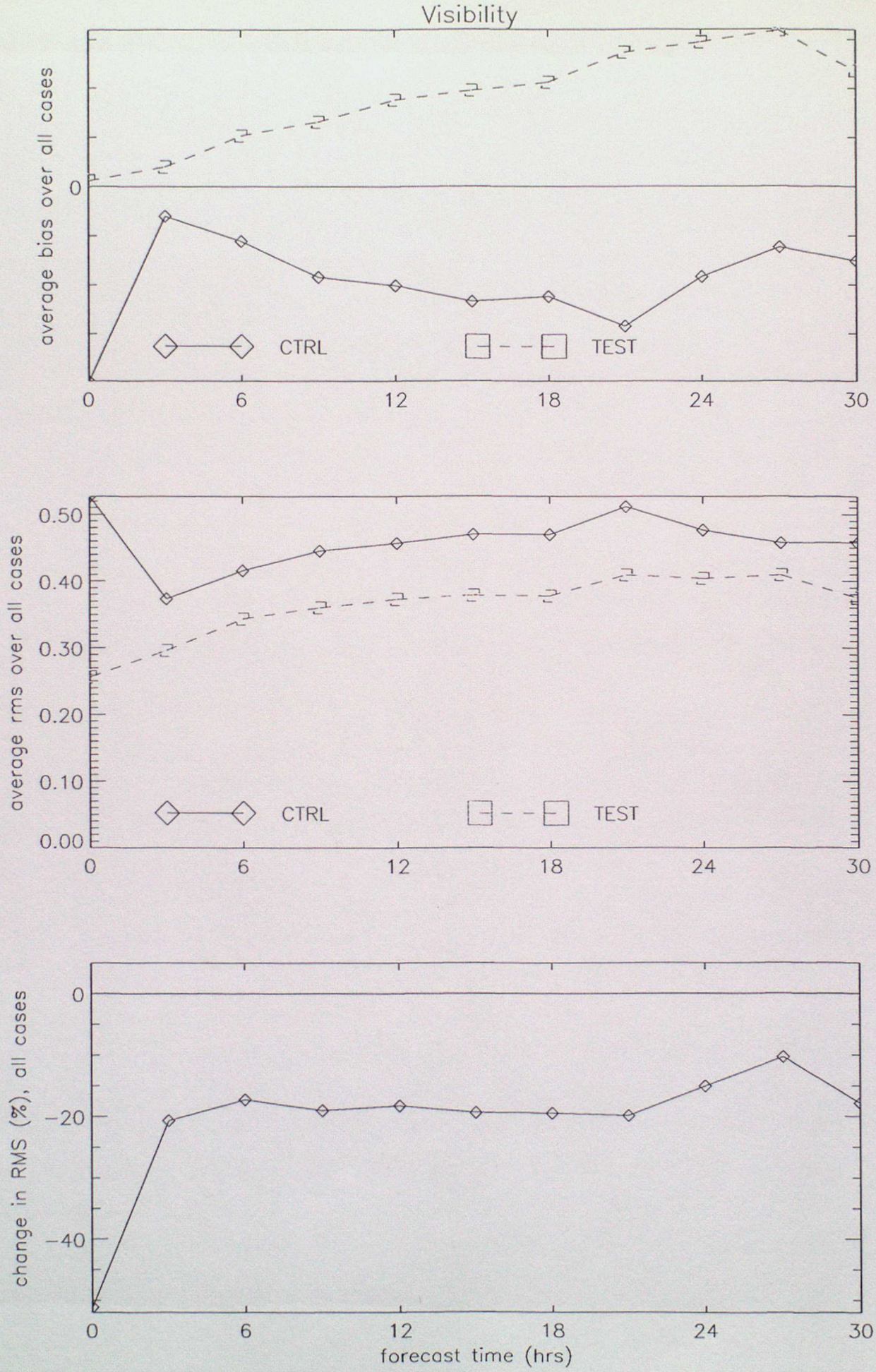
Visibility
average bias over all cases
0
CTRL
TEST
0
6
12
18
24
30
average rms over all cases
0.50
0.40
0.30
0.20
0.10
0.00
CTRL
TEST
0
6
12
18
24
30
change in RMS (%), all cases
0
-20
-40
0
6
12
18
24
30
forecast time (hrs)

Fig. 4.1.3

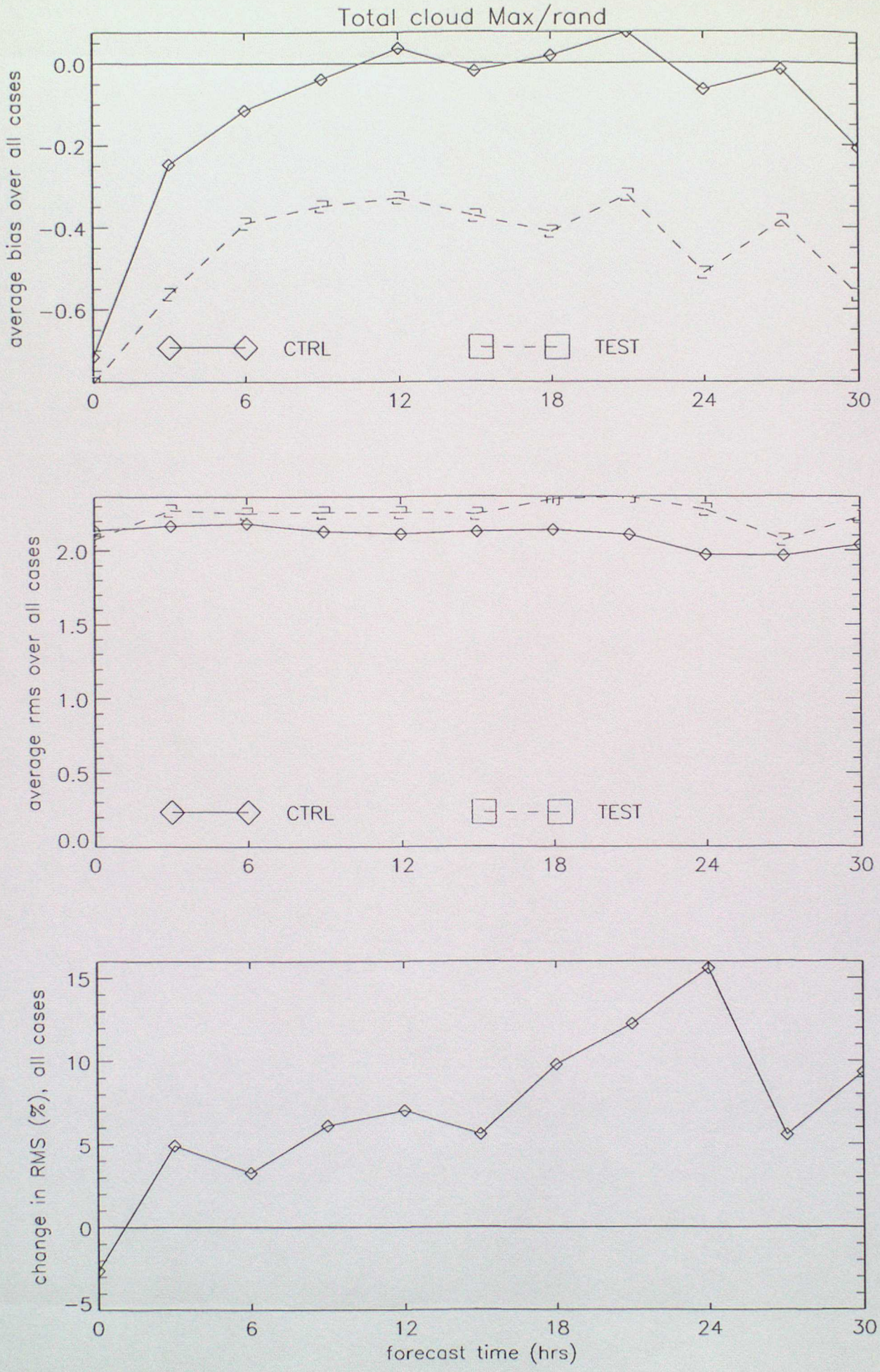
Total cloud Max/rand
average bias over all cases
0.0
−0.2
−0.4
−0.6
CTRL
TEST
0
6
12
18
24
30
average rms over all cases
2.0
1.5
1.0
0.5
0.0
CTRL
TEST
0
6
12
18
24
30
change in RMS (%), all cases
15
10
5
0
−5
0
6
12
18
24
30
forecast time (hrs)

Fig. 4.1.4

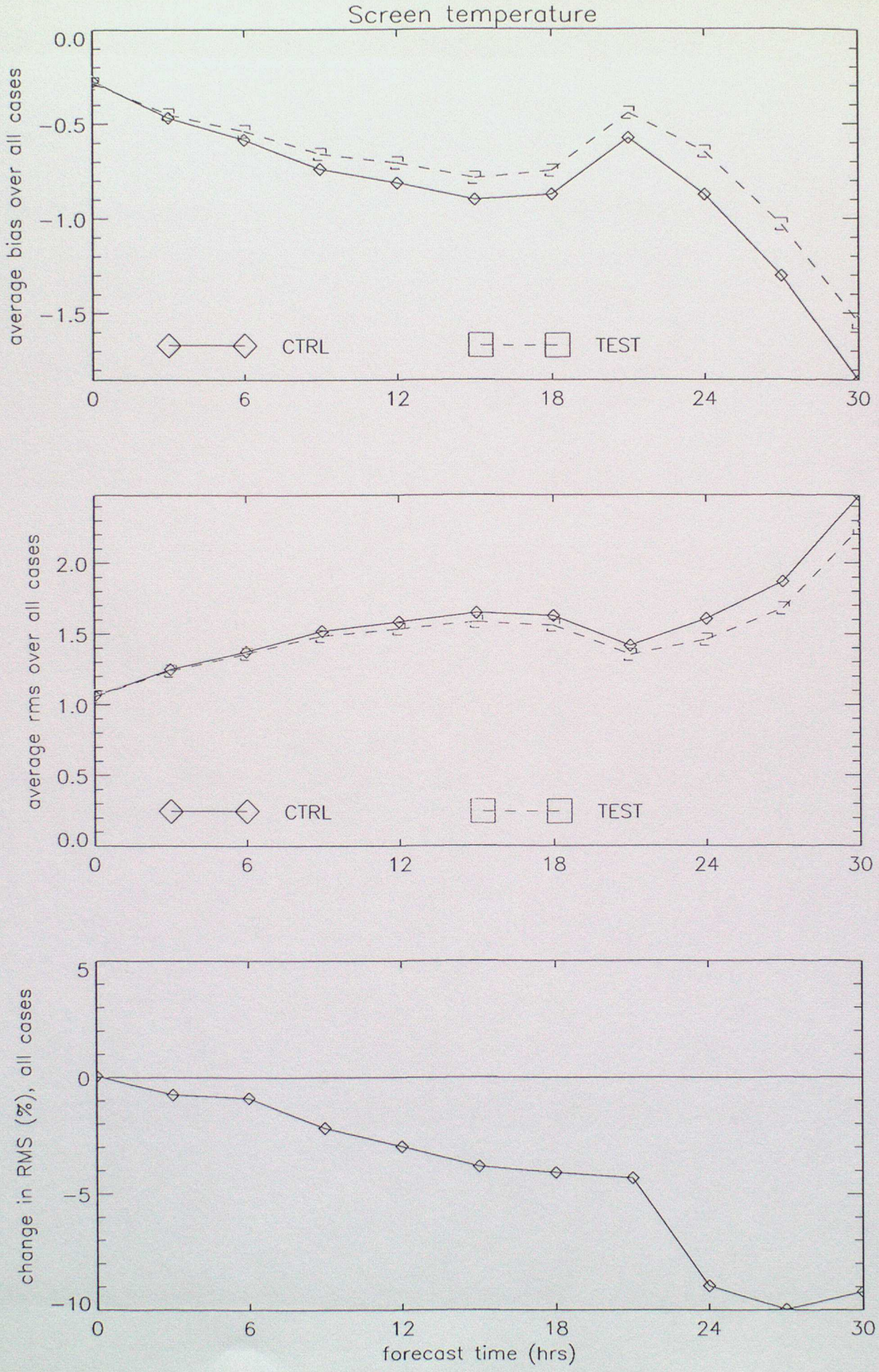
Screen temperature
average bias over all cases
0.0
−0.5
−1.0
−1.5
CTRL
TEST
0
6
12
18
24
30
average rms over all cases
2.0
1.5
1.0
0.5
0.0
CTRL
TEST
0
6
12
18
24
30
change in RMS (%), all cases
5
0
−5
−10
0
6
12
18
24
30
forecast time (hrs)

Fig. 4.1.5

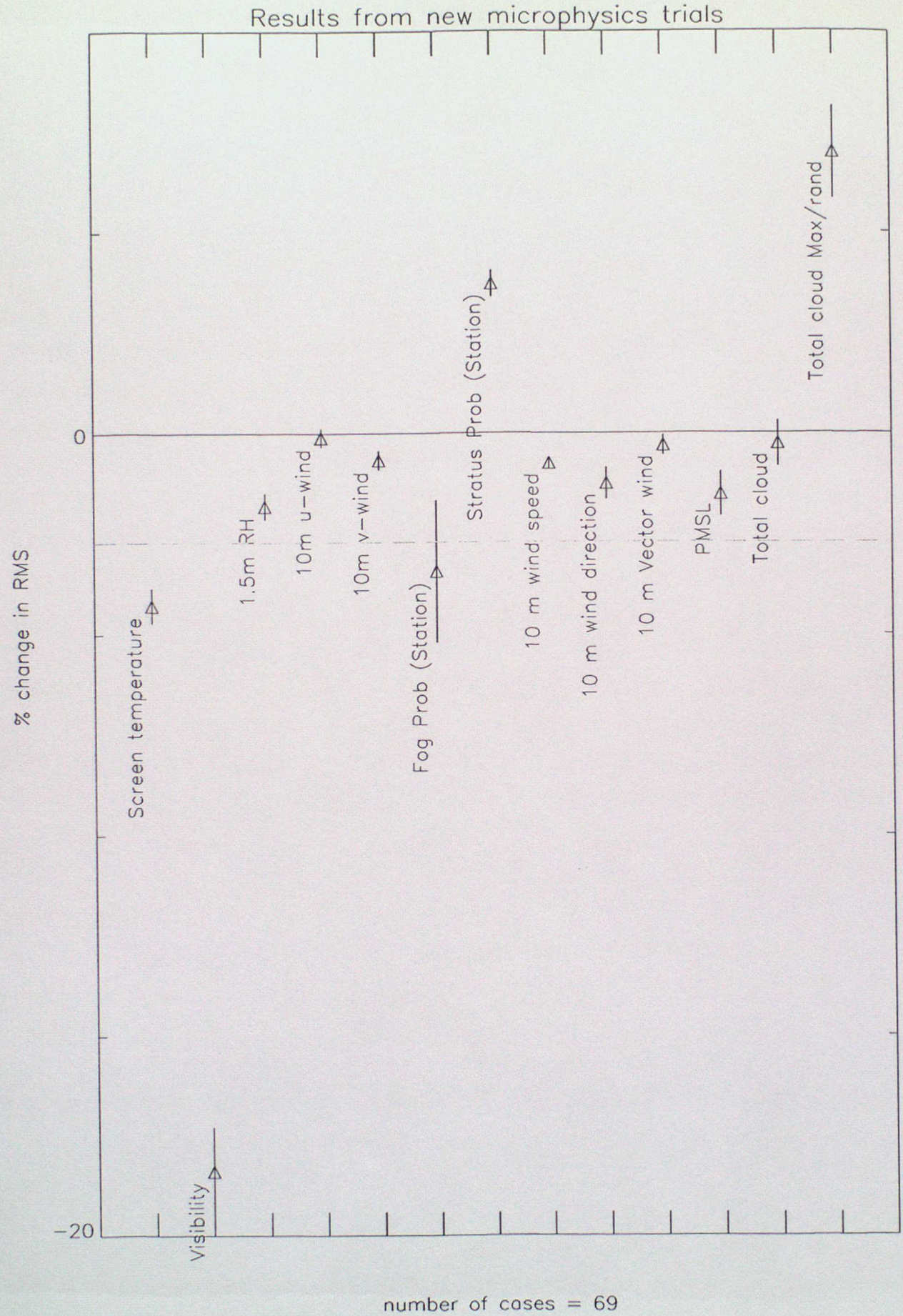
Results from new microphysics trials
% change in RMS
0
−20
Screen temperature
1.5m RH
10m u−wind
10m v−wind
Fog Prob (Station)
Stratus Prob (Station)
10 m wind speed
10 m wind direction
10 m Vector wind
PMSL
Total cloud
Total cloud Max/rand
Visibility
number of cases = 69

Fig. 4.1.6

Fig 4.2.1(a)

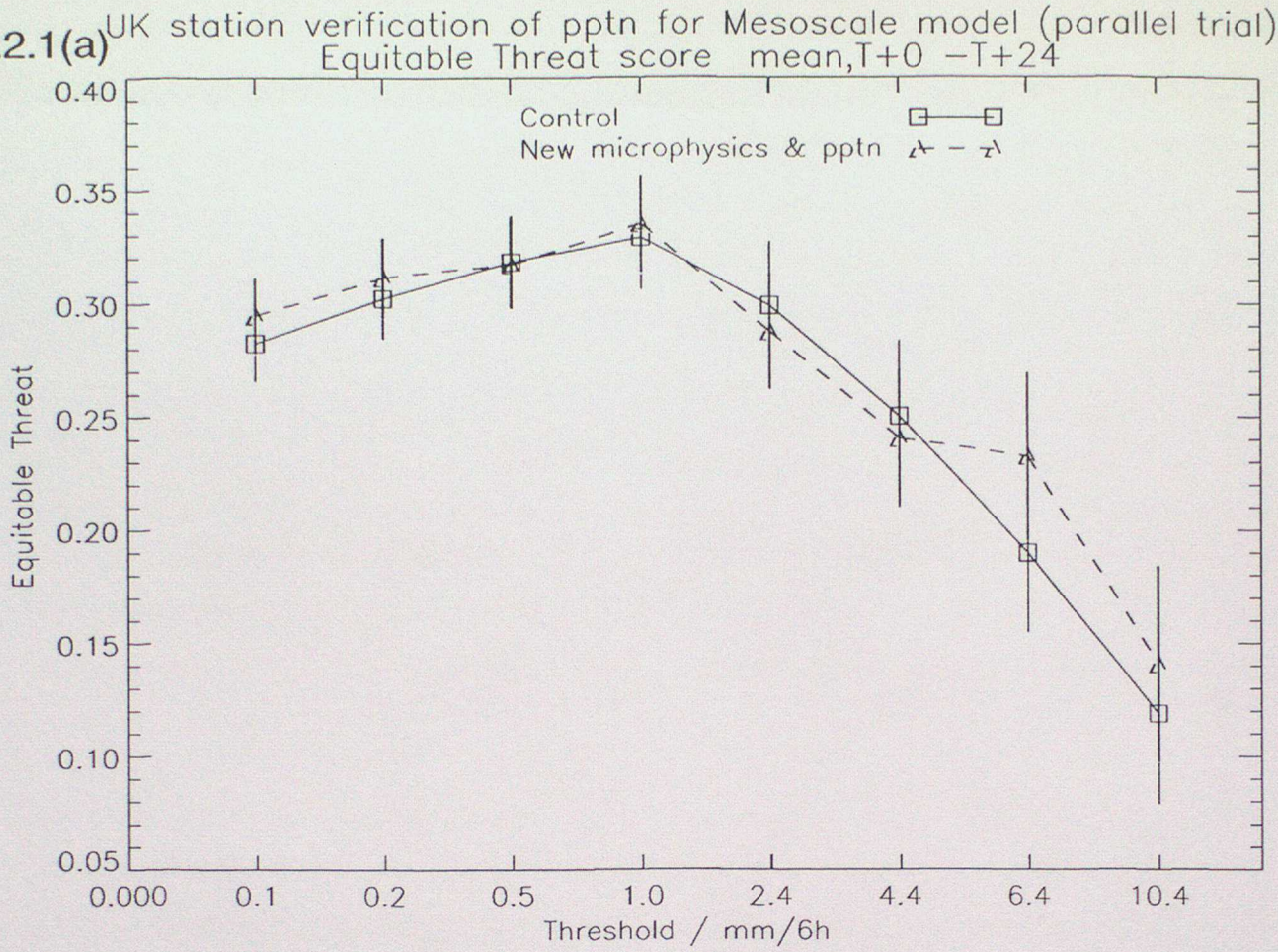

Fig 4.2.1(b)

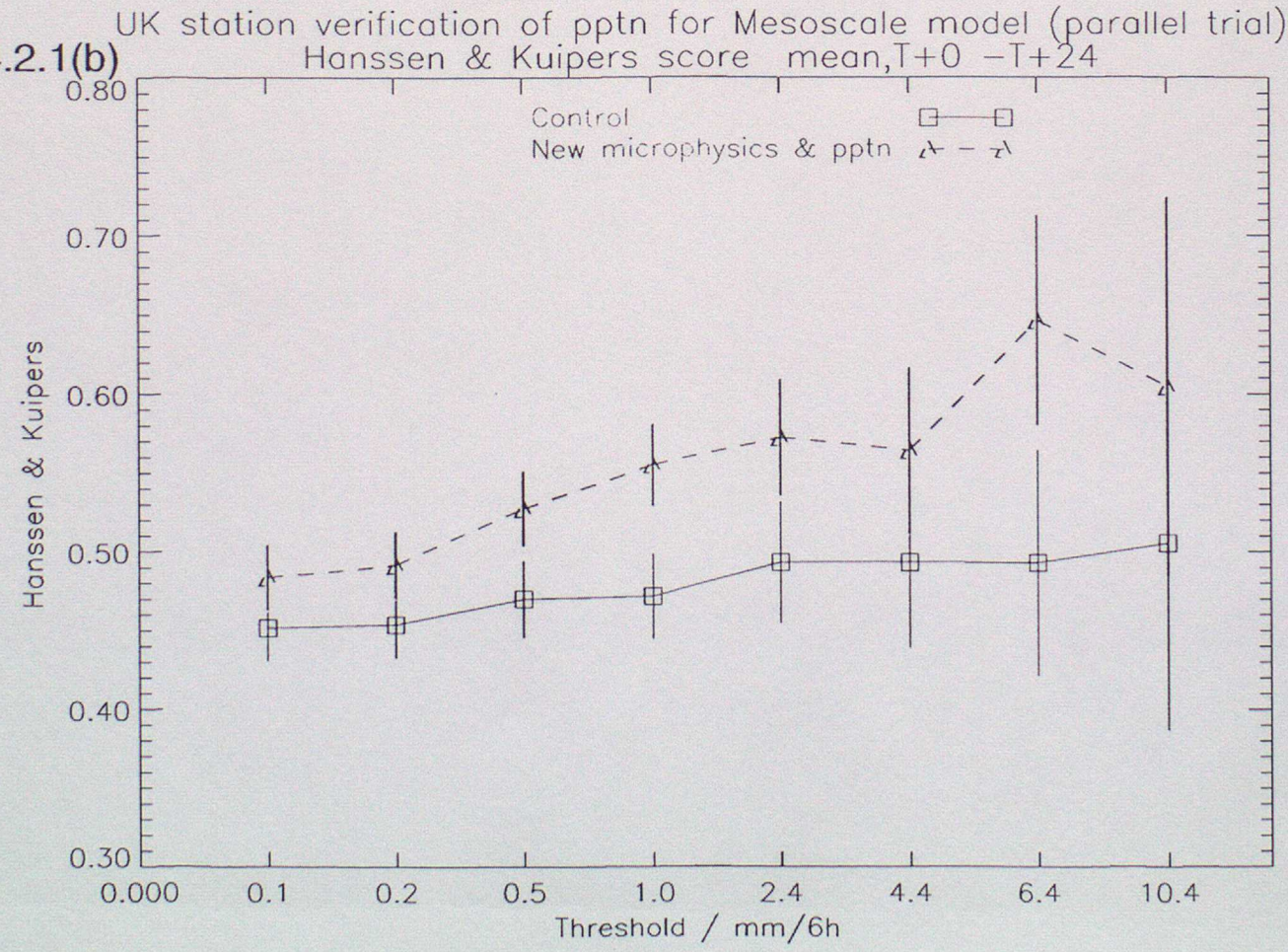

Fig 4.2.2(a)

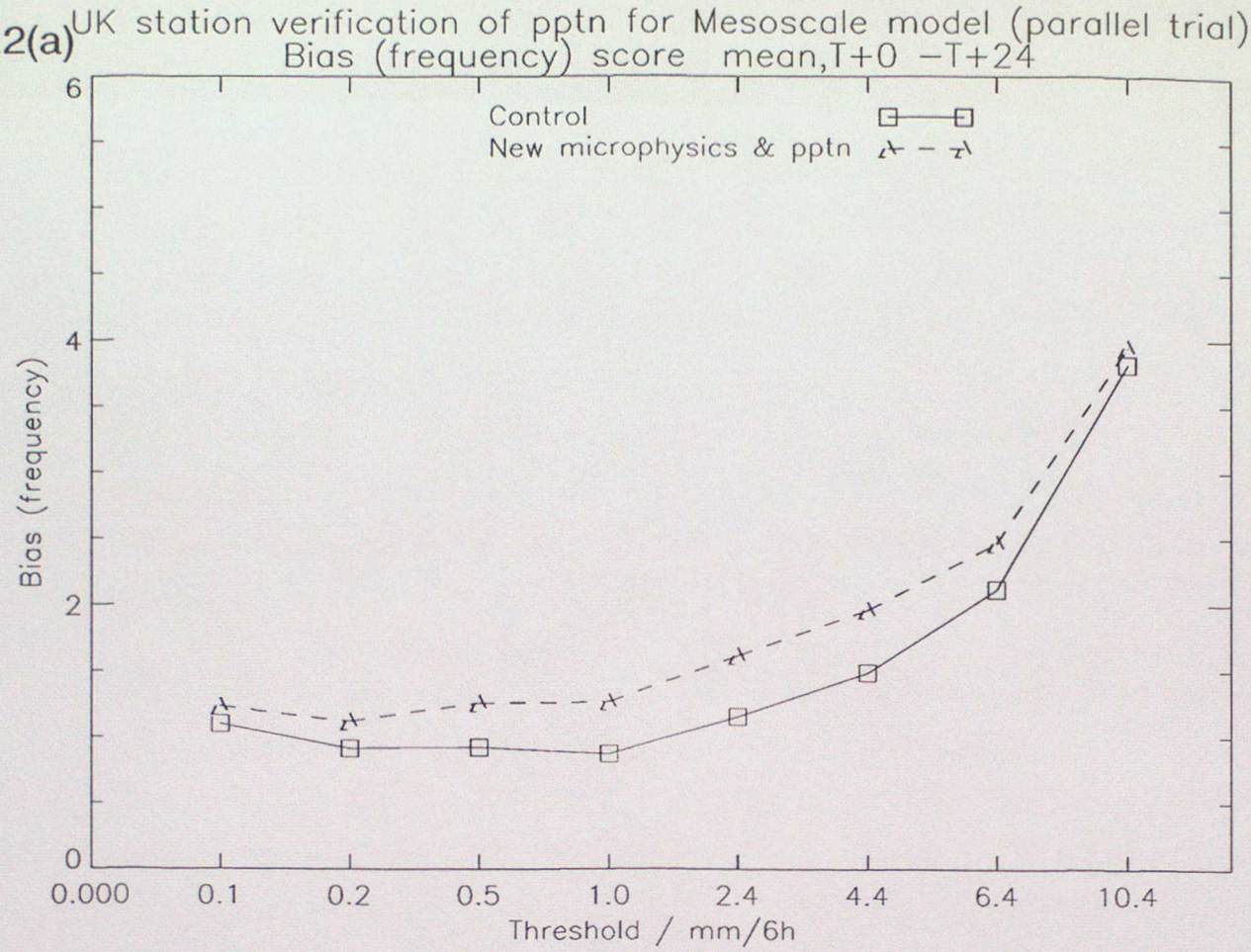

Fig 4.2.2(b)

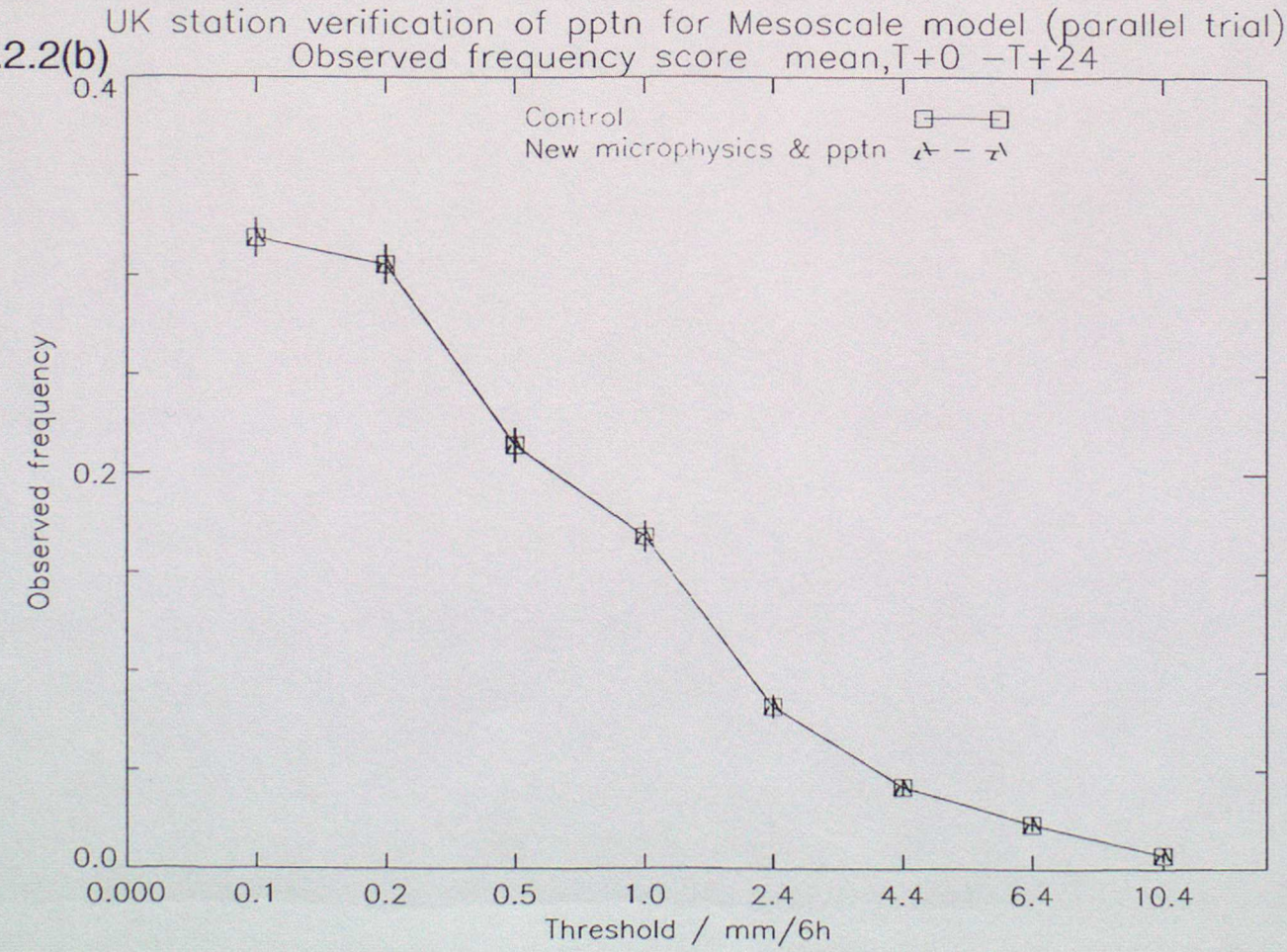

control

test

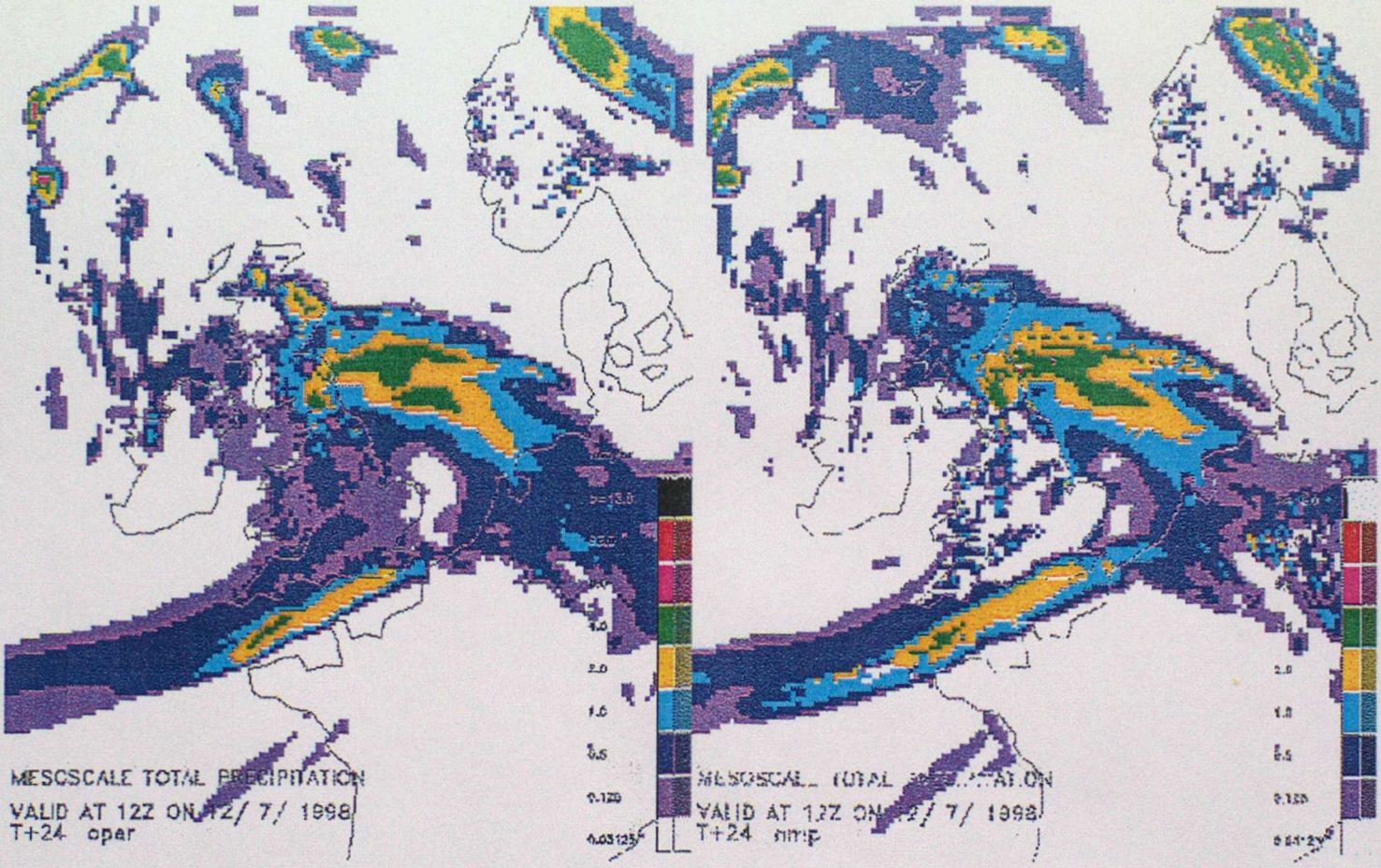

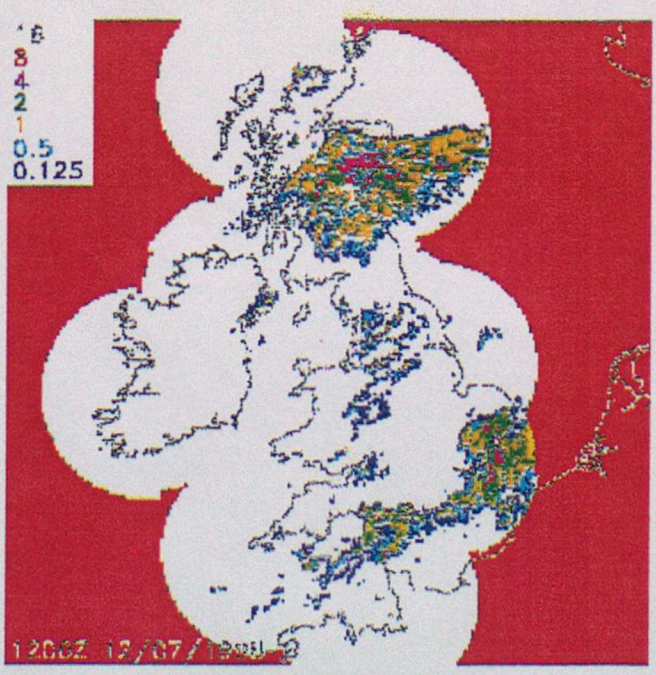

verifying radar image

Fig. 4.3.1 July 12th 1998, 12z, T+24

control

test

Fig. 4.3.2

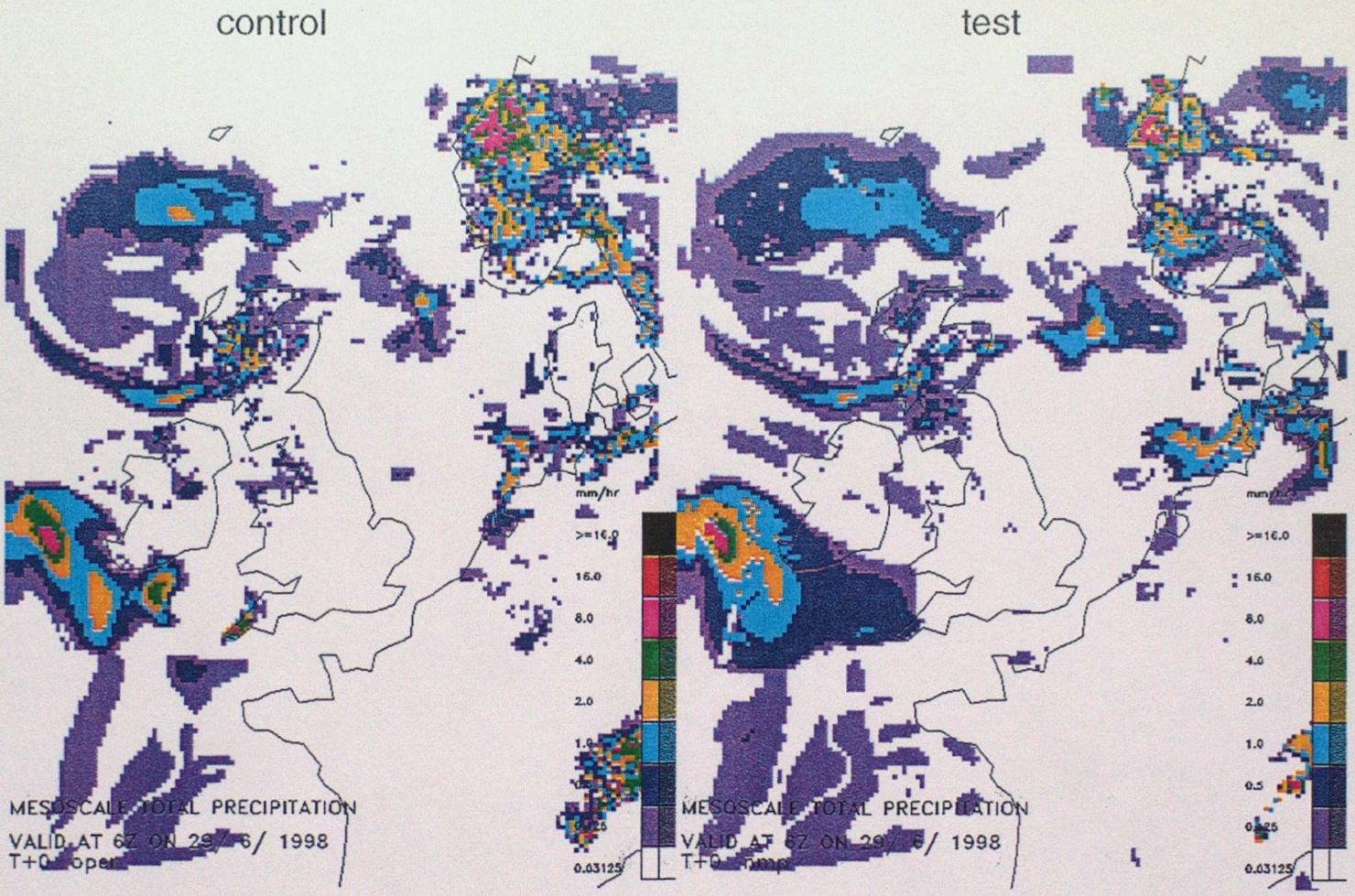

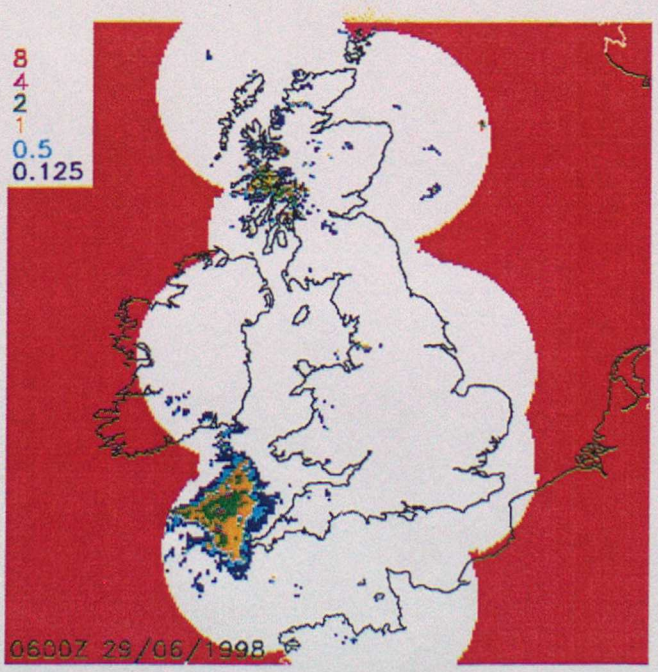

verifying radar image

Fig. 4.3.3 June 29th 1998, 6z, T+0

Appendix A - Assimilation of MOPS cloud data with the new cloud microphysics scheme

We document first of all the formulation of the present MOPS assimilation scheme, before describing the revised version for the new microphysics. Possible variations of this new formulation, and the results of some experiments to evaluate them, are summarised in a final section.

A1 Current MOPS assimilation scheme

The target layer cloud fraction C_L' is calculated from the observed (MOPS) cloud fraction C^{obs} and the current model convective cloud fraction C_{CV}.

$$C_L' = \max \{ (C^{obs} - C_{CV})/(1-C_{CV}) , 0 \} \quad (1)$$

The updated relative humidity rh' is calculated from the inverse f^{-1} of the function relating rh and cloud fraction defined in Appendix B of UM Documentation Paper 29, equations P292.B1 to P292.B6:

$$C=f(rh) \quad (2)$$

so the rh increment is

$$rh'-rh = f^{-1}(C_L') - rh \quad (3)$$

The updated vapour mixing ratio q' is calculated from

$$q' = rh' \, q_{sat}(T,p) \quad (4)$$

where

q_{sat} is over ice for $T<0$ and over water for $T>0$

There are no increments to liquid or frozen water during assimilation. It is true that the $q_c^{L/F}$ values at the end of assimilation are not in 'equilibrium' with the new rh'. If some of the rh increment gets transferred to $q_c^{L/F}$ to restore equilibrium during the next timestep, then the next assimilation step will add another increment to restore rh towards rh'. This is the benefit of a 'nudging' type of assimilation. In an effort to hasten convergence, an attempt was made to re-initialise $q_c^{L/F}$ after assimilation to be consistent with rh' through the equations in UMDP 29 Appendix C, but this proved to make very little difference to the cloud analysis, and was not adopted.

A2 MOPS assimilation scheme for new cloud microphysics

Relevant considerations:

(a) Since the new cloud microphysics scheme predicts the phase of the cloud, it is desirable to minimise any assumptions about phase during the assimilation scheme which might work against the new scheme.

(b) Liquid cloud fraction at any temperature obeys the relationship $C_{liq}=f(rh)$ where rh is defined with respect to water, and f is the same function as in (2) above.

(c) Ice cloud fraction C_{ice} is no longer directly related to rh eg ice can exist when rh (with respect to ice) is less than rh_{crit}. There is a relationship between ice cloud fraction C_{ice} and q_c^F.

(d) The overlap assumption for liquid and ice cloud in the same grid box is to set total cloud to the sum of ice and liquid cloud fractions (limited to 1). However, this could change in future versions of the scheme, so it would be better to keep the assimilation scheme free from any overlap assumption.

It seems sensible in the light of (a) to add any assimilation increments to q, as in the current scheme, leaving the cloud/precipitation scheme to assign the phase of the condensate (For attempts to make direct increments to $q_c^{L/F}$, see section A3).

We consider in turn the assimilation algorithm when the model has: liquid cloud only, ice cloud only, mixed phase cloud, no cloud. Assume we have values q, q_c^L and q_c^F prior to assimilation.

A2.1 Liquid cloud

Define a total rh with respect to *water*,

$$rh_{TOT}\,(wat) = (q+q_c^L+q_c^F)/q_{sat}^{wat}(T_L\,,p) \qquad (5)$$

where T_L is the liquid/frozen water temperature. Derive the target cloud fraction C_L' from equation (1) as before. Apply a relationship between rh_{TOT} and cloud fraction:

$$rh_{TOT}'\,(wat) = g\,(C_L'\,) \qquad (6)$$

Compute

$$q_{TOT}' = rh_{TOT}'\; q_{sat}^{wat}(T_L\,,p) \qquad (7)$$

and hence add a humidity increment:

$$q'-q = q_{TOT}' - q - q_c^L - q_c^F \qquad (8)$$

A2.2 The function $rh_{TOT}=g(C)$

In equation (3), we have a relationship between rh for vapour and cloud fraction in the current scheme. The corresponding relationship between *total rh* and cloud fraction in the current scheme still holds for liquid-only cloud in the new scheme, provided $q_{sat}^{wat}(T_L\,,p)$ is used. It is:

$$rh_{TOT} = \{\sqrt{(2C)} - 1\}\{1-rh_{crit}\} + 1 \qquad 0<C<0.5 \qquad (9a)$$

$$\{1 - \sqrt{(2[1-C])}\}\{1-rh_{crit}\} + 1 \qquad 0.5<C<1.0 \qquad (9b)$$

and follows from equations P292.A1 and P292.15 of UM Documentation Paper 29.

A2.3 Ice cloud

While ice cloud fraction in the new scheme is not directly related to rh, it is nevertheless true that in the absence of forcing, the new scheme will tend to an equilibrium relationship where rh_{TOT} with respect to ice approximately satisfies equation (9). Since the adjustment timescale for ice cloud in the new scheme is of order 2 hours and since the nudging timescale during assimilation is 3 hours, it is reasonable to use this equilibrium relationship. We are only attempting to analyse clouds which change little on the timescale of several hours. Also, if we

abandon the equilibrium relationship, then we are forced to consider a less satisfactory option, that of parametrising the 'best-fit' relationship between rh_{TOT} and C_{ice}. Experiment has shown that this is different for growing ice clouds and decaying ice clouds, because there is hysteresis in the system. Also, the 'best-fit' relationships from a forecast run away from equilibrium are likely to vary with synoptic situation.

So we proceed for ice-only cloud as follows:

Define a total rh with respect to *ice*,

$$rh_{TOT}\,(ice) = (q+q_c^{L}+q_c^{F})/q_{sat}^{ice}(T_L\,,p) \qquad (10)$$

Derive the target cloud fraction C_L' from (1) as before. Apply the equilibrium relationship between rh_{TOT} (ice) and cloud fraction:

$$rh_{TOT}'\,(ice) = g\,(C_L'\,) \qquad (11)$$

Convert to obtain rh_{TOT} with respect to water:

$$rh_{TOT}'\,(wat) = rh_{TOT}'\,(ice)\;q_{sat}^{ice}(T_L\,,p)\;/q_{sat}^{wat}(T_L\,,p) \qquad (12)$$

Finally, apply (7) and (8) as for liquid cloud.

A2.4 Mixed phase cloud

Although we don't wish to predict phase during assimilation, the target total water should be better represented if the model's existing phase partitioning is respected. So we combine (6) and (12) and apply them in a weighted manner according to the liquid/ice already present in the model

$$rh_{TOT}'\,(wat) = g(C_L')\,\{\;q_c^{L} + \;q_c^{F}\,q_{sat}^{ice}(T_L\,,p)\;/q_{sat}^{wat}(T_L\,,p)\;\}\;/\;(\;q_c^{L}+q_c^{F}\;) \qquad (13)$$

followed once more by (7) and (8). The weighting in (13) could be done in other ways, eg with C_{liq} and C_{ice}, but this may not be better.

A2.5 No cloud

When there is no cloud initially in the model, it is uncertain whether any cloud created by the assimilation should be treated as ice or liquid. This means we are uncertain whether to convert the target rh_{TOT}' to q_{TOT}' with q_{sat}^{wat} or q_{sat}^{ice}. We can be confident that the cloud should be ice below, say, -35 deg C, and should allow for the possibility of the cloud being liquid down to, say, -25 deg C. So the value of qsat will vary from the water value to the ice value over this temperature range, with a linear weighting in between. Where we use q_{sat}^{wat} but the cloud should be ice, this will mean the target q_{TOT}' is too high, but this will only serve to hasten the model's initial convergence to the observed cloud. Once a little ice cloud is present, the target humidity will be derived appropriately as in section 2.3, or section 2.4 if liquid is also present.

A2.6 Limitations

Since ice cloud is in practice, not in equilibrium, it would be possible for the model rh_{TOT} to be less than the value $g(C_L')$, but with the model's layer cloud fraction greater than C_L'. The reverse could also happen. In either case, the humidity increment computed as above would take the model away from the observed cloud fraction. The best way to tackle this problem is to check that the humidity increment q'-q is of the same sign as the cloud fraction increment (C_L'- C_L), and if it is not, then allow no humidity increment. This does introduce some

dependence of the assimilation scheme on the derivation of the model's total layer cloud fraction from its liquid and ice components, but this cannot be easily avoided.

When the cloud fraction increment is zero (ie both model and observation have zero cloud or both have full cover), then the humidity increment will be zero.

A3 Initial Assimilation Tests

The new assimilation scheme was tested initially on 4 winter cases, with 12 hours of assimilation of all observation types, including MOPS cloud data. The performance of the scheme was assessed to begin with on the fit to cloud data at the end of the 12 hour assimilation. Control runs were supplied by running the old microphysics and/or running without cloud data. No forecasts were run at this stage.

Generally, the new scheme gave a closer fit to the cloud data in the lower troposphere, at some levels by a significant margin. In two cases, the improved fit at lower levels with assimilation went along with an improved fit without assimilation ie the microphysics scheme was responsible for the improvement. In one case, however, (DT 6 UTC, 8/1/97) the test and control runs without assimilation gave a similar fit, and the improvement with the new microphysics came only with assimilation of cloud data switched on (Figure A1). The reason for this interesting difference is not known.

Above about 500hPa, the new scheme gave a poorer fit and this was most noticeable at cirrus levels (see Figure A2). At level 24 (~250hPa), the new scheme's bias is worse than the control by some 2.5 oktas. The assimilation of cloud data does reduce the bias a little, but by less than assimilation with the control scheme, where the bias is less to start with.

Given the characteristic of excess cirrus in the new scheme, it seemed worth exploring a revised assimilation scheme, with increments directly to cloud ice water content, based on its relationship to ice cloud fraction.

A4 Attempts to improve ice cloud assimilation

Three variants of the scheme in A2 (which we will label vn1.0) were tested, all on the 5/12/97 case.

vn2.0 Wherever the model has ice cloud only, an ice increment is calculated from the 'target' cloud by an inversion of the new scheme's $C_{ice}(q_c^F)$ relationship. There is no vapour increment unless the observed cloud is zero and the model has $rh>rh_{crit}$, in which case rh is reduced to rh_{crit}.. At points with any liquid cloud in the model background, there is a vapour increment calculated as in vn1.0, and no ice increment. If the model cloud is zero, and the observed cloud non-zero, then cloud is created via a vapour increment as in vn1.0 for temperatures above -25 deg C. For temperatures below -25 deg C, cloud is created by an ice increment and, if necessary, a vapour increment is added to ensure $rh>rh_{crit}$.

vn2.1 As vn2.0, but when aiming to reduce ice cloud, the scheme adds a vapour increment designed to reduce rh to rh_{crit}.

vn2.2 In this version, vapour increments were calculated as in vn1.0, and ice increments as in vn2.0. The vapour increment from vn1.0 was then reduced by the amount of any ice increment added.

The version 2 code options with different combinations of vapour and ice increments did not improve the fit to cirrus, but in fact slightly degraded it (Figure A3). This is a little puzzling,

since the vapour-cloud relationship is not exact for ice cloud, and the ice content-cloud relationship is exact. However, the version 2 options perhaps suffer from a poorer description of the vapour increment than n It was decided to remain with vn1.0 for the case studies in forecast mode, for which the results are reported in section 2.3.

A5 Test of a linearised cloud assimilation

Lorenc (personal communication) suggested that instead of using equation (9) to calculate the target total rh, it might be preferable to linearise (9) and apply it to increments ie

$$\Delta rh_{TOT} = g'(C)\,\Delta C \qquad (14)$$

This would get round the need to check if the cloud and humidity increments were of opposite sign. Possibly, if the mixed phase does not obey (9) very well, then the changes in rh_{TOT} and C might obey the linearisation to a better approximation, though this is not known a priori. One problem with (14) is that the derivative g' gets large near C=0 and C=1. In tests it was limited to a value of +/- $2(1-rh_{crit})$, which is the average gradient over the range C=0 to C=1. The same 5 cases described in section 2.3 were rerun with the linearised version of the scheme. The relative impact of the linearisation was approximately neutral, average rms scores for cloud, temperature, wind and fog probability being within 1% of the scores for vn1.0.

In the absence of a clear advantage for the linearised scheme, it was decided to retain vn1.0 as the version to put forward for full operational trials. It is possible that a larger number of cases may reveal a more systematic impact from the linearisation. The linearisation may be useful in future when developing an 'observation operator' and its adjoint for a 3D-Variational version of the cloud assimilation.

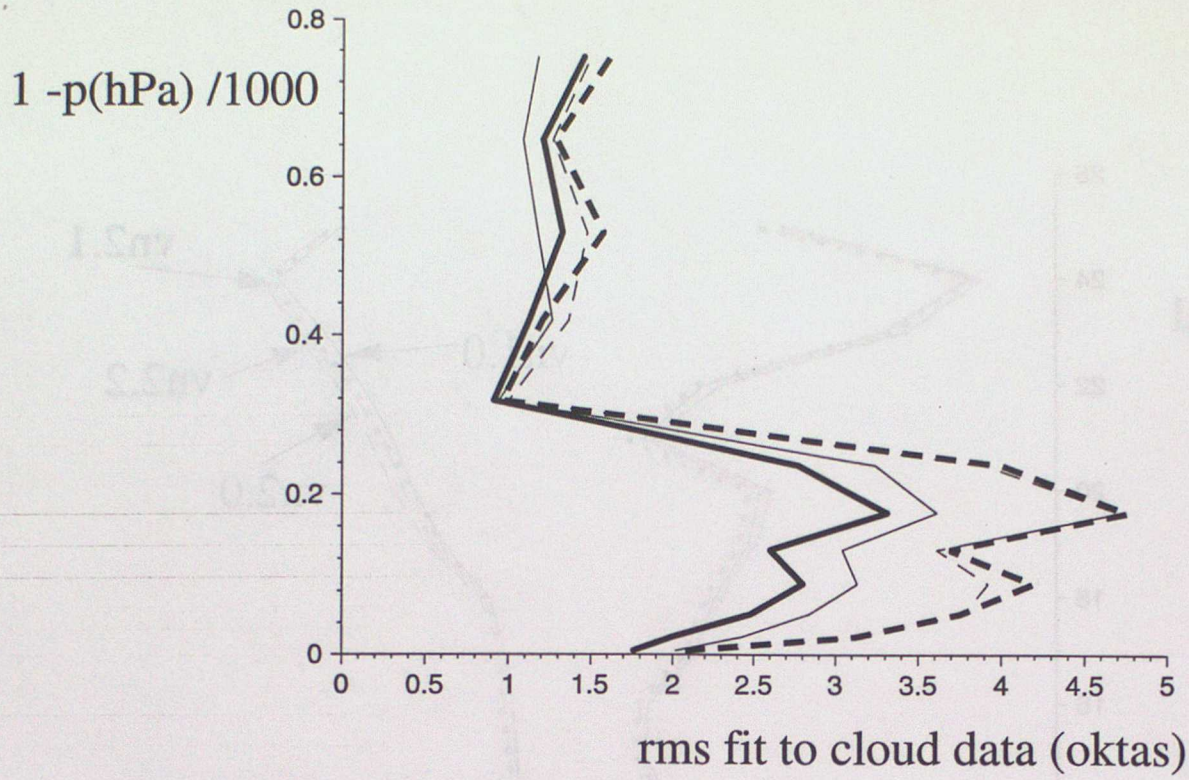

Figure A1: Rms fit to MOPS cloud data at 6z 8/1/97, after 12 hours of assimilation. Bold lines are for new microphysics, normal lines for old microphysics. Full lines are for runs where the cloud data were assimilated, dashed lines are for runs where NO cloud data were assimilated. The vertical co-ordinate increases as pressure decreases, according to the formula shown.

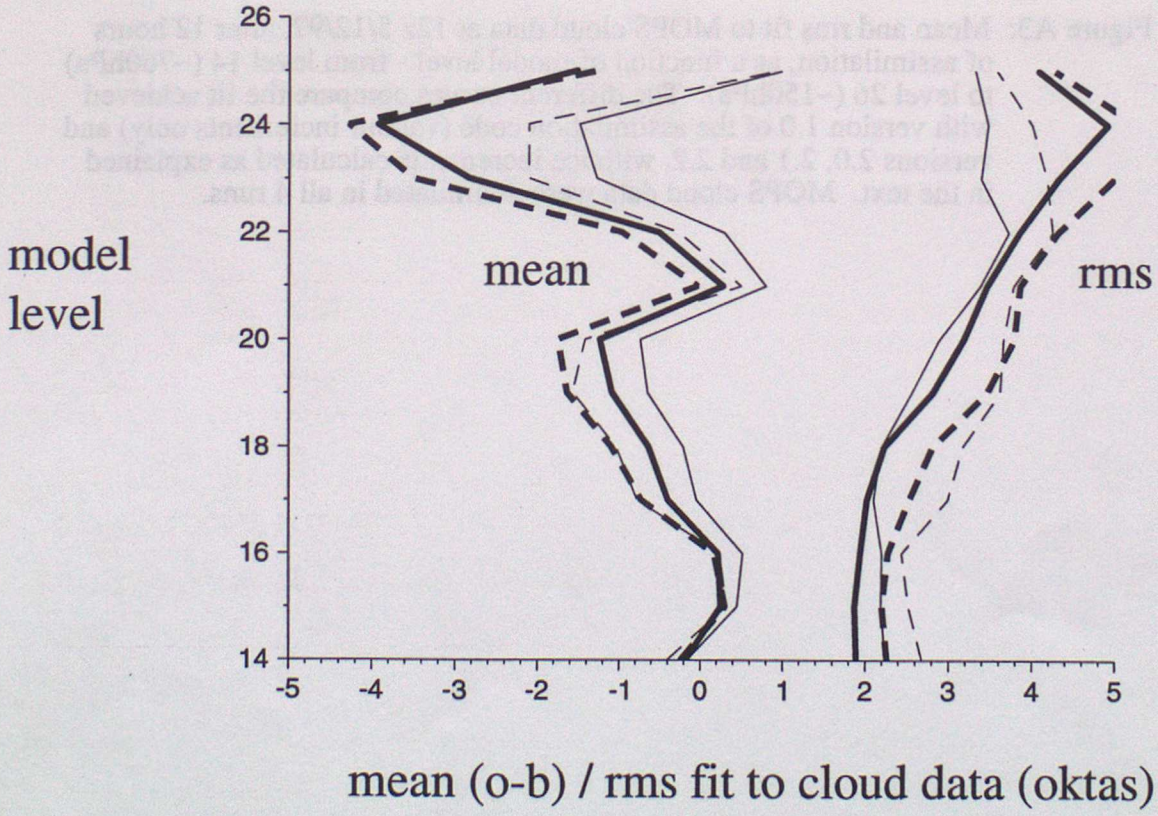

Figure A2: Mean and rms fit to MOPS cloud data at 12z 5/12/97, after 12 hours of assimilation, as a function of model level - from level 14 (~760hPa) to level 26 (~150hPa). Bold lines are for new microphysics. Normal lines are for old microphysics. Full lines are for runs where the cloud data were assimilated, dashed lines are for runs where NO cloud data were assimilated. The mean figures (o-b) are observation - background.

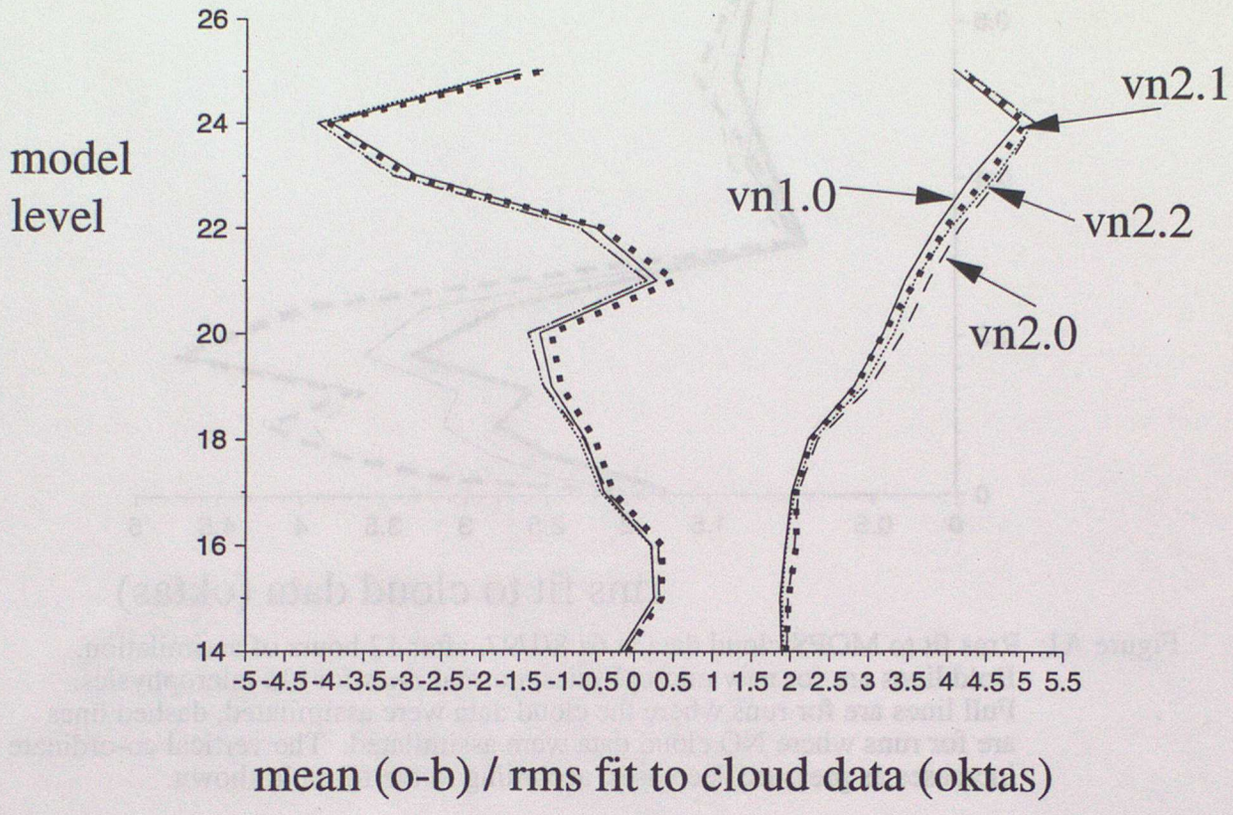

Figure A3: Mean and rms fit to MOPS cloud data at 12z 5/12/97, after 12 hours of assimilation, as a function of model level - from level 14 (~760hPa) to level 26 (~150hPa). The different curves compare the fit achieved with version 1.0 of the assimilation code (vapour increments only) and versions 2.0, 2.1 and 2.2, with ice increments calculated as explained in the text. MOPS cloud data were assimilated in all 4 runs.

The New Visibility Diagnostic

Scientific Description.

Visibility diagnosis in the Unified Model (UM) relies on a simplistic estimation of particle scattering cross section and number density. Only the contribution to scattering from aerosol and cloud particles which form on them are currently considered. Treatment of precipitation will be a future upgrade. The parametrization of particle scattering cross-section and number density relies on the model humidity and a dry aerosol mass mixing ratio. The latter provides a number density and average dry radius.

The current UM scheme uses a mean relative humidity or a mean liquid water content, both of which are produced from the UM cloud scheme assuming a triangular distribution of states about the prognostic total water content (the critical RH (RHcrit) value is used to characterise the width of the distribution). An approximation of the equilibrium equation for water droplet growth (relative humidity versus droplet radius), with RH limited to 99.9%, gives particle radius in subsaturated conditions. Where cloud is diagnosed, the particle size is estimated by distributing it equally amongst the aerosol particles. The largest droplet radius (lowest visibility) obtained from the two approaches is then selected. Although the scheme is analytic in both directions, it is not consistent, due to the rather arbitrary method of switching between the RH-based and liquid water-based approaches. In practice, as soon RHcrit is reached, liquid water is present and this dominates. The scheme thus derives a visibility from a 'gridbox average' cloud water. Given the large difference between visibility inside and outside cloud, the scheme has the characteristic of readily producing 'poor' visibility (e.g. 500-1000m) while rarely diagnosing very low visibility (e.g. 50 m), since this would require very high gridbox average liquid water content.

The new scheme is based more rigorously on the assumption that there is a distribution of humidity within a gridbox in the same way as the cloud scheme. It is formulated to compute the visibility at any probability level, but for current purposes diagnoses the median visibility. It takes the prognostic value total water content directly, which is equivalent to using median values of RH and liquid water. The equilibrium RH as a function of radius for a moist aerosol particle is given by the Kohler curve:

$$RH = \exp\left(\frac{A_0}{r} - \frac{B_0}{(r/r_d)^3 - 1}\right)$$

with A_0 and B_0 constants and r_d the dry aerosol radius. The liquid water content is given trivially by:

$$q_L = \max\left(\tfrac{4}{3}\pi (r^3 - r_d^3)\rho_w N,\ 0\right)$$

where N is the particle number density.

The equilibrium curve is shown in Figure 1. The full form of the equilibrium curve is used, but it is forced to be single-valued in RH, by holding RH at the activation value for radii above the activation radius. Rather than being treated separately to the geometric solution, the

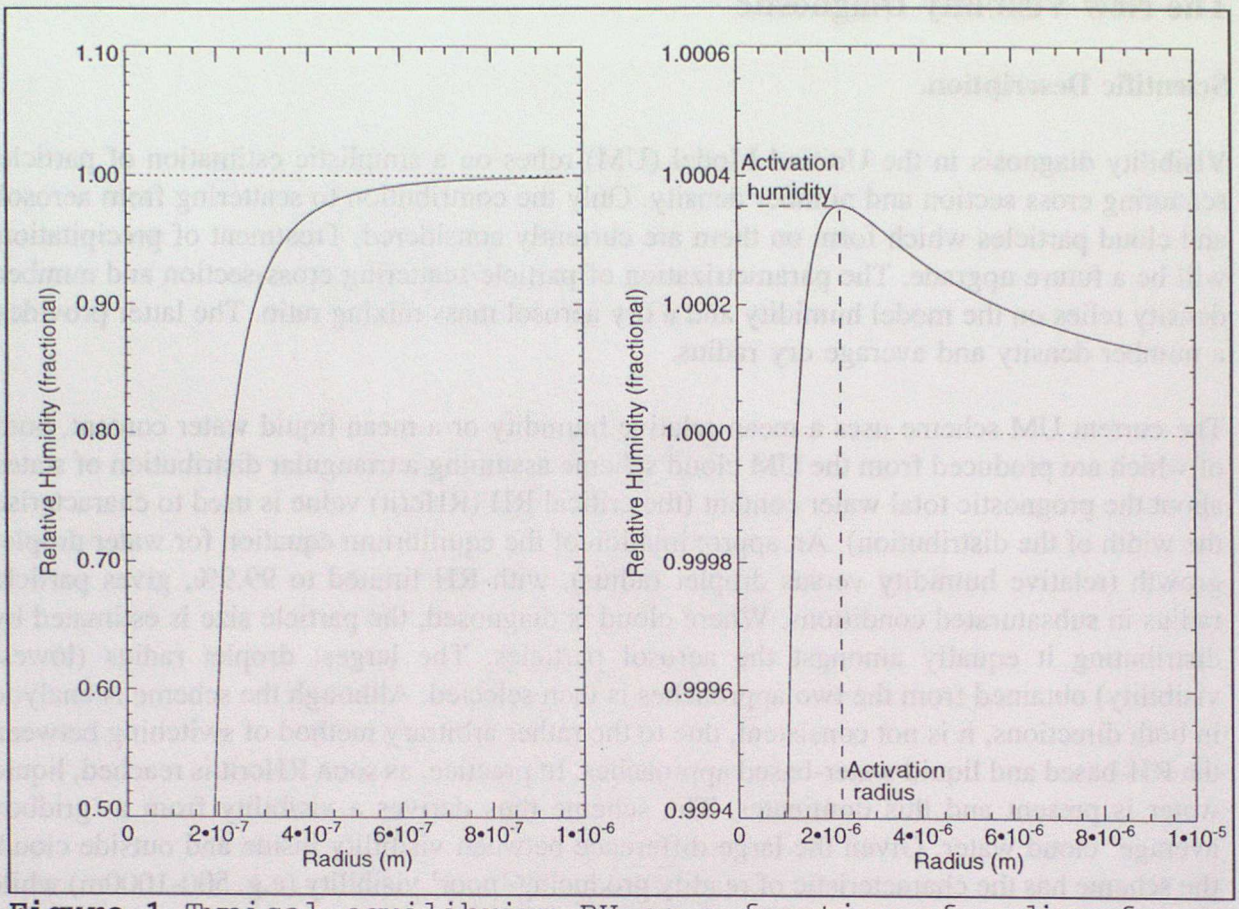

Figure 1 Typical equilibrium RH as a function of radius for an aerosol particle; right hand plot shows detailed behaviour around saturation.

two contributions are added, to obtain a continuous scheme shown in Figure 2 This requires an iterative solution of the following equation (expressing conservation of water) to recover droplet radius:

$$q_t = RH(r)\,q_s(T,p) + q_L(r)$$

Here q_s is the saturation specific humidity. The inverse solution is analytic and the scheme is consistent in both directions. Importantly for future applications, it is differentiable, with a derivative continuous in both humidity and aerosol. Liquid water is not present in this scheme until the median RH reaches 100%, so the diagnosed visibility is not as low as in the current scheme in the range RHcrit to 100%; outside these ranges it is similar.

Both schemes also require aerosol mass content, pressure and temperature. A probability of visibility below a given threshold diagnostic is available from both schemes, and is almost identical for a threshold visibility of 1km or above; for lower threshold visibilities, the new probability diagnostic gives a more rigorous result.

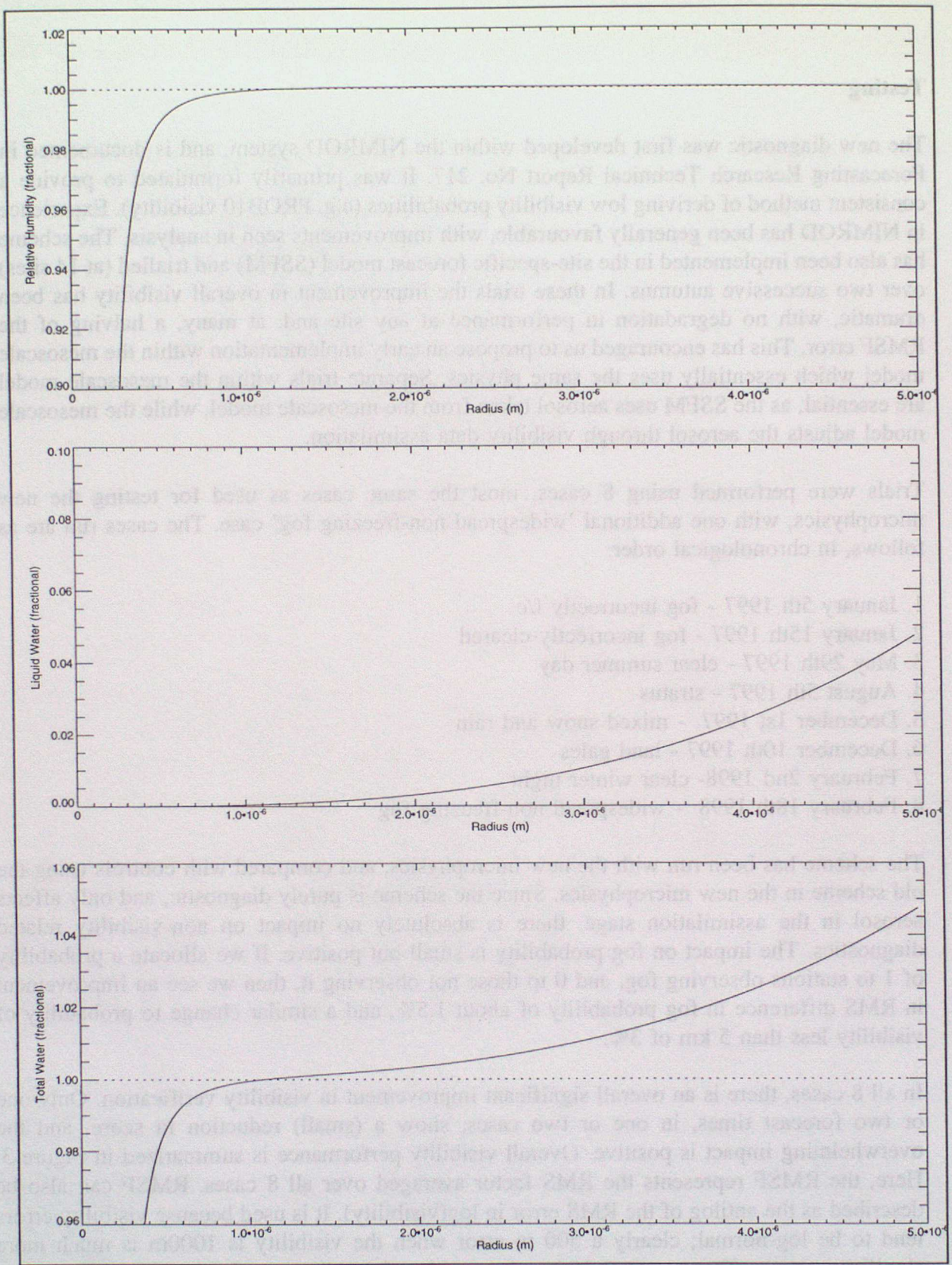

Figure 2 Equilibrium RH (top), liquid water content normalized by q_s (middle) and sum of two (bottom).

Testing

The new diagnostic was first developed within the NIMROD system, and is documented in Forecasting Research Technical Report No. 217. It was primarily formulated to provide a consistent method of deriving low visibility probabilities (e.g. PROB10 visibility). Experience in NIMROD has been generally favourable, with improvements seen in analysis. The scheme has also been implemented in the site-specific forecast model (SSFM) and trialled (at 14 sites) over two successive autumns. In these trials the improvement in overall visibility has been dramatic, with no degradation in performance at any site and, at many, a halving of the RMSF error. This has encouraged us to propose an early implementation within the mesoscale model which essentially uses the same physics. Separate trials within the mesoscale model are essential, as the SSFM uses aerosol taken from the mesoscale model, while the mesoscale model adjusts the aerosol through visibility data assimilation.

Trials were performed using 8 cases, most the same cases as used for testing the new microphysics, with one additional 'widespread non-freezing fog' case. The cases run are as follows, in chronological order:

1. January 5th 1997 - fog incorrectly f/c
2. January 15th 1997 - fog incorrectly cleared
3. May 29th 1997 - clear summer day
4. August 5th 1997 - stratus
5. December 1st 1997 - mixed snow and rain
6. December 10th 1997 - land gales
7. February 2nd 1998- clear winter night
8. February 18th 1998 - widespread non-freezing fog

The scheme has been run with the new microphysics, and compared with controls using the old scheme in the new microphysics. Since the scheme is purely diagnostic, and only affects aerosol in the assimilation stage, there is absolutely no impact on non-visibility related diagnostics. The impact on fog probability is small but positive. If we allocate a probability of 1 to stations observing fog, and 0 to those not observing it, then we see an improvement in RMS difference in fog probability of about 1.5%, and a similar change to probability of visibility less than 5 km of 3%.

In all 8 cases, there is an overall significant improvement in visibility verification. Only one or two forecast times, in one or two cases, show a (small) reduction in score, and the overwhelming impact is positive. Overall visibility performance is summarized in Figure 3. Here, the RMSF represents the RMS factor averaged over all 8 cases. RMSF can also be described as the antilog of the RMS error in log(visibility). It is used because visibility errors tend to be log-normal; clearly a 500 m error when the visibility is 1000m is much more significant than a 500 m error at 20 km. It is evident from these results that the improvement is substantial. It is not meaningful to quote a percentage improvement in RMSF, as the scale is not really linear. However, the underlying RMS log(Vis) reduction is 20% at best (at T+0),

3.5% at worst and about 9% on average.

The improvement in analysis is particularly noticeable, and arises because the log(visibility) errors are much more evenly distributed around the log of median visibility diagnostic: since the old scheme was essentially giving the log of visibility derived from the mean cloud water, rather than the mean log(visibility) there was a systematic error introduced. In practice, we find log(visibility) errors to be very symmetrically distributed, so the log of the median visibility (which equals the median log(visibility) corresponds closely to the mean log(visibility).

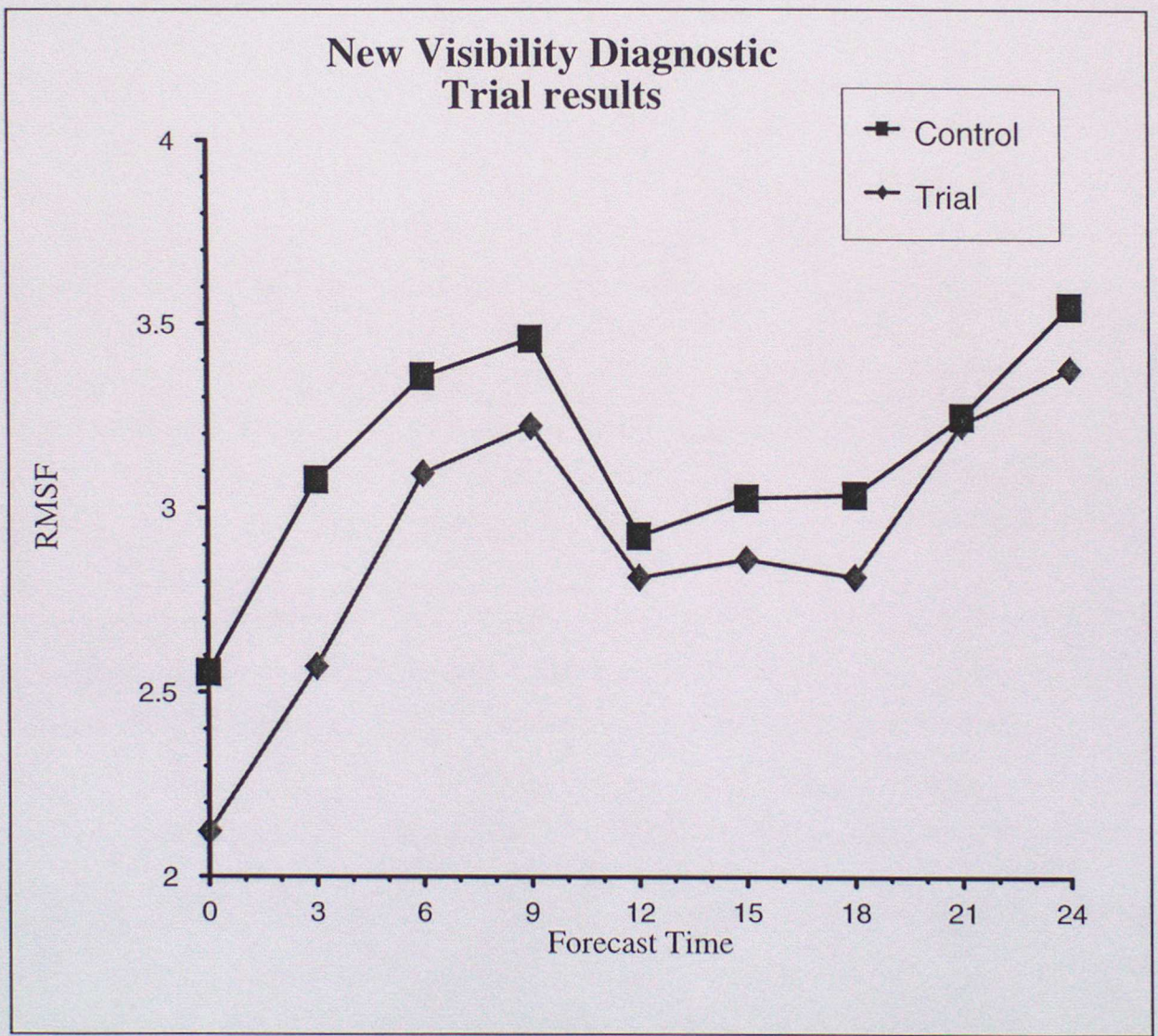

Figure 3 RMSF Errors in visibility, averaged over all eight cases in trial.

Conclusions and Recommendations

The visibility diagnostic in the UM has no impact on other variables (except aerosol) and does not affect forecast evolution. The results from SSFM trials and the mesoscale model trials reported here show a substantial improvement in verification of visibility. Improvement arises both in fog and non-fog cases, though diagnosis of fog is better achieved using the 'fog probability' diagnostic. This is itself slightly improved by the new diagnostic system. Further advantages of the scheme are its sounder and more internally consistent scientific basis, and its mathematical characteristics which make it more suitable for future use in variational schemes.

Given these conclusions, it is strongly recommended that the scheme be implemented in the operational mesoscale model, and that it become the standard UM visibility diagnosis method.